Understanding the post-translational control of CD86 in regulating T cell stimulation

&

What is the role of Lyp phosphatase (PTPN22) in phagocyte signaling?

by

Emily Elisabeth Halford

A thesis submitted to the University of Birmingham in partial fulfilment of the requirements for the award of MASTERS OF RESEARCH in Biomedical Research

School of Immunity and Infection
College of Medical and Dental Sciences
University of Birmingham
August 2012

Project 1:

Understanding the post-translational control of CD86 in regulating T cell stimulation

This project is submitted in partial fulfilment of the requirements for the award of the MRes

ABSTRACT

Background: T cell activation requires two signals, the first of which is provided by the interaction between the TCR and MHC-peptide complex and the second which is provided by the interaction between CD86 and CD28. CD86 is upregulated on antigen presenting cells (APCs) upon encounter with pathogen, and therefore its expression acts as a critical checkpoint for T cell activation. MARCH 1 and 8 ligases have been shown to regulate CD86 expression via a post-translational mechanism in immature APCs, preventing the balance of T cell activation versus anergy being shifted and auto-reactive T cells potentially becoming activated.

Methods: Cyclohexamide, an inhibitor of protein synthesis, was used to investigate the stability of CD86 on the surface of human APCs and MARCH 1 and 8 ligases were overexpressed in Chinese Hamster Ovary (CHO)-CD86 cells.

Results: Overexpression led to a 98-99% decrease in the level of surface CD86. This was shown to be via endocytosis and was associated with a high level of ubiquitination. However CD86 was found to be stable on human APCs.

Conclusions: These results demonstrate the potential for potent downregulation of CD86 by MARCH 1 and 8 and raise questions about how such a mechanism operates and is regulated in primary cells.

ACKNOWLEDGEMENTS

Thank you to Professor David Sansom for allowing me to work on such an interesting area and for providing excellent supervision. Thank you to the Sansom lab for being so helpful, especially Dr Omar Qureshi who was always happy to help, to impart wisdom and make me laugh. In particular I am grateful to Dr Qureshi for teaching me to use the confocal microscope. Special thanks to Satdip Kaur for running the Western Blot included in this report and to Louisa Jeffrey for teaching me PCR after I had officially left. Thank you to Dr Kesley Attridge and Lucasz Wardzinski for the mouse cells and generally to the Sansom and Walker labs for being so welcoming.

CONTENTS

LIST OF FIGURES

INTRODUCTION

T cell activation

T cells are lymphocytes which play a key role in driving the immune response against pathogens. There are two main types, T helper cells ($CD4^+$), and cytotoxic T cells ($CD8^+$). For a naïve T cell to be activated it must interact with an antigen presenting cell (APC) such as a dendritic cell, B cell or monocyte. This principally occurs in the lymph nodes, which T cells pass through, sampling antigen, as they circulate through the blood. Two signals are needed for activation; Signal 1 is delivered via the interaction of the T cell receptor of a $CD4^+$ T cell with antigenic peptide presented by Major Histocompatibility Complex (MHC) class II molecules on the surface of the APC and Signal 2 is delivered by interaction of CD28 on the surface of the T cell with co-stimulatory molecules CD80 and CD86 which are expressed on the surface of the APC (Linsley *et al.*, 1991).

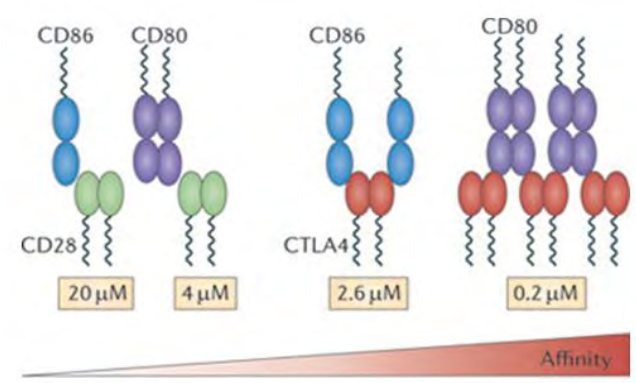

Figure 1: CD28 and CTLA-4 and their ligands, CD80 and CD86 (Manzotti et al. 2006)

CD80 and CD86 are members of the immunoglobulin superfamily (Freeman *et al.,* 1993); and each monomer consists of two immunoglobulin-like domains, a transmembrane region and a cytosolic tail. CD86 is primarily found as a monomer (Zhang *et al.*, 2003) whereas

CD80 forms a dimer (Ikemizu *et al.*, 2000) (**Figure 1**). CD80 and CD86 are also the ligands for CTLA-4 (CD152), which is expressed on mature T cells as well as constitutively on regulatory T cells. CTLA-4 acts via its interaction with CD80/86 as a negative regulator of T cell activation, instead leading to T cell anergy; a state of unresponsiveness.

CD86 is expressed at low levels on immature dendritic cells (DCs) and rapidly upregulated upon receipt of maturation stimuli whereas CD80 is expressed only upon receipt of these stimuli and is upregulated less rapidly (Sansom *et al.* 2000). These maturation stimuli include recognition of pathogen associated molecular patterns (PAMPS), such as Lipopolysaccharide (LPS), a component of the cell wall of gram negative bacteria, by pattern recognition receptors (PRRs), such as Toll-like receptors. These maturation stimuli also lead to the upregulation of MHC class II molecules, decreased endocytic ability, increased motility and production of pro-inflammatory cytokines (Thery and Amigorena, 2001). The requirement of such stimuli for upregulation of CD80 and CD86 acts as a safeguard against autoimmunity because if the DC has not encountered a pathogen and is instead potentially presenting an auto-antigen, then the levels of CD80 and CD86 will be too low to activate what could be autoreactive T cells.

Although CD80 and 86 are both ligands for the same receptor, they share only 25% sequence homology (Freeman *et al.*, 1993) and have been shown to have distinct functional identities (Sansom *et al.* 2003). CD86 is important in initiating an immune response, whereas CD80 is more important in prolonging that immune response (Boriello *et al.* 1997) and indeed CD28 and CTLA-4 have higher affinity for CD80 than CD86 (Manzotti *et al.* 2006).

Post-translational control of CD86

Considering the key role of CD86 in T cell activation, it is important that a low level of cell surface expression is maintained on immature DCs and that upon maturation signals, high levels are induced. As well as the previously described transcriptional controls, there are also

thought to be post-translational mechanisms which contribute to the regulation of surface CD86.

It was reported by Goto *et al.* (2003) that the protein c-MIR, can downregulate the expression of CD86 on the surface of human monocyte derived DCs. c-MIR was identified via a screen for human proteins with structural and functional homology to the MIR (Modulator of Immune Recognition) 1 and 2 proteins of Kaposi's Sarcoma-associated Herpesvirus (Goto *et al.*, 2003). MIR 1 and 2 are E3 ubiquitin ligases which are able to circumvent recognition by the host immune system by downregulating the surface expression of MHC class I, CD86 and ICAM-1 (Coscoy *et al.*, 2001). cMIR, on the other hand, was found to affect CD86 and not MHC class I or ICAM-1 expression (Goto *et al.*, 2003). Interestingly their findings suggest that MIR 1 and 2 originated in the host genome and were 'hijacked' by KSHV to avoid recognition by the immune system.

Subsequently additional human proteins were found which shared homology with MIR1 and 2 and these were named as the MARCH (Membrane Associated RING-CH) family. MARCH 1 was found to downregulate surface expression of CD86 in a similar manner to c-MIR, which was renamed MARCH 8 (Bartee *et al.*, 2004). MARCH 1 is primarily expressed in secondary lymphoid tissue (Matsuki *et al.*, 2007) whereas MARCH 8 is reported to be ubiquitously expressed (Bartee *et al.*, 2004). Both MARCH 1 and 8 have been shown to be located in the endolysosomal compartment (Jabbor *et al.*, 2009; Goto *et al.*, 2003).

Indeed multiple publications have shown that MARCH 1 and CD86 associate with one another (De Gassart *et al.*, 2008; Matsuki *et al.*, 2007; Thibodeau *et al.*, 2008) and further to this DCs from MARCH 1 knockout mice have been observed to exhibit increased surface expression of CD86 and MHC class II (Ohmura-Hoshino *et al.*, 2007). In addition overexpression of MARCH 1 and 8 in a human melanoma cell line has been shown to lead to

a 65-75% decrease in surface levels of CD86, a similar decrease in MHC class II and only a 0-8% decrease in CD80 (Lapaque *et al.*, 2009).

The downregulation of surface CD86 and MHC class II by MARCH 1 and 8 is thought to be important in maintaining DC function in the steady state and may therefore be a 'housekeeper' for immature DCs (Ohmura-Hoshino *et al.*, 2009). Upon receipt of maturation signals MARCH 1 is downregulated and is therefore not detected in mature human monocyte derived DCs (De Gassart *et al.*, 2008).

Molecular mechanism of CD86 downregulation

MARCH 1 and CD86 mutation studies have shown that the transmembrane domains of MARCH 1 and CD86 (as well as the cytosolic region of CD86) are necessary for their association and therefore they may interact via this domain (Corcoran *et al.*, 2011). MARCH 1 and 8 are E3 ubiquitin ligases, the third of the three enzymes which catalyse the series of reactions necessary for ubiqutination, which is a post-translational modification involving the conjugation of 76-amino acid polypeptide, ubiquitin, via its C terminus to a lysine side chain of a protein (Pickart *et al.*, 2001). It is the Really Interesting New Gene (RING)-CH domain of the MARCH ligases, a zinc finger in the cytosolic region, which conveys the ubiquitin ligase activity of the protein (Bartee *et al.*, 2003).

The addition of one or a few ubiquitin molecules to a protein has been shown to be able to promote endocytosis from the surface of the cell and to result in destruction of that protein in the lysosome (Pickart *et al.*, 2001) and indeed pulse chase experiments with a mouse cell line which overexpresses MARCH 1 ligase have shown that the kinetics of CD86 loss from the surface is indicative of endocytosis and a role for the lysosome (Corcoran *et al.*, 2011). Lysine mutagenesis studies have shown that ubiquitination is necessary for the observed downregulation of both human and mouse CD86 upon MARCH 1 or 8 overexpression (Goto *et al.*, 2003; Baravalle *et al.*, 2011). There are multiple lysines in the cytoplasmic tail of CD86

, all of which are able to be ubiquitinated by MARCH 1 (Baravalle *et al.*, 2011) and indeed it has been reported that CD86 is polyubiquitinated by MARCH 1 (Corcoran *et al.*, 2011). In particular it has been reported that ubiquitination of lysines closest to the transmembrane domain, such as at Lys267, is important for the downregulation of surface CD86 on murine APCs (Baravalle *et al.*, 2011; Corcoran *et al.*, 2011).

Regulation of MARCH 1 and 8

It has been reported that MARCH 1 has a half-life of less than 30 minutes and is degraded in the lysosome by multiple lysosomal proteases such as Cathepsin L (Jabbor *et al.*, 2009). This would therefore allow any transcriptional changes in the level of the MARCH ligases, such as the downregulation upon maturation, to rapidly become apparent at the protein level. In addition, CD83, a member of the immunoglobulin superfamily which is upregulated on the surface of DCs upon receipt of maturation stimuli, has been observed to inhibit MARCH 1 via its transmembrane region in mouse DCs (Tze et al., 2011). This prevents ubiquitination and hence downregulation of CD86 by any remaining MARCH 1 by blocking their interaction (**Figure 2**). In addition this would block the interaction of MARCH 1 and MHC class II, therefore higher levels of both MHC class II and CD86 would be available to contribute to signal 1 and 2, respectively. In addition it has been suggested that MARCH 1 may be able to inhibit CD83 (Tze *et al.*, 2011). Interestingly a recent paper has shown that MARCH 1 may in fact regulate itself through dimerization and autophosphorylation (Borgeois-Daigneault and Thibodeau, 2012).

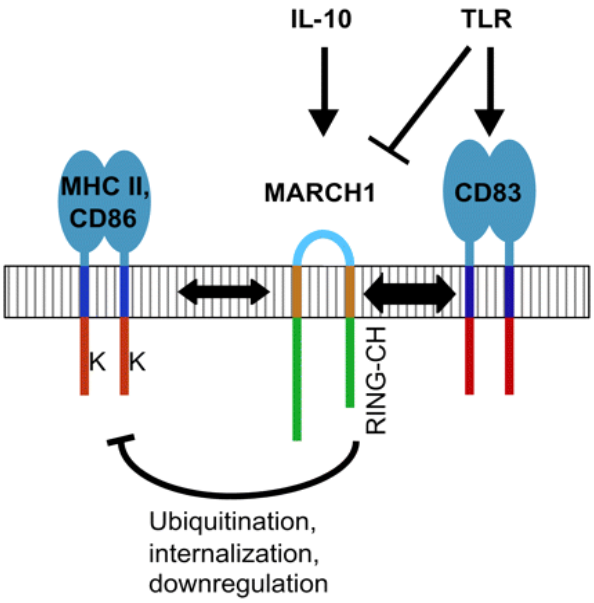

Figure 2: The influence of CD83 and Interleukin-10 (IL-10) on the downregulation of MHC Class II and CD86 by MARCH 1 ligase (Tze et al., 2011).

The anti-inflammatory cytokine Interleukin-10 (IL-10), on the other hand, is able to strongly induce an increase in MARCH 1 mRNA levels via interaction with its receptor on the surface of the APC and hence decrease levels of surface MHC class II and CD86 in the case of both human and mouse cells (Thibodeau *et al.*, 2008; Tze *et al.*, 2011) (**Figure 2**). This reduces the ability of the APC to activate T cells and is hence a mechanism of regulating T cell activation. IL-10 can be produced by the DC which it acts upon, therefore acting in an autocrine fashion, or may be produced by surrounding cells, therefore acting in a paracrine fashion (Haase *et al.*, 2002). A recent publication has shown that indeed in mouse DCs which have been stimulated with LPS, CD86 is continuously ubiquitinated which is due in part to the action of autocrine IL-10 (Baravalle *et al.*, 2011).

Taking into account the findings of the recent publications in this field, we hypothesise that CD86 will be unstable on the surface of human APCs, but stable on those which have

received maturation stimuli. In addition we hypothesise that MARCH 1 and 8 are able to downregulate CD86.

The aims of this study are:

- To investigate the stability of CD86 on the surface of immature antigen presenting cells
- To determine the effect of MARCH 1 and 8 ligase overexpression on the surface CD86

MATERIALS AND METHODS

DNA Constructs and Transfectants

Full length CD80, CD86, CTLA-4 and HLA-DR DNA was provided by Prof. David Sansom and GFP tagged MARCH ligase constructs by Dr. Adrian Kelly (University of Cambridge, U.K.). The constructs were cloned into CMV expression vector pcDNA3.1 as described by Mead *et al.* (2005).

Cell purification and Culture

All cell cultures were maintained at 37°C in a humidified incubator containing 5% CO_2.

CHO cells

Chinese Hamster Ovary cells expressing different DNA constructs were generated by electroporation of human cDNAs cloned into a CMV expression vector. Cells were grown in 1x Dulbeccos Modified Eagle Medium (Gibco, Invitrogen) supplemented with 2mM L-glutamine (Sigma), 10% foetal bovine serum (FBS) (Biosera or Invitrogen) and 1% penicillin and streptomycin (Invitrogen). Cells expressing the plasmid were selected using G418 (500µg/ml) treatment and by cell sorting. Cultures were maintained as previously described and passaged by trypsinization. Cells were transfected with the MARCH ligase constructs via electroporation using a Neon® Transfection System (Life Technologies) and were cultured for 24 hours before further experiments were carried out.

Akata B cells

Akata B cells were cultured in complete RPMI 1640 medium supplemented with 2mM L-glutamine (Sigma), 10% foetal bovine serum (FBS) (Biosera or Invitrogen) and 1% penicillin and streptomycin (Invitrogen).

Human Monocytes and Monocyte-Derived Dendritic Cells

For $CD14^+$ $CD16^-$ monocyte isolation, peripheral human blood mononuclear cells (PBMCs) were isolated from leukocyte reduction system cones (LC) (Provided by the national Blood Transfusion Service, Birmingham, UK) by Ficoll-paque density gradient centrifugation (GE Healthcare). Cells were washed twice in PBS and resuspended at 1×10^8/ml in MACS buffer (0.5% BSA and 2mM EDTA in PBS). Unless otherwise stated, all washes were carried out by centrifugation for 5 minutes at 1500rpm.

$CD14^+$ $CD16^-$ cells were isolated via negative selection by incubating PBMCs with human monocyte enrichment cocktail and magnetic colloid according to the manufacturer's instructions (Stem Cell Technologies, France). Blood was obtained from anonymous donors following informed consent and in line with institutional and ethical committee approval. To generate monocyte-derived dendritic cells (MoDCs) $CD14^+$ $CD16^-$ monocytes were cultured for 7 days with Granulocyte Macrophage-Colony Stimulating Factor (GM-CSF) (800U/ml; Peprotech) and Interleukin-4 (IL-4) (400U/ml; Peprotech) at 37°C in a humidified incubator. When required the MoDCs were matured by overnight treatment with LPS (1µg/ml; Sigma). All human and murine cells were cultured in complete RPMI 1640 medium supplemented with 10% FBS, 50 U/ml penicillin and streptomycin, and 200µM glutamine (Life Technologies/Invitrogen).

Murine B cells and dendritic cells

Murine $CD19^+$ B cells and Bone Marrow-derived Dendritic Cells (BMDC) from BALB/c mice (purchased from The Jackson Laboratory) were provided by Dr Kesley Attridge and Lukasz Wardzinski. The B cells were isolated by negative selection from single cell suspensions obtained from the spleen using CD19 microbeads (Miltenyi Biotech). BMDCs were obtained by treatment of cultured bone marrow from with 200U/ml rmGM-CSF (Peprotech) for 11 days.

Flow Cytometry Assays

Rate of degradation assay

For the rate of degradation assay cells were pre-incubated at 37°C with cyclohexamide (100µg/ml; Calbiochem) for the indicated period of time. Alternatively cells were incubated with 10mM MG132 (Sigma) or 100mM Ammonium Chloride (NH_4Cl) (Sigma) to inhibit the proteosome or lysosome. During the time course experiments all cells were treated with the relevant inhibitor or control media and were placed on ice when the appropriate time point was reached to stop the activity of the inhibitor from continuing.

Cell lines and human cells were stained with monoclonal antibodies against human CD80, CD86, CTLA-4 and HLA-DR. Murine cells were stained with monoclonal antibodies against mouse CD80, CD86 and IAd. All Antibodies were purchased from BD Pharmingen. At least 200,000 cells were used for each stain and staining was carried out in polystyrene tubes.

For analysis of surface protein, cells were incubated with the indicated antibody (1:200 in media) at 4°C for 1 hour and subsequently washed in 1ml PBS. For total staining, cells were washed after a 10 min incubation in 3% paraformaldehyde at RT. Cells were washed twice in 1ml PBS and once in 1ml of permeabilising solution (0.1% Saponin) before being stained with the indicated antibody (1 in 200 in permeabilising solution) and incubated at RT for 30 min. After staining cells were washed in 1ml permeabilising solution and twice in 1ml PBS.

Flow cytometry was performed using a FACSCalibur flow cytometer (BD Biosciences) and analysed using FlowJo software (Tree Star). 10000 events were collected for each sample. When using transfected cells 5000 events were collected from a transfected gate. Dead cells were excluded by forward and side scatter characteristics.

Confocal Microscopy

Imaging was carried out using a Zeiss LSM 780 inverted laser scanning confocal microscope. Constant laser powers and acquisition parameters were maintained throughout each experiment. Analysis was performed using Image J (Wayne Rasband, NIH) and quantification of cells was carried out by outlining cells and measuring the mean fluorescence intensity (MFI). All images shown are representative of at least 5 micrographs.

Immunofluorescence staining

CHO cells expressing CD86 were transfected with each MARCH ligase construct and plated on poly-L-lysine-coated coverslips overnight. Cells were treated with media, 10mM MG132 or 100mM NH_4Cl and incubated at 37°C for 4 hours. After this time cells were washed with 1ml PBS and fixed by treatment with 250µl of 3% PFA for 10 min at RT. Cells were washed in 1ml PBS and subsequently twice in 1ml permeabilising solution (0.1% Saponin) before being incubated at RT with 250µl of donkey serum solution (1:1000 serum in 0.1% Saponin) for 30 min. Cells were labelled at RT with an unconjugated mouse anti-human CD86 antibody (BU63) (Invitrogen; 1:200 in the donkey serum solution) for 30 min. Cells were washed three times in 1ml permeabilising solution and labelled with an Alexa555-conjugated donkey anti-mouse antibody (Invitrogen) diluted 1:500 in permeabilising solution for 30 min. Subsequently cells were washed three times in 1ml permeabilising solution followed by 1ml PBS.

Endocytosis assay

CHO cells expressing CD86 were transfected with each MARCH ligase construct and plated on poly-L-lysine-coated coverslips overnight. The media was aspirated and cells incubated at RT with 250µl of donkey serum solution (1:1000 serum in 0.1% Saponin) for 30 min. An unconjugated mouse anti-human CD86 antibody (BU63) (Invitrogen; 1:200 in the donkey serum solution) was subsequently added and cells were incubated at 37°C for 30 min. Cells

were washed twice with 1ml DMEM (10% FBS) and 1ml PBS and subsequently fixed by incubation for 10min at RT in 250µl of 3% PFA. After being fixed, cells were washed in 1ml PBS and twice in 1ml permeabilising solution (0.1% Saponin). Cells were labelled at RT with an Alexa555-conjugated donkey anti-mouse antibody (Invitrogen) diluted 1:500 in permeabilising solution for 30 min, washed three times in 1ml permeabilising solution followed by 1ml PBS.

Immunoprecipitation

To obtain surface CD86 only, anti-CD86 antibody (BU63) (Invitrogen 1µg) was incubated with $2.5x10^6$ control cells or MARCH 8 ligase wildtype or mutant transfected CHO-CD86 cells for 1hr at 4°C. Cells were subsequently centrifuged at 5000rpm for 3min at 4°C and the supernatant discarded. Cells were lysed by addition of 1% Triton buffer containing 100x protease cocktail inhibitor and incubated on ice for 30min. The supernatant was transferred to new tubes and a 20µl aliquot was removed and labelled as the whole cell lysate. Protein-G-Sepharose beads (20µl per immune-precipitation) were added to the supernatant and the samples were kept at 4°C overnight on a rotating wheel.

To obtain total CD86 Protein-G-Sepharose beads (20µl per immune-precipitation) and 1µg Anti-CD86 antibody (BU63) (Invitrogen) were added to 1% Triton buffer and kept at 4°C overnight on a rotating wheel. The beads were washed 3x with Triton (lysis) buffer. $2.5x10^6$ control cells or MARCH 8 ligase wildtype or mutant transfected CHO-CD86 cells were lysed by addition of 1ml 1% Triton buffer containing 100x protease inhibitor cocktail and incubated on ice for 30min. The supernatant was added to the antibody coated beads and kept at 4°C on a rotating wheel for 1 ½ hours.

The total and surface CD86 samples were washed 3 times in 1% Triton (lysis) buffer and following the final wash the supernatant was discarded and 20µl 2x sample loading buffer was added.

Western blotting

The total and surface CD86 samples were boiled for 5min at 100°C and electrophoresed on an 8-16% gradient SDS-polyacrylamide gel. The samples were subsequently transferred to a nitrocellulose membrane for 90 minutes at 400mA using a wet-blotting system. The transfer membrane was blocked with 5% (w/v) milk powder in PBS/0.05% Tween 20 (PBST) for an hour at room temperature to prevent non-specific binding and subsequently incubated with 1µg/ml of an anti-ubiquitin primary antibody in 5% (w/v) milk powder in PBST overnight at 4°C. The membrane was washed 3x in 50ml PBST high salt for 5mins before incubation with the secondary goat anti-mouse HRP antibody overnight at 4°C. Subsequently the membrane was washed 5x in 50ml PBST high salt for 5mins, rinsing the lid and gel in dH_20 after the first wash. After the last wash the PBST was discarded and Amersham ECL western blotting reagents (Thermo Scientific, Perbio) were added for 30 seconds. The blot was placed in an X-ray cassette and the film was developed in a dark room.

Statistics

For the results in Figures 11-14 a paired Student's T-TEST was performed. All error bars show the standard error of the mean.

RESULTS

Stability of surface and total CD80 and CD86, investigated by CHX treatment

We investigated the stability of surface and total CD80 and CD86 as an indicator of whether the MARCH 1 and or 8 ligases are targeting these co-stimulatory molecules for degradation. Treatment of cells with an inhibitor of protein synthesis, cyclohexamide (CHX) prevents cells replacing any CD80 or CD86 which has been degraded, therefore enabling us to investigate the rate of degradation.

Cells were treated with either media or CHX for up to 4 hours, over 5 time points. After this time cells were stained for surface protein and this was analysed by flow cytometry. Chinese Hamster Ovary (CHO) cells expressing recombinant human CD86 or CD80 were initially used for this assay (**Figure 3**). It has previously been reported that CHX treatment of T cells over 2-4 hours leads to a significant decrease in intracellular CTLA-4 (Iida *et al.,* 2000) and therefore CHO cells expressing CTLA-4 were used as a control for CHX activity. After 1 hour of CHX treatment the level of CTLA-4 on the CHX-treated cells was considerably lower than on the media-treated cells and remained this way for the next 3 hours, indicating rapid protein degradation (**Figure 3A and 3B**) and therefore CTLA-4 was a useful control for CHX activity.

In contrast there was little difference in the level of CD80 between the media and CHX-treated cells and this was the case over all five time points (**Figure 3A and 3B**). Similarly the level of CD86 also remains constant over the four hours, with both CHX and media treatment. Therefore CD80 and CD86 appear stable when expressed on the surface of CHO cells.

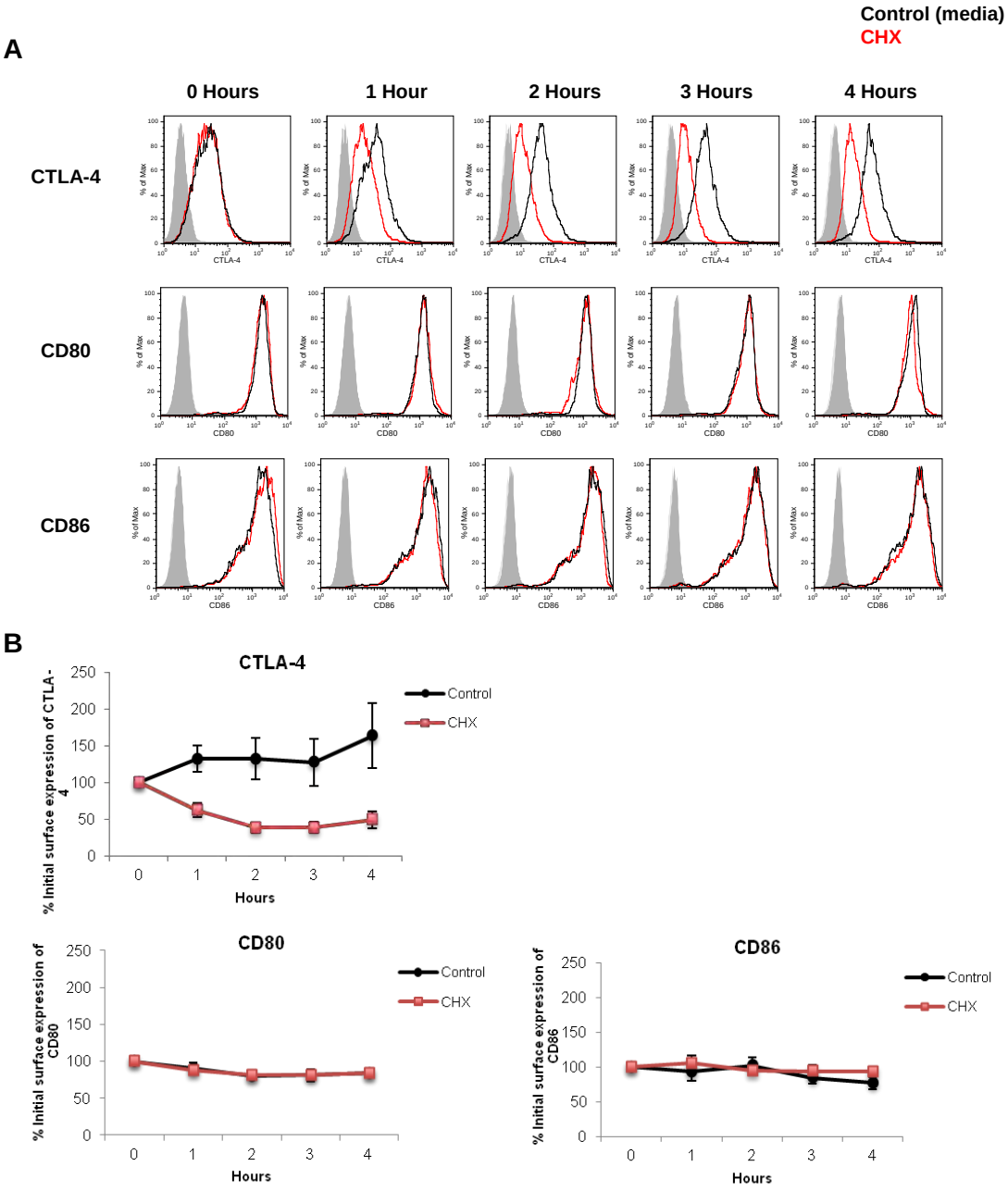

Figure 3: Stability of CTLA-4, CD80 and CD86 on the surface of CHO-CTLA-4, CHO-CD80 and CHO-CD86 cells. Cells were incubated with media or 100µg/ml cyclohexamide (CHX) for 0-4 hours at 37°C, surface stained with PE-conjugated anti-CTLA-4, CD80 or CD86 and analysed by flow cytometry. (A) Histograms of CTLA-4, CD80 and CD86 levels on control cells (media-treated) (black) and levels on CHX treated cells (red). Isotype controls are shown in grey. Data are representative of three independent experiments. (B) Graphical representation of the results of the three independent experiments.

To investigate the stability of CD80 and CD86 on the surface of APCs, Akata B cells were treated with media or CHX for four hours, over 5 time points, stained for surface CD80 or CD86 and analysed by flow cytometry. This revealed that these cells express CD80 and CD86 and that the level of CD80 and CD86 does not decrease upon CHX-treatment of these cells (**Figure 4A and 4B**). The levels remained similar to the initial level except for a slight peak increase on the CHX-treated B cells at the two hour time point, which then returned to the initial level over the next hour. Therefore CD80 and CD86 appear stable on the surface of Akata B cells.

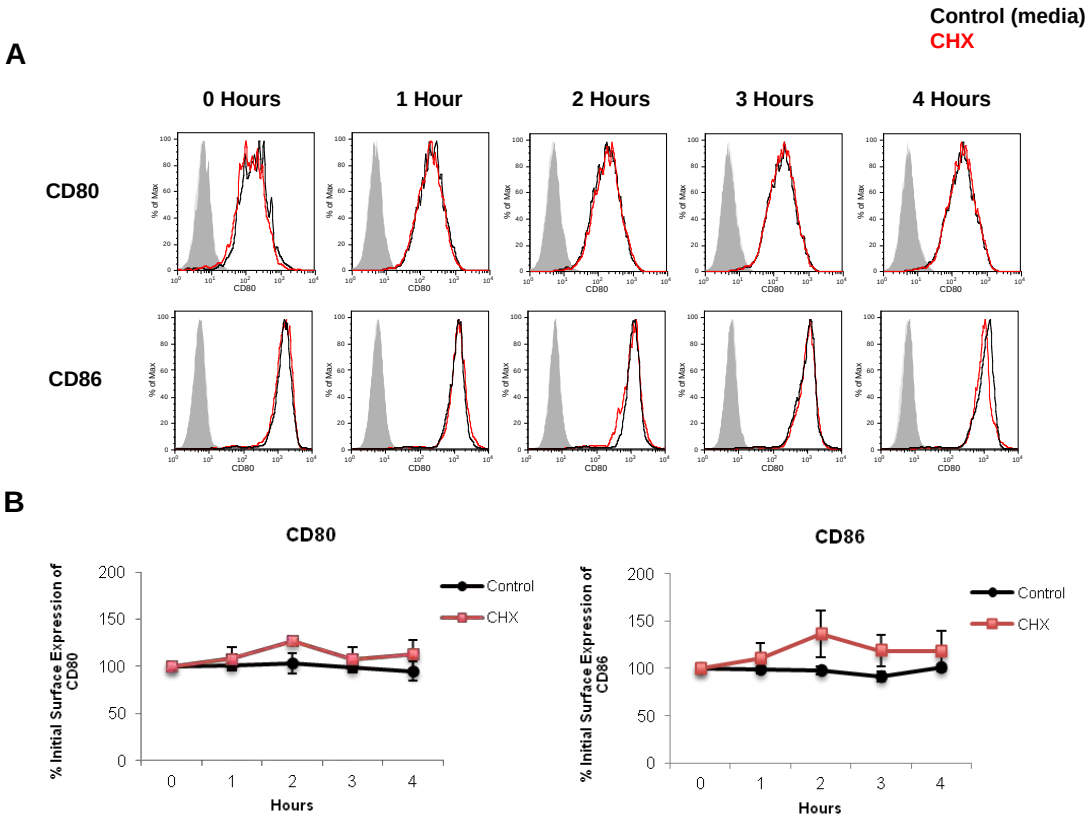

Figure 4: Stability of CD80 and CD86 on the surface of Akata B cells. Cells were incubated with media or 100µg/ml cyclohexamide (CHX) for 0-4 hours at 37°C, surface stained with PE-conjugated anti-CD80 or CD86 and analysed by flow cytometry. (A) Histograms of CD80 and CD86 levels on control cells (media-treated) (black) and levels on CHX treated cells (red). Isotype controls are shown in grey. Data are representative of three independent experiments. (B) Graphical representation of the results of the three independent experiments.

We subsequently tested the stability of CD80 and CD86 in two further types of APC: human monocyte derived dendritic cells (MoDCs) and monocytes. Cells were treated with media or CHX for four hours, over 3 time points, stained for surface CD80 or CD86 and analysed by flow cytometry. The results of this experiment showed that these cells express CD80 and CD86 and that CHX-treatment does not lead to a decrease in the level of CD80 (**Figure 5A and 5B**). From these histograms it would appear that CD86 is unstable on these cells as the CHX-treated cells expressed less CD86 than the media treated. However the CD86 graph in section B shows that this difference in the level of CD86 is due to an upregulation in the media treated cells which is unable to occur in the CHX-treated cells as we have blocked protein synthesis and does not show instability of CD86. The histogram in **Figure 5C** shows that CHX-treatment does not reduce the surface level of CD86 on the human monocytes. Therefore CD80 and CD86 appear to be stable on the surface of human monocytes and MoDCs.

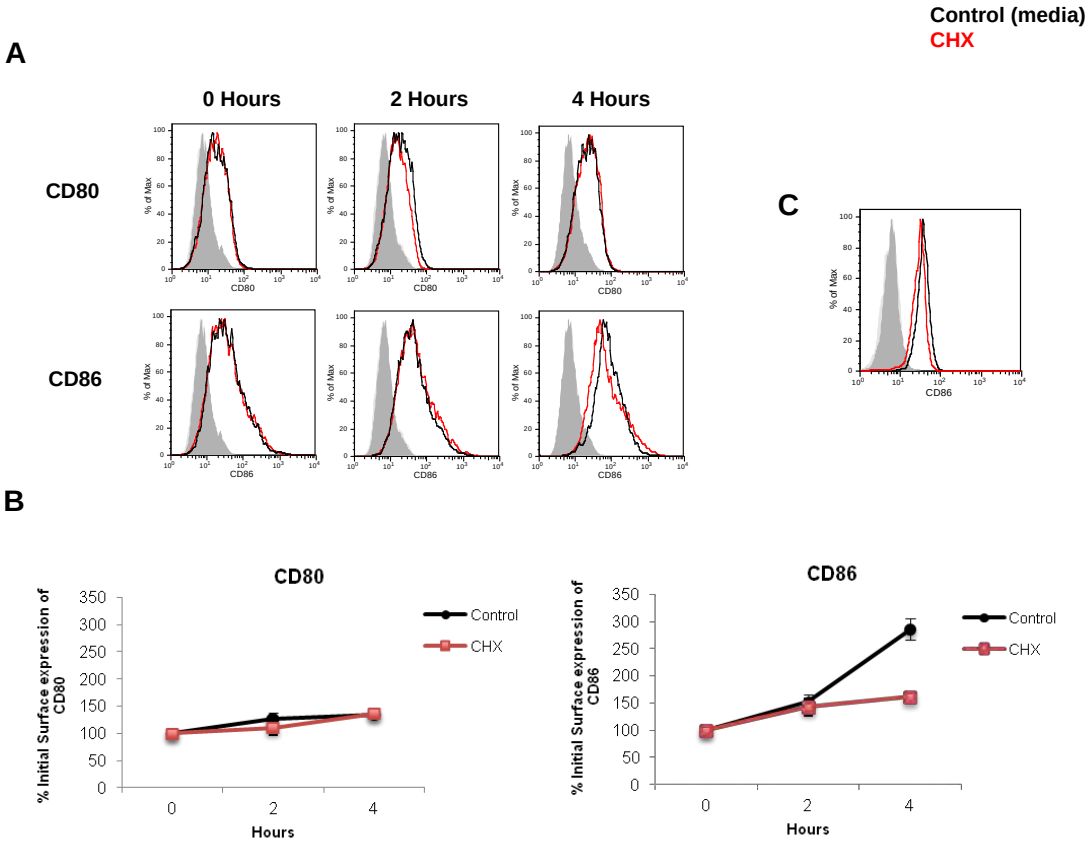

Figure 5: Stability of CD80 and CD86 on the surface of human immature monocyte-derived dendritic cells and monocytes. Cells were incubated with media or 100µg/ml cyclohexamide (CHX) for 0-4 hours at 37°C, surface stained with PE-conjugated anti-CD80 and/or CD86 and analysed by flow cytometry. (A) Histograms of CD80 and CD86 levels on control (media-treated) (black) and CHX treated (red) monocyte-derived dendritic cells. Isotype controls are shown in grey. Data are representative of three independent experiments. (B) Graphical representation of the results of the three independent monocyte-derived dendritic cell experiments. (C) Histograms of CD86 levels on control (media-treated) (black) and CHX treated (red) monocytes. Isotype controls are shown in grey.

One possibility for the observed stability of surface CD86 could be that only intracellular protein is degraded. To investigate this, CHO cells, Akata B cells and MoDCs were again treated with either media or CHX for up to 4 hours, with 5 time points (3 for the MoDCs) and stained for total CD86 before being analysed by flow cytometry. We observed that the total level of CD86 did not decrease upon CHX-treatment within the CHO-CD86, Akata B and MoDCs (**Figure 6**) and therefore it does not appear that the intracellular CD86 is degraded. Overall these results indicate that total and surface CD86 is stable in CHO-CD86, human B cells, human monocytes and immature MoDCs.

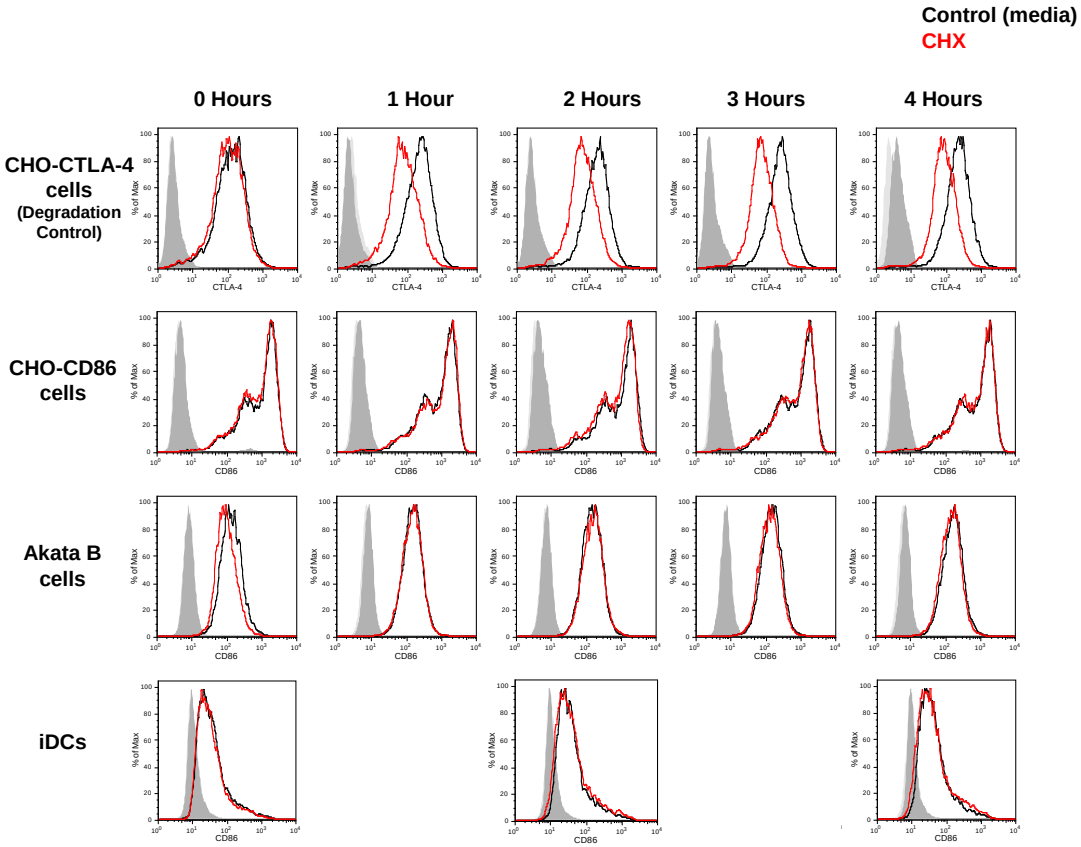

Figure 6: Stability of total CD86 in CHO-CD86, Akata B and immature human monocyte-derived dendritic cells. Cells were incubated with media or 100µg/ml cyclohexamide (CHX) for 0-4 hours at 37°C, total stained with PE-conjugated anti-CD86 and analysed by flow cytometry. Histograms show levels of CD86 on control cells (media-treated) (black) and on CHX treated cells (red). Isotype controls are shown in grey. CTLA-4 levels on control and CHX-treated CHO-CTLA-4 cells were also measured as a control for CHX activity.

Stability of surface CD80 and CD86 on mouse cells, investigated via CHX treatment

To test if the lack of degradation was only seen in human APCs, the rate of degradation assay was also carried out using mouse splenic B cells (**Figure 7**). Cells were treated with CHX for 3 hours before staining and analysis by flow cytometry. Cells were stained for surface MHC class II molecules (IAd) in addition to CD80 and CD86 as a marker of B cells, which are MHC class II^{hi}. Both the whole population and cells within the MHC class II^{hi} population were studied.

As shown in **Figure 7** the mouse B cells do not express CD80, however they do express CD86 and expression of CD86 was considerably lower on the surface of the CHX-treated cells than media treated cells. Along with the observation that the CD86 expression is not very high, this suggests that CD86 is unstable on the surface of these cells, however we would need to determine whether the difference observed between the surface level of CD86 on the media and CHX-treated cells was not just due to an upregulation in the level of CD86 on the media treated cells which was prevented in the CHX-treated cells because of the inhibition on CD86 synthesis. The results of this experiment indicate that CD86 is unstable on the surface of mouse B cells.

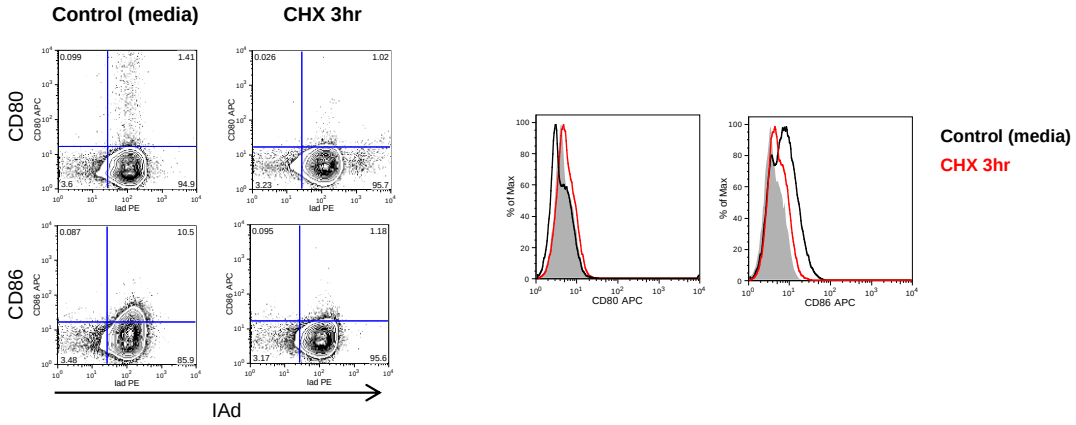

Figure 7: Stability of CD80 and CD86 on the surface of Mouse splenic B cells. Cells were incubated with media or 100µg/ml cyclohexamide (CHX) for 3 hours at 37°C, surface stained with PE-conjugated anti-CD80 or CD86 and analysed by flow cytometry. Contour plots of CD80 and CD86 expression against IAd expression and histograms showing CD80 and CD86 levels on control (media-treated) (black) and CHX treated (red) mouse splenic B cells are shown. Isotype controls are shown in grey.

Next we wished to establish whether CD80 and CD86 are unstable on the surface of mouse bone marrow derived dendritic cells (BMDCs) and whether the receipt of maturation stimuli then leads to stabilisation, as the literature suggests (**Figure 8**). Cells were treated with CHX for 3 hours before staining and analysis by flow cytometry. These cells were stained for surface MHC class II molecules (IAd) in addition to CD80 and CD86 as a marker of DCs, which are MHC class II^{hi}. Both the ungated population and the cells within the MHC class II^{hi} population were studied. This was simultaneously carried out at 4°C to investigate whether CD80 and CD86 are upregulated in culture.

Similar levels of CD80 were observed on the media and CHX treated cells from both the ungated and the IAd^{hi} populations (**Figure 8A**). Similar levels of CD86 were also observed on the media and CHX treated cells from the IAd^{hi} population but a lower level of CD86 was observed on the surface of the CHX treated than the media treated cells from the ungated population (**Figure 8A**). However the level of CD86 on the media treated cells was higher than on the 4°C media treated cells (**Figure 8B**) and therefore the difference between the level of CD86 on the CHX and media treated cells may have been due to CD86 being upregulated in culture. Therefore this data indicates that CD80 and CD86 are relatively stable on the surface of both immature and mature mouse DCs; however more repeats would be needed to confirm this finding.

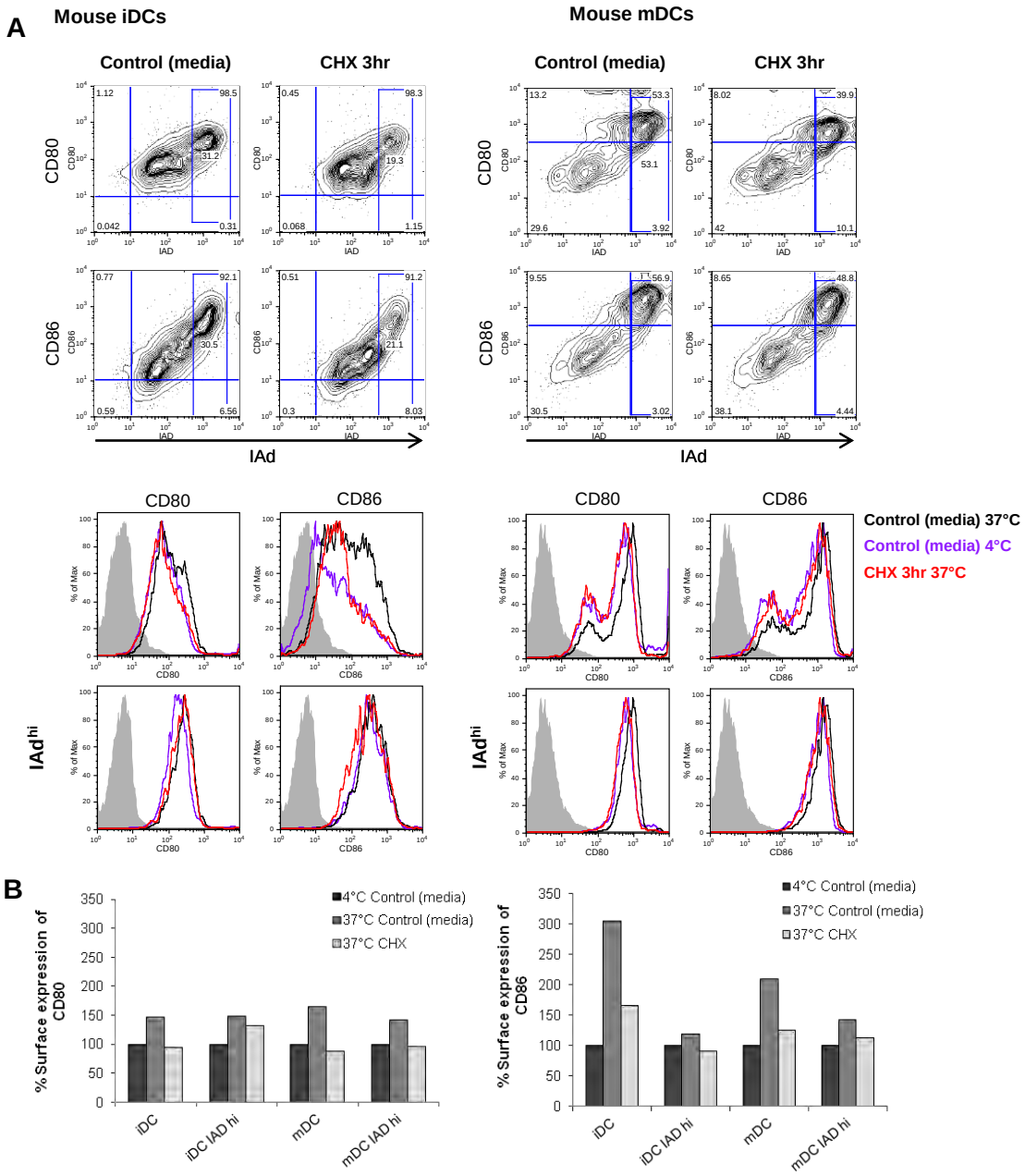

Figure 8: Stability of CD80 and CD86 on the surface of Mouse immature and mature bone marrow-derived dendritic cells. Cells were incubated with media or 100µg/ml cyclohexamide (CHX) for 3 hours at 37°C or 4°C, surface stained with APC-conjugated anti-CD80 or CD86 and analysed by flow cytometry. Contour plots of CD80 and CD86 expression against IAd expression and histograms showing CD80 and CD86 levels on control (media-treated) (black) and CHX treated (red) mouse immature and mature bone marrow-derived dendritic cells are shown. Isotype controls are shown in grey. Data are representative of two independent experiments. Graphical representation of the results of the two independent experiments are also shown.

The stability of CD80 and CD86 on the surface of immature and mature human MoDCs was also investigated, so that a comparison could be made, with staining for HLA-DR to ensure that the MHC class II^{hi} population could be gated upon (**Figure 9**). Cells were treated with CHX for 3 hours before staining and analysed by flow cytometry. No difference in the level of CD80 was observed in the CHX-treated immature and mature DCs compared to media-treated cells (**Figure 9A**). Similarly there was no difference between the levels of CD86 on the surface of the whole population of immature DCs under the two conditions, however in the HLA-DR^{hi} population there was a reduced level of CD86 on the surface of the CHX-treated immature DCs compared to media treated cells (**Figure 9A**). This was statistically significant ($p<0.05$) across two independent experiments (**Figure 9B**) however again we would need to determine whether the difference observed between the surface level of CD86 on the media and CHX-treated cells was not just due to an upregulation in the level of CD86 on the media treated cells which was prevented in the CHX-treated cells because of the inhibition on CD86 synthesis. The level of CD86 on the surface of the mature DCs was similar under both the CHX and media conditions. Therefore CD80 was shown to be stable on the surface of human immature and mature DCs. CD86 was also shown to be stable on the surface of mature DCs and on the ungated but not the MHC class II^{hi} immature DCs.

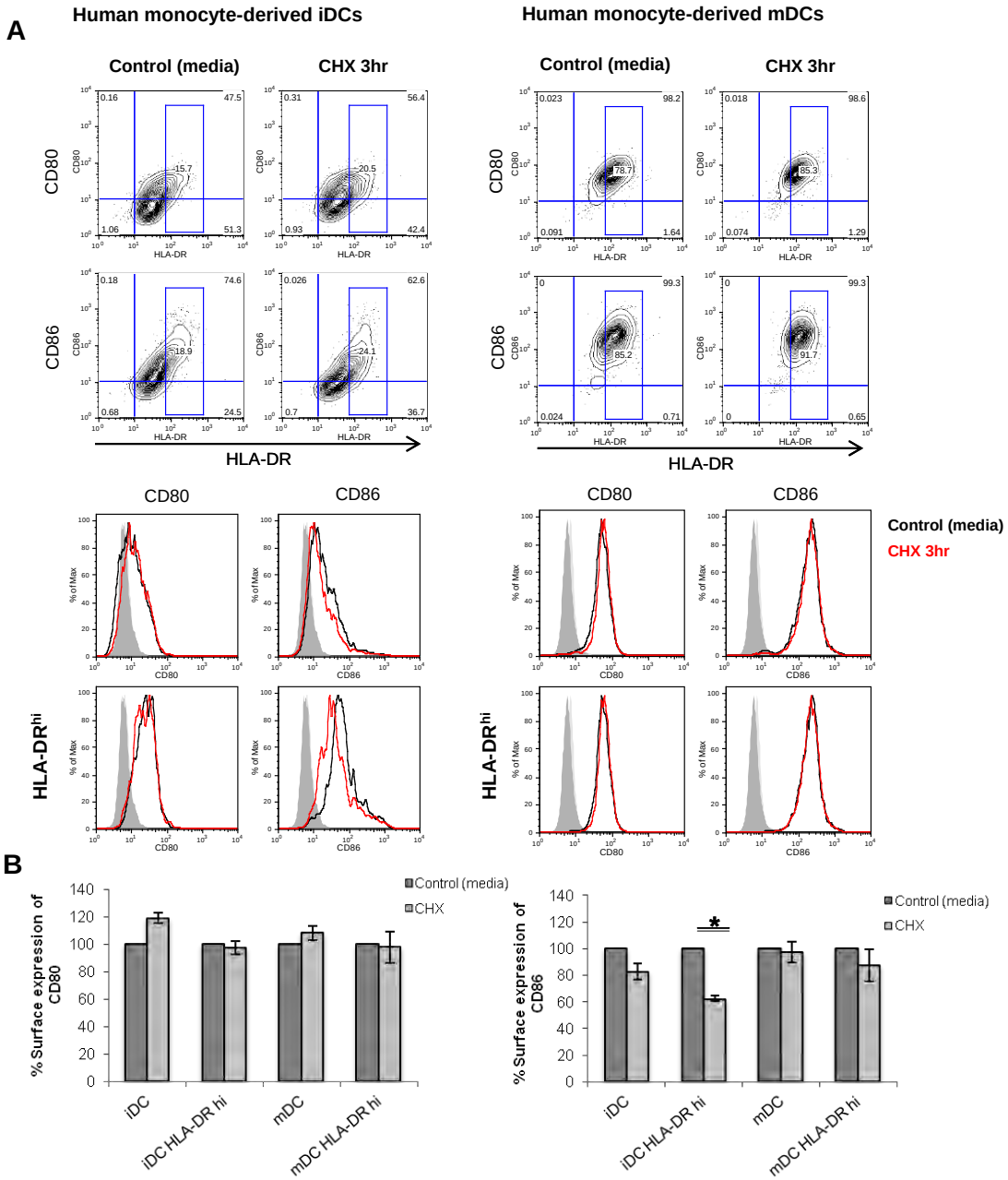

Figure 9: Stability of CD80 and CD86 on the surface of human immature and mature monocyte-derived dendritic cells. Cells were incubated with media or 100µg/ml cyclohexamide (CHX) for 3 hours at 37°C, surface stained with PE-conjugated anti-CD80 or CD86 and analysed by flow cytometry. Contour plots of CD80 and CD86 expression against HLA-DR expression and histograms showing CD80 and CD86 levels on control (media-treated) (black) and CHX treated (red) cells are shown. Isotype controls are shown in grey. Data are representative of two independent experiments. Graphical representation of the results of the two independent experiments are also shown.

Effect of MARCH transfection on the level of surface CD80 and CD86

To determine whether MARCH 1 or 8 ligases are able to affect the surface expression of CD80 and CD86; wildtype or mutant MARCH 1 or 8 ligase constructs were transfected into CHO-CD80, CHO-CD86 or CHO-CTLA4 cells and the surface level was measured. As shown in **Figure 10A**, four amino acid substitutions were made to generate the mutants. These cells were treated with media or MG132, an inhibitor of the 26S proteasome, for 4 hours, stained for the relevant surface protein and analysed by flow cytometry.

Figure 10B shows surface expression of CTLA-4 was not reduced in the MARCH transfected cells when compared to the untransfected cells. MG132 treatment of the MARCH transfected CHO-CTLA-4 cells led to a dramatic increase in the level of CTLA-4. This was as expected because CTLA-4 is known to be targeted for degradation by ubiqutination (Iida et al., 2000) and inhibition of the proteasome reduces the level of free ubiquitin. This therefore serves as a control for MG132 activity. There was a slight decrease in the level of CD80 compared to the untransfected cells but this was also seen in the cells transfected with the mutant. The level of CD86 on wildtype MARCH transfected cells was found to be considerably lower than on untransfected cells and this effect was not seen for cells transfected with the MARCH 1 and 8 mutants (**Figure 10B**). We also observed that treatment with MG132 was able to partially rescue the level of CD86 on the wildtype MARCH 1 and 8 transfected cells. Therefore overexpression of wildtype MARCH 1 or 8 led to a remarkable downregulation in the level of surface CD86 but not CD80 or CTLA-4 on CHO cells.

A

MARCH 1 WT: ^{61}DICRICHCEG DEESPLITPC RCTGTLRFVH QSCLHQWIKS SDTRCCELCK^{110}
MARCH 1 MUTANT: ^{61}DISRISHCEG DEESPLITPC RCTGTLRFVH QSCLHQWIKS SDTRCSELSK^{110}

MARCH 8 WT: ^{81}RICHCEGDDESPLITPCHCTQSLHFVHQACLQQWIKSSDTRCCELCKYEF^{130}
MARCH 8 MUTANT: ^{81}RISHSEGDDESPLITPCHCTQSLHFVHQACLQQWIKSSDTRCSELSKYEF^{130}

B

Untransfected
Control (transfected + media)
Transfected + MG132

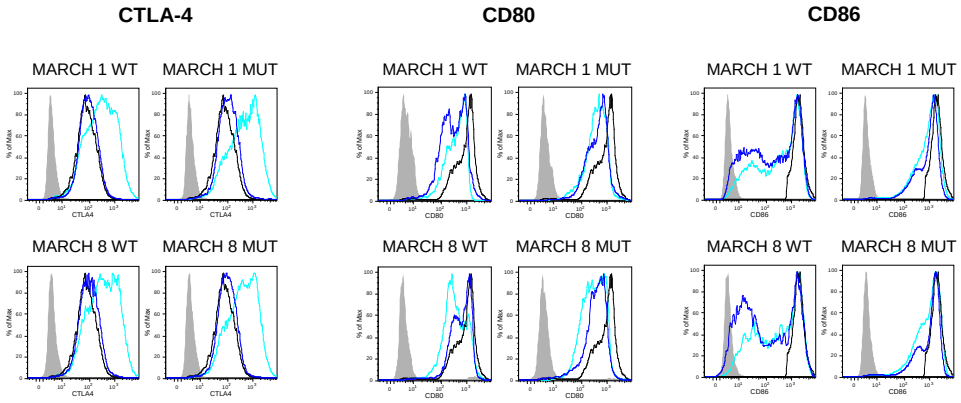

Figure 10: Effect of MARCH transfection on CTLA-4, CD80 and CD86 surface expression. MARCH transfected CHO-CTLA-4, CHO-CD80 and CHO-CD86 cells were pre-incubated with media or MG132 (10mM) for four hours at 37°C before being stained with PE-conjugated anti-CTLA-4, CD80 or CD86 and analysed by flow cytometry (A) Sections of peptide sequence from the MARCH constructs showing the differences between wildtype and mutant (B) Histograms of CTLA-4, CD80 and CD86 surface staining on MARCH transfected CHO-CTLA-4, -CD80 and –CD86 cells. The level of each surface protein on untransfected cells is shown in black, the level on the cells transfected with each MARCH ligase is shown in blue and the level on MG132 treated MARCH transfected cells is shown in cyan. Isotype controls are shown in grey.

Further investigations into the stability of surface and total CD86 on MARCH 1 and 8 transfected cells

To further investigate the effect of MARCH 1 expression on the surface level of CD86, MARCH 1 wildtype or mutant transfected cells were either treated with media, CHX, MG132 or Ammonium Chloride (NH_4Cl), an inhibitor of lysosomal degradation for 4 hours. Cells were stained for surface CD86 and analysed by flow cytometry. Transfection of CHO-CD86 cells with wildtype MARCH 1 led to a dramatic decrease in the surface level of CD86 compared to transfection with mutant MARCH 1 (**Figure 11A**). This was observed in the MARCH 1 positive population but not the MARCH 1 negative population of the transfected sample (**Figure 11B**) and was statistically significant ($P<0.001$) across three independent experiments. The level of CD86 expressed on the surface of the MARCH 1 positive population was found to be approximately 1.3% of the level expressed on the surface of the negative population within the same sample (**Figure 11C**).

Neither CHX nor NH_4Cl were found to affect the observed decrease in the surface level of CD86 (**Figure 11B and 11C**). In contrast the level of CD86 on the surface of the MG132 treated MARCH 1 positive cells was higher than the media-treated MARCH 1 positive cells (2.6% across three independent experiments) (**Figure 11B and 11C**). Therefore MARCH 1 overexpression led to a 98-99% downregulation in the level of surface CD86 which was rescued slightly by MG132.

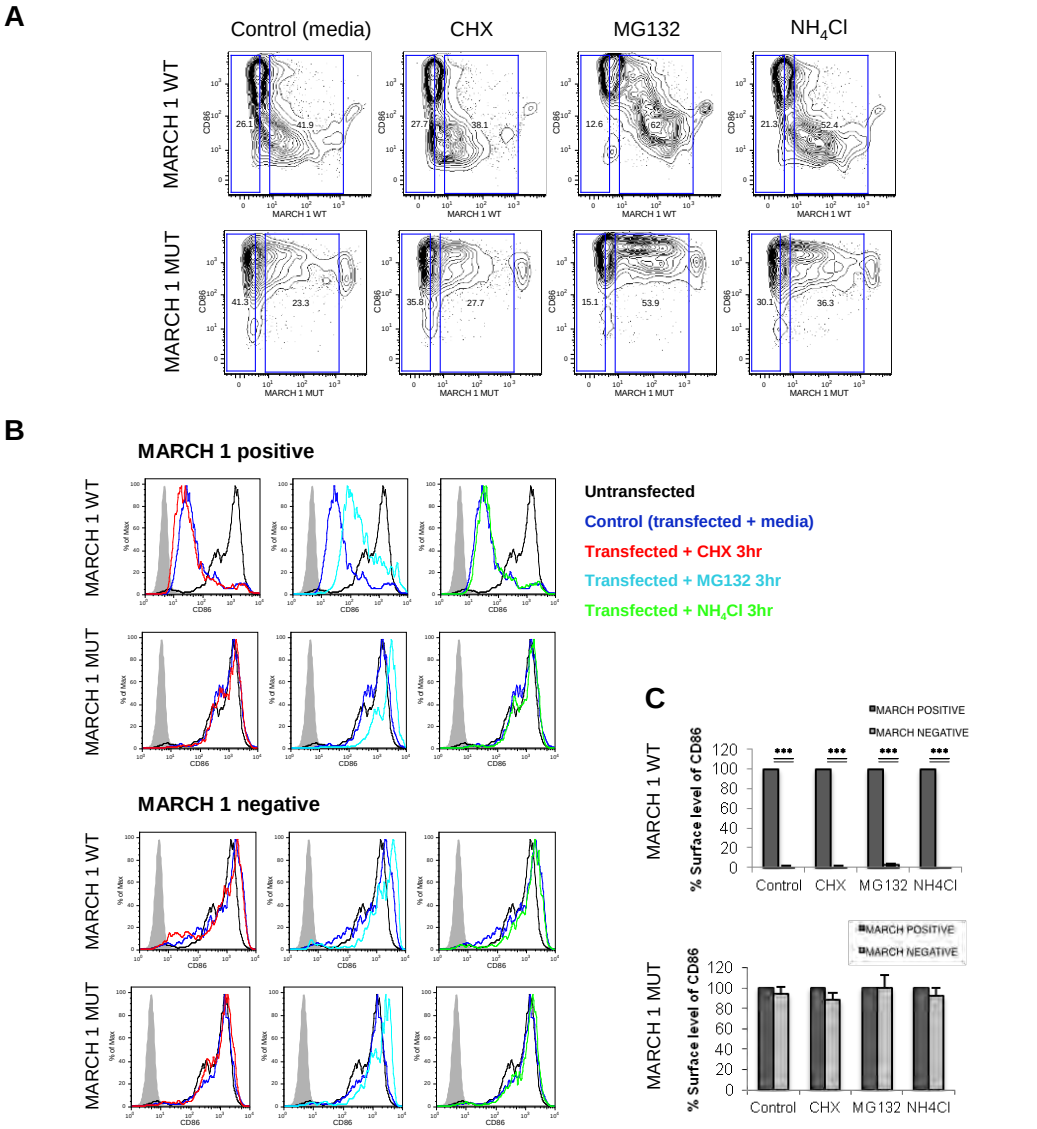

Figure 11: Effect of MARCH 1 transfection on CD86 surface expression. MARCH 1 wildtype and MARCH 1 mutant transfected CHO-CD86 cells were pre-incubated with media, 100µg/ml cyclohexamide (CHX), 10mM MG132 or 100mM Ammonium Chloride (NH_4Cl) for four hours at 37°C before being stained with PE-conjugated anti-CD86 and analysed by flow cytometry. (A) Contour plots of MARCH ligase against CD86 expression showing the MARCH positive and negative gates used. Data are representative of three independent experiments. (B) Histograms showing CD86 surface staining on MARCH 1 wildtype and mutant positive and negative CHO-CD86 cells. The level of CD86 on untransfected cells is shown in black, the level on the cells transfected with each MARCH ligase is shown in blue, the level on MG132 treated MARCH transfected cells is shown in cyan and the level on NH_4Cl treated MARCH transfected cells is shown in green. Isotype controls are shown in grey. (C) Graphical representations of the level of CD86 on the MARCH positive and negative cells within each transfected sample. Data is from three independent experiments.

To determine whether similar effects would be observed with MARCH 8 expression, MARCH 8 wildtype or mutant transfected cells were either treated with media, CHX, MG132 or Ammonium Chloride (NH_4Cl) for 4 hours. Cells were stained for surface CD86 and analysed by flow cytometry. We observed that MARCH 8 wildtype expression led to a reduction in surface expression of CD86, which was not observed for the mutant MARCH 8 (**Figure 12A**). This was not observed in the MARCH 8 mutant transfected cells or the MARCH 8 negative cells of the wildtype transfected sample (**Figure 12B**). This was statistically significant ($p<0.001$) across three independent experiments, where the surface levels of CD86 on the MARCH 8 wildtype positive cells were on average 1.2% of those on the MARCH 8 wildtype negative cells within the same sample (**Figure 12C**).

CHX treatment of wildtype transfected cells led to a greater reduction in surface CD86 compared to media-treated transfected cells (0.6% across three independent experiments) (**Figure 12B and 12C**). NH_4Cl had little effect but the level of CD86 on the surface of MG132 treated MARCH 8 positive cells was higher than on media-treated MARCH 8 positive cells (4.1% across three independent experiments) (**Figure 12B and 12C**). Therefore MARCH 8 overexpression leads to a 98-99% downregulation in the level of surface CD86, which was exacerbated by CHX and rescued slightly by MG132.

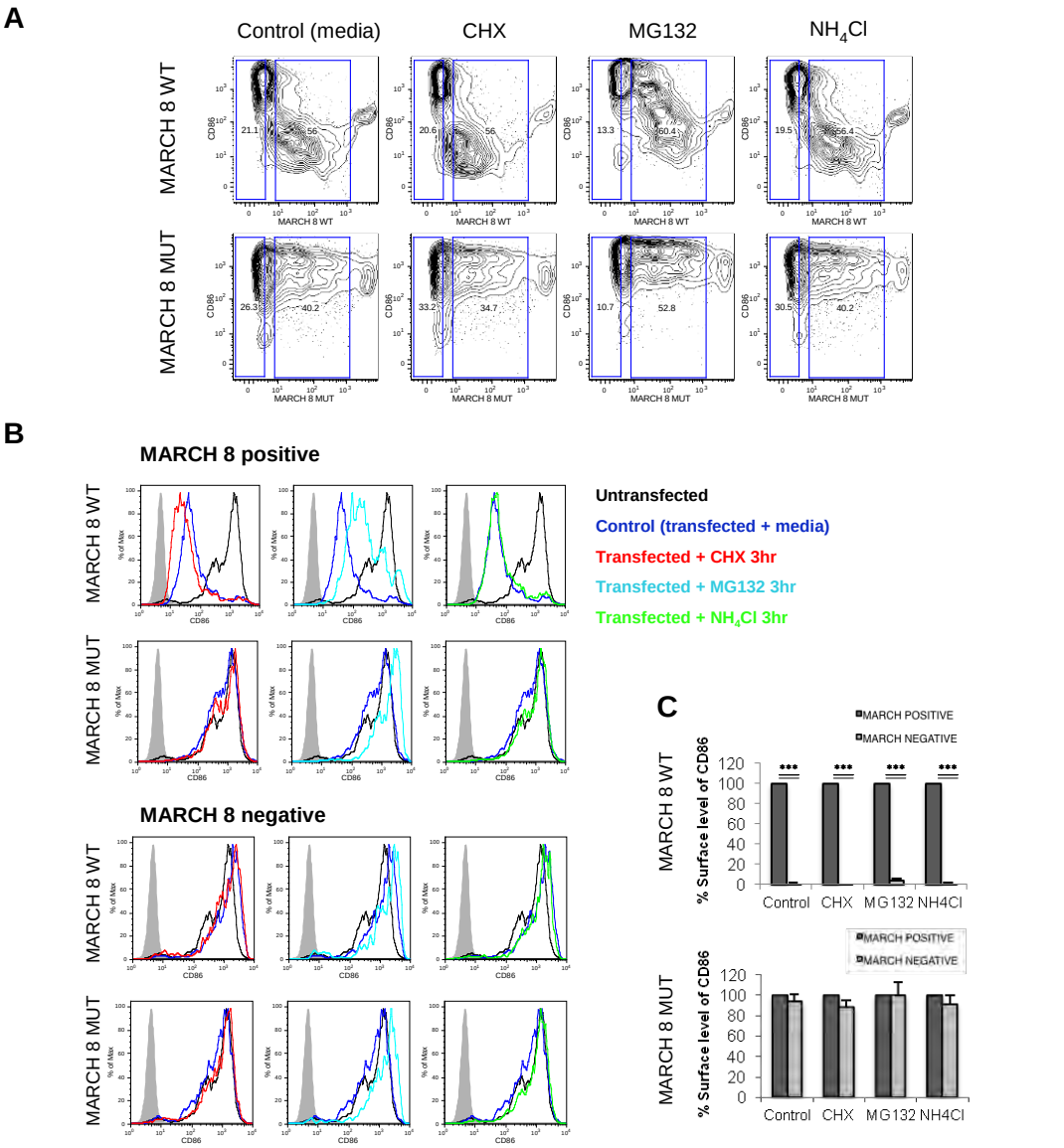

Figure 12: Effect of MARCH 8 transfection on CD86 surface expression. MARCH 8 wildtype and MARCH 8 mutant transfected CHO-CD86 cells were pre-incubated with media, 100µg/ml cyclohexamide (CHX), 10mM MG132 or 100mM Ammonium Chloride (NH_4Cl) for four hours at 37°C before being stained with PE-conjugated anti-CD86 and analysed by flow cytometry. (A) Contour plots of MARCH ligase against CD86 expression showing the MARCH positive and negative gates used. Data are representative of three independent experiments. (B) Histograms showing CD86 surface staining on MARCH 1 wildtype and mutant positive and negative CHO-CD86 cells. The level of CD86 on untransfected cells is shown in black, the level on the cells transfected with each MARCH ligase is shown in blue, the level on MG132 treated MARCH transfected cells is shown in cyan and the level on NH_4Cl treated MARCH transfected cells is shown in green. Isotype controls are shown in grey. (C) Graphical representations of the level of CD86 on the MARCH positive and negative cells within each transfected sample. Data is from three independent experiments.

To investigate whether a similar downregulation in CD86 would be observed on the total level of CD86 upon transfection, MARCH 1 wildtype or mutant transfected cells were either treated with media, CHX, MG132 or Ammonium Chloride (NH_4Cl) for 4 hours, before total staining was carried out and the levels of CD86 analysed by flow cytometry. We observed that MARCH 1 wildtype expression did indeed lead to a reduction in the total level of CD86 (**Figure 13A**). This was not observed in the MARCH 1 mutant transfected cells or the MARCH 1 negative cells of the wildtype transfected sample (**Figure 13B**). This was found to be statistically significant ($p<0.001$) across three independent experiments, where the total level of CD86 within the MARCH 1 wildtype positive cells was on average 27% of the total level within the MARCH 1 wildtype negative cells (**Figure 13C**).

CHX treatment of the MARCH 1 wildtype transfected cells was able to cause a further reduction in the level of CD86 (6.4% across three independent experiments) (**Figure 13B and 13C**). MG132 treatment of the MARCH 1 wildtype transfected cells had little effect on the total level of CD86. NH_4Cl treatment was able to partially rescue the total level of CD86 in one of the experiments however this was not reproducible across three independent experiments (**Figure 13B and 13C**). Therefore MARCH 1 overexpression leads to downregulation in the level of total CD86, which was exacerbated by CHX and may be rescued by NH_4Cl.

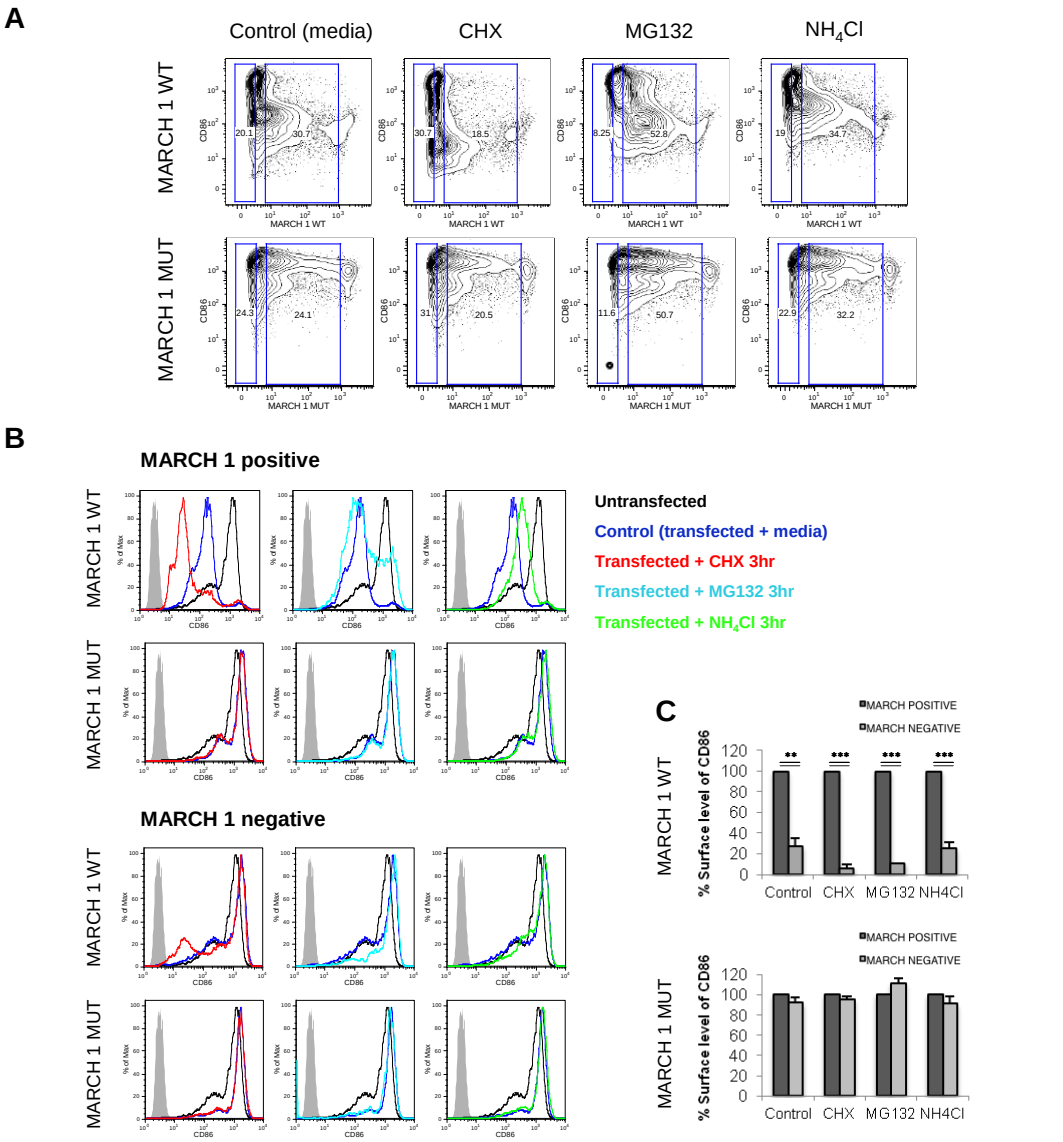

Figure 13: Effect of MARCH 1 transfection on total CD86 expression. MARCH 1 wildtype and MARCH 1 mutant transfected CHO-CD86 cells were pre-incubated with media, 100µg/ml cyclohexamide (CHX), 10mM MG132 or 100mM Ammonium Chloride (NH_4Cl) for four hours at 37°C before being fixed, permeabilized and stained with PE-conjugated anti-CD86 and analysed by flow cytometry. (A) Contour plots of MARCH ligase against CD86 expression showing the MARCH positive and negative gates used. Data are representative of three independent experiments. (B) Histograms showing CD86 staining in MARCH 1 wildtype and mutant positive and negative CHO-CD86 cells. CD86 expression for untransfected cells are shown in black, for cells transfected with each MARCH ligase CD86 expression is shown in blue and for MG132 or NH_4Cl treated MARCH transfected cells the level of CD86 expression is shown in cyan or green respectively. Isotype controls are shown in grey. (C) Graphical representations of the level of CD86 on the MARCH positive and negative cells within each transfected sample. Data is from three independent experiments.

To determine whether similar effects would be observed with MARCH 8 expression, MARCH 8 wildtype or mutant transfected cells were either treated with media, CHX, MG132 or Ammonium Chloride (NH_4Cl) for 4 hours. Cells were stained for total CD86 and analysed by flow cytometry. We observed that MARCH 8 wildtype expression did indeed lead to a reduction in the total level of CD86 (**Figure 14A**). This was not observed in the MARCH 8 mutant transfected cells or the MARCH 8 negative cells of the wildtype transfected sample (**Figure 14B**). This was found to be statistically significant across the three experiments ($p<0.001$), where the total level of CD86 within the MARCH 8 wildtype positive cells was on average 10% of the total level within the MARCH 8 wildtype negative cells (**Figure 14C**).

CHX treatment of the MARCH 8 wildtype transfected cells was able to cause a further reduction in the level of CD86 (**Figure 14B**). MG132 treatment had little effect on the level of CD86 but NH_4Cl was able to partially rescue the total level of CD86 in the MARCH 8 wildtype transfected cells. This was reproducible across the three experiments (**Figure 14B and 14C**) where the average level of total CD86 was 18%. Therefore MARCH 8 overexpression leads to downregulation in the level of total CD86, which was exacerbated by CHX and rescued by NH_4Cl.

Overall both MARCH 1 and 8 overexpression led to a 73-90% decrease in the level of CD86, both surface and total. This was exacerbated by CHX, the surface level was partially rescued by MG132 and the total level was partially rescued by NH_4Cl.

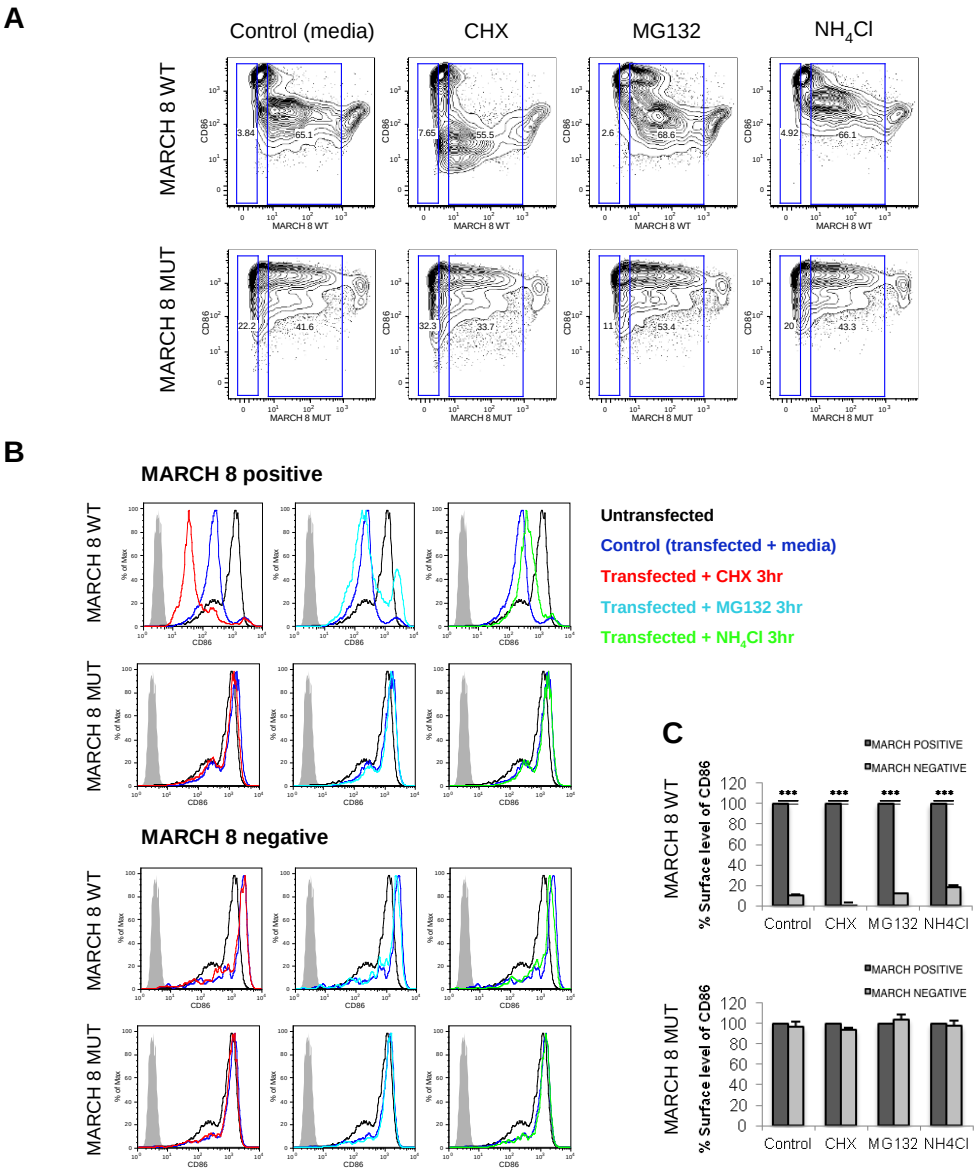

Figure 14: Effect of MARCH 8 transfection on total CD86 expression. MARCH 8 wildtype and MARCH 8 mutant transfected CHO-CD86 cells were pre-incubated with media, 100µg/ml cyclohexamide (CHX), 10mM MG132 or 100mM Ammonium Chloride (NH_4Cl) for four hours at 37°C before being fixed, permeabilized and stained with PE-conjugated anti-CD86 and analysed by flow cytometry. (A) Contour plots of MARCH ligase against CD86 expression showing the MARCH positive and negative gates used. Data are representative of three independent experiments. (B) Histograms showing CD86 staining in MARCH 1 wildtype and mutant positive and negative CHO-CD86 cells. CD86 expression for untransfected cells are shown in black, for cells transfected with each MARCH ligase CD86 expression is shown in blue and for MG132 or NH_4Cl treated MARCH transfected cells the level of CD86 expression is shown in cyan or green respectively. Isotype controls are shown in grey. (C) Graphical representations of the level of CD86 on the MARCH positive and negative cells within each transfected sample. Data is from three independent experiments.

Visualisation of the effect of MARCH 1 and 8 transfection on CD86 expression

To investigate whether this downregulation of CD86 upon transfection with MARCH 1 and 8 wildtype could be visualised, confocal microscopy was performed (**Figure 15**). CHO-CD86 cells were transfected with wildtype or mutant MARCH 1 or 8 and either treated with media, MG132 or NH_4Cl for 4 hours at 37°C. They were stained for total CD86 and visualised using the confocal microscope. We observed that the cells transfected with wildtype MARCH 1 or 8 expressed no surface CD86 whereas untransfected cells within the same sample expressed high levels of surface CD86 (**Figure 15A and 15B**). The level of surface CD86 also remained high in cells which were transfected with mutant MARCH 1 or 8. Quantification revealed that there was an inverse correlation between the level of wildtype MARCH 1 and CD86. Similarly it was evident that when the level of wildtype MARCH 8 expression was high the level of CD86 was low (**Figure 15B**). Neither MG132 nor NH_4Cl were able to prevent the downregulation of CD86. Therefore we confirmed by a second technique that MARCH 1 and 8 expression leads to a downregulation of CD86 in CHO-CD86 cells.

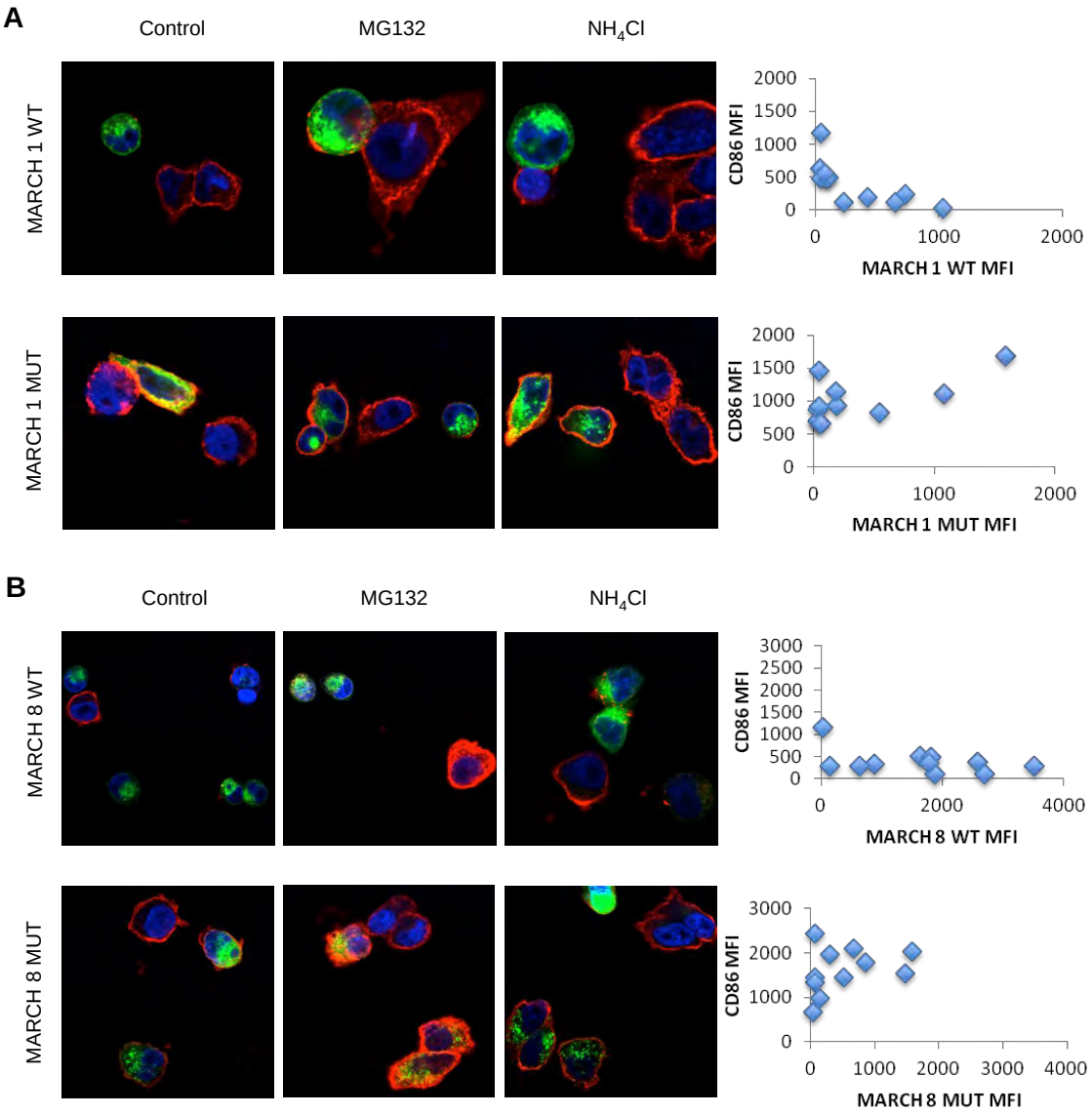

Figure 15: Visualisation of the effect of MARCH transfection upon CD86 expression. MARCH transfected CHO-CD86 cells were pre-incubated with media, MG132 (10mM) or NH_4Cl (100mM) for four hours at 37°C before being stained for CD86. (A) Confocal micrographs of GFP-tagged MARCH 1 wildtype or MARCH 1 mutant transfected CHO-CD86 cells. MARCH-GFP is shown in green and CD86-PE in red. (B) Confocal micrographs of GFP-tagged MARCH 8 wildtype or MARCH 8 mutant transfected CHO-CD86 cells. MARCH-GFP is shown in green and CD86-PE in red. All confocal images shown are representative of at least 5 micrographs. For quantification cells from four micrographs were outlined and mean fluorescence intensity (MFI) for GFP-tagged MARCH and CD86 staining was calculated and plotted graphically.

We also sought to determine whether CD86 is endocytosed in CHO-CD86 cells transfected with wildtype MARCH 1 and 8 (**Figure 16**). Transfected cells were incubated at 4°C with an unconjugated mouse anti-CD86 antibody, fixed, permeabilised and incubated with a fluorochrome conjugated anti-mouse antibody. These were visualized using the confocal microscope. Again we observed that there was no CD86 (red) on the surface of the MARCH 1 and 8 wildtype transfected cells. In addition colocalization between MARCH (green) and CD86 (red) within vesicles could be seen (orange) within these cells. In contrast cells transfected with the mutant MARCH ligases had high levels of surface CD86 expression and no colocalization was observed. This suggests that the MARCH 1 and 8 ligases interact with CD86 on the surface of CHO-CD86 cells, resulting in endocytosis of CD86.

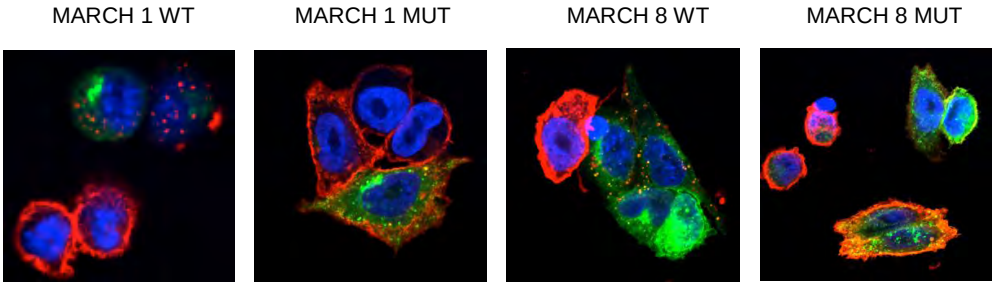

Figure 16: Endocytosis of CD86 from the surface of MARCH transfected CHO-CD86 cells. MARCH transfected CHO-CD86 cells were incubated with unconjugated mouse anti-CD86 at 37°C before being stained with a fluorochrome-conjugated anti-mouse antibody. Confocal micrographs of GFP-tagged MARCH 1 wt, MARCH 1 mutant, MARCH 8 wt and MARCH 8 mutant transfected cells are displayed. MARCH-GFP is shown in green and CD86-PE in red.

Detection of ubiquitinated CD86 in CHO-CD86 cells overexpressing MARCH 8 ligase

Previous research has shown that downregulation of both human and mouse CD86 upon MARCH 1 or 8 overexpression is ubiquitin dependent (Goto *et al.*, 2003; Baravalle *et al.*, 2011). We therefore sought to determine whether MARCH expression would lead to increased ubiquitination of CD86. A Western blot for ubiquitin was performed on samples containing surface or total CD86 from CHO-CD86 cells which had been transfected with MARCH 8 wildtype or MARCH 8 mutant (upper panel). To obtain surface CD86 only, the anti-CD86 antibody was added before cells were lysed and to obtain total CD86, cells were lysed before the antibody was added. **Figure 17** shows that we observed a denser band for ubiquitin in the MARCH 8 wildtype transfected sample containing total CD86 when compared to the untransfected and the mutant MARCH 8 transfected CHO-CD86 cells. The band for ubiquitinated surface CD86 in the MARCH 8 wildtype transfected sample was less dense. Levels of CD86 were found to be similar between all cell types (lower panel). The results of this figure indicate that MARCH 8 expression leads to increased ubiquitination of CD86.

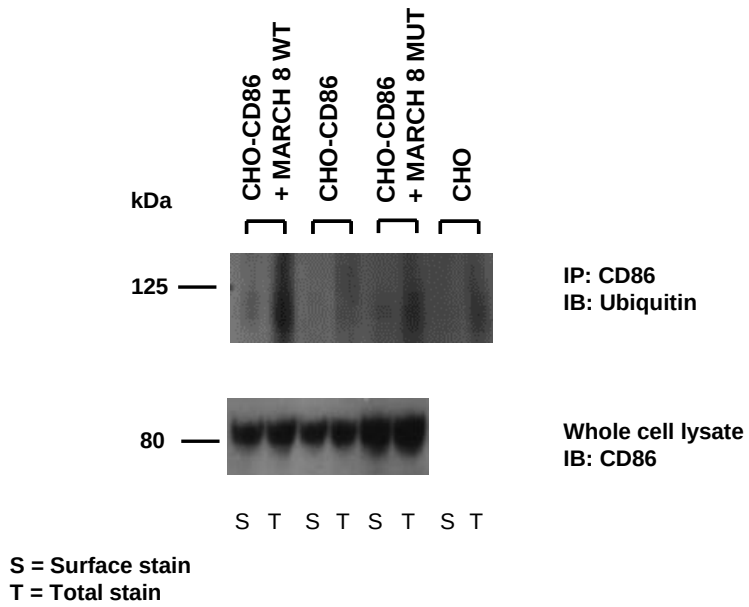

Figure 17: Ubiquitination of CD86 in cells overexpressing MARCH 8 ligase. CD86 was immuno-precipitated from MARCH 8 wildtype transfected CHO-CD86 cells, untransfected CHO-CD86 cells, MARCH 8 mutant transfected cells or untransfected CHO cells. This was done either before or after lysis to obtain surface or total CD86. The samples were then run on a polyacrylamide gel and a Western Blot was performed for ubiquitin (top panel). Whole cell lysates were also run and a Western Blot for CD86 was performed as a control for levels of CD86 (lower panel). IP: Immunoprecipitate; IB: Immunoblot.

DISCUSSION

The level of CD86 on the surface of an antigen presenting cell is crucial in determining whether a T cell is activated and is hence critical in maintaining the balance between hypo- and hyper-responsiveness of the immune system. We have observed that CD80 and CD86 are stable on the surface of CHO cells, human Akata B cells and human monocyes as well as MoDCs. It was expected that CD80 may be more stable than CD86 as it does not contain any lysine residues in its cytosolic tail and the literature suggests that it is not a target of MARCH 1 and 8 (Lapaque *et al.*, 2009). In addition as it is only expressed on the surface of DCs upon receipt of maturation stimuli there is no need for it to be downregulated on immature DCs.

The observed stability of CD86 was unexpected as MARCH 1 and 8 overexpression experiments in the recent literature show that CD86 is downregulated from the surface of the cell by these ligases (Goto *et al.*, 2003; Lapaque *et al.*, 2009). We therefore expected that a decrease in surface CD86 would be observed upon CHX treatment, much like for the degradation control, CTLA-4. Instead CD86 appears to have a slow turnover, so although new CD86 is not being synthesised the existing CD86 is not being degraded.

CD86 was also found to be relatively stable on the surface of immature and mature mouse BMDCs but not mouse B cells. However we cannot be confident at this stage that the apparent decrease in CD86 in the CHX treated cells is not due to upregulation of CD86 in the media treated cells. Additional repeats would need to be carried out with 4°C controls. In the HLA-DR^{hi} gated immature human monocytes there was a significant decrease in the level of surface CD86 expression upon CHX treatment but again 4°C controls would be needed to determine whether this shows CD86 instability.

The stability of CD86 observed is not in line with our hypothesis which was that CD86 would be unstable on the surface of immature APCs. A possible explanation may be that these cells do not express these MARCH ligases, however recent publications show that human B cells, monocytes and immature DCs do express MARCH 1 and 8 (Matsuki *et al.*, 2007; De Gassart *et al.*, 2008). In future we could determine MARCH 1 and 8 expression in our cells using PCR.

Alternatively the MARCH ligases may be present but could themselves be unstable and hence be sensitive to CHX. If this is the case the level of MARCH 1 and potentially MARCH 8 would decrease upon CHX treatment. Indeed Jabbor *et al.* (2009) showed that MARCH 1 has a half-life of 30 minutes and therefore has a high turnover. Interestingly the peak in CD86 surface levels on the Akata B cells after 2 hours of CHX treatment could potentially be explained by this CHX-sensitivity. However, when MARCH 1 and 8 transfected B cells were treated with CHX for 4 hours, the level of MARCH 1 and 8, which are tagged with GFP, did not decrease (unpublished data), which would suggest that these MARCH ligases are not unstable.

Another possible explanation for the observed stability of CD86 may be that the MARCH 1 and 8 ligases require accessory proteins to downregulate CD86 and that these proteins are sensitive to CHX. Indeed previous literature has suggested that MARCH 1 and 8 do not use a substrate specific motif because mouse MARCH 1 has been shown to be able to act upon human CD86, which shares little homology in the cytosolic region to mouse CD86 (Corcoran *et al.*, 2011). This group suggest that adapter molecules may be involved which facilitate the interaction between MARCH 1 and 8 and their substrates, perhaps by targeting them both to the same part of the membrane.

The results of the MARCH overexpression experiments suggest that, as hypothesised, human MARCH 1 and 8 can downregulate the surface level of human CD86 and are in

accordance with those of Lapaque *et al.* (2009), who used flow cytometry to observe a similarly dramatic decrease in surface CD86 but not CD80 levels upon transfection of a human melanoma cell line with MARCH 1 and MARCH 8. We were able to observe this both by flow cytometry and confocal microscopy. Like this group, we were able to show that MARCH 1 and 8 overexpression can also downregulate surface levels of HLA-DR (**Supplementary Figure 1**). It is interesting that although CTLA-4 has been shown to also be targeted for degradation by ubiquitination (unpublished data); overexpression of the MARCH ligases in CHO-CTLA-4 cells does not reduce the surface level of CTLA-4. This suggests either specificity of the ligases or their accessory proteins.

Previous research has shown that ubiquitination is necessary for downregulation of human surface CD86 upon MARCH 1 and 8 overexpression. The increased level of ubiquitinated CD86 observed in the CHO-CD86 cells which overexpress MARCH 8 indicates that CD86 is indeed ubiquitinated by the MARCH ligases. This effect was seen for total CD86 but not surface CD86 as we know from previous data that most of the CD86 would have been already removed from the surface. In addition no downregulation of CD86 was seen in response to transfection with the MARCH 1 and 8 mutant ligases and seeing as these are mutated in their RING-CH region, which confers their E3 ubiquitin ligase activity; this also suggests that ubiquitination is necessary for down regulation of CD86. The partial rescue in the surface level of CD86 seen with MG132, which reduces the level of free ubiquitin in the cell, would also suggest a role for ubiquitination. We would have expected MG132 to have rescued the surface level of CD86 more than it did, however it may be that it would have if added sooner after transfection. A partial rescue in the total level of CD86 was observed when cells were treated with NH_4Cl, which may add weight to the proposed mechanism that ubiquitination of CD86 by the MARCH ligases leads to endocytosis and degradation in the lysosome. However, this rescue was also only slight and at this point we cannot conclusively say whether CD86 is degraded in the lysosome, proteasome, or both.

This is to our knowledge, the first time that endocytosis of CD86, mediated by MARCH 1 and MARCH 8, has been observed via microscopy. The co-localization of these two proteins has previously been shown via immunoprecipitation (De Gassart *et al.*, 2008) and the kinetics of downregulation of CD86 in cells overexpressing CD86 have indicated that surface CD86 is endocytosed (Corcoran *et al.*, 2011) but these images provide clearer evidence. This will need to be repeated and investigated in greater detail before we can conclusively say that MARCH 1 and 8 induce endocytosis of CD86.

In terms of future work, we could establish a CHO cell line which expresses a tail-less mutant of CD86 (thus lacking lysine residues) and transfect these cells with the MARCH ligases to determine whether this would prevent the down regulation of CD86. This would allow us to further investigate the importance of ubiquitination. In addition it would be interesting to see if the tail-less CD86 and the MARCH ligases are able to associate with one another. It is curious that mouse MARCH 1 ligase can act upon human as well as mouse CD86 seeing as there is little homology between the cytosolic regions of CD86 between the two species (Corcoran *et al.*, 2009) and using this tail-less mutant would allow us to investigate which domains are important in this association. Previous work by Corcoran *et al.* (2009) has shown that the transmembrane region, as well as the cytosolic region is necessary for the interaction between MARCH 1 and CD86 in mice and it may be that this extends to human CD86 as well.

In addition, to further explore this system a CHO cell line could be established which expresses human CD83 as well as CD86. The MARCH ligases could then be transfected in and the level of CD86 measured by flow cytometry and confocal microscopy to determine whether human CD83 can inhibit the activity of the human MARCH 1 and 8 ligases, increasing the stability of CD86, as was indicated by Tze *et al.* (2011).

Understanding the threshold for T cell activation in humans is of vital importance to be able to treat autoimmune diseases such as Rheumatoid Arthritis; a condition in which autoreactive T cells drive tissue destruction in the joints. As binding of CD86 and CD80 to CD28 contributes signal two for T cell activation, maintaining the appropriate level of expression of these proteins on the surface of immature and mature antigen presenting cells is crucial in maintaining the balance of T cell activation versus T cell anergy. When considering regulation of the level of CD86 on the surface of the antigen presenting cells we must investigate post-translational as well as translational controls. The results of this report show that human CD86 is downregulated from the surface of a CHO cell line by expression of human MARCH 1 and 8 ligases and that this may be by inducing endocytosis of this co-stimulatory molecule. Much of the recent literature has used murine systems and centred upon MARCH 1, therefore this report provides valuable insight into the post-translational controls upon human CD86 expression within antigen presenting cells.

APPENDIX

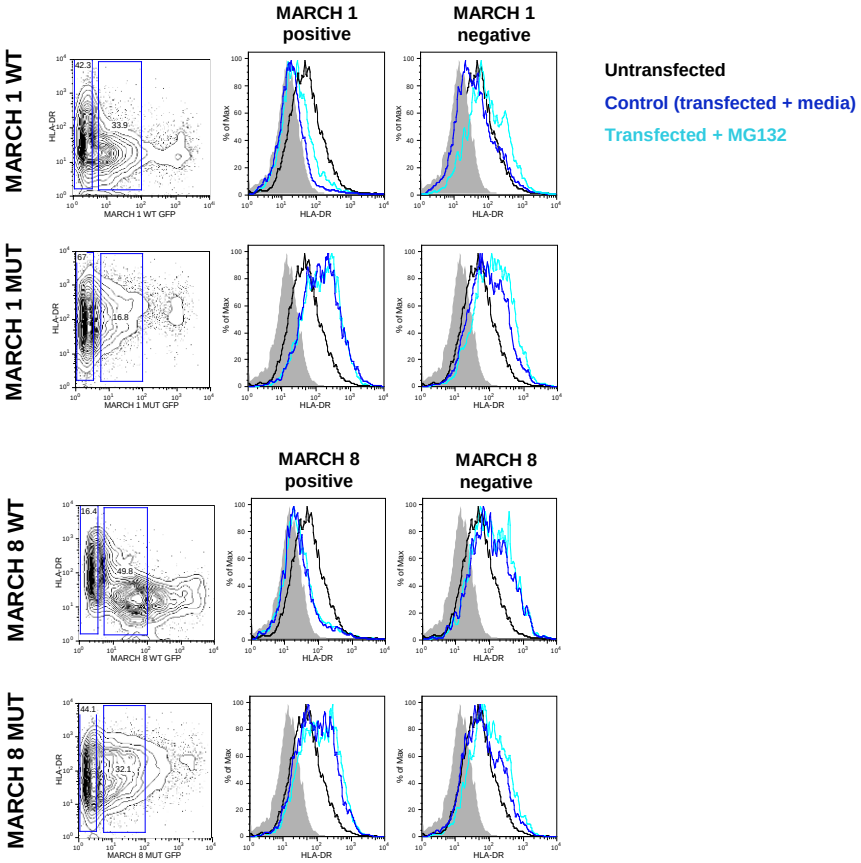

Supplementary Figure 1: Effect of MARCH transfection on HLA-DR surface expression. MARCH transfected CHO-HLA-DR cells were pre-incubated with media or MG132 (10mM) for four hours at 37°C before being stained with APC-conjugated anti-HLA-DR. The level of HLA-DR on untransfected cells is shown in black, the level on the cells transfected with each MARCH ligase is shown in blue and the level on MG132 treated MARCH transfected cells is shown in cyan. Isotype controls are shown in grey.

REFERENCES

Bartee, E., M. Mansouri, B. T. H. Nerenberg, K. Gouveia, and K. Fruh. 2004. Downregulation of major histocompatibility complex class I by human ubiquitin ligases related to viral immune evasion proteins. *J. Virol.* 78: 1109-1120.

Borgeois-Daigneault, M. C. and J. Thibodeau. 2012. Autoregulation of MARCH1 Expression by Dimerization and Autoubiquitination. *Journal of Immunology* 188: 4959–4970.

Borriello, F., M. P. Sethna, S. D. Boyd, A. N. Schweitzer, E. A. Tivol, D. Jacoby, T. B. Strom, E. M. Simpson, G. J. Freeman, and A. H. Sharpe. 1997. B7-1 and B7-2 have overlapping, critical roles in immunoglobulin class switching and germinal center formation.*Immunity* 6: 303-313.

Brunner, M. C., C. A. Chambers, F. K. M. Chan, J. Hanke, A. Winoto, and J. P. Allison. 1999. CTLA-4-mediated inhibition of early events of T cell proliferation. *Journal of Immunology* 162: 5813-5820.

Coscoy, L., D. Sanchez, and D. Ganem. 2001. A novel class of herpesvirus-encoded membrane-bound E3 ubiquitin ligases regulates endocytosis of proteins involved in immune recognition. *J. Cell Biol.* 155: 1265-1273.

Corcoran, K., M. Jabbour, C. Bhagwandin, M. J. Deymier, D. L. Theisen, and L. Lybarger. 2011. Ubiquitin-mediated Regulation of CD86 Protein Expression by the Ubiquitin Ligase Membrane-associated RING-CH-1 (MARCH1). *J. Biol. Chem.* 286: 37168-37180.

De Gassart, A., V. Camosseto, J. Thibodeau, M. Ceppi, N. Catalan, P. Pierre, and E. Gatti. 2008. MHC class II stabilization at the surface of human dendritic cells is the result of

maturation-dependent MARCH I down-regulation. *Proc. Natl. Acad. Sci. U. S. A.*105: 3491-3496.

Freeman, G. J., F. Borriello, R. J. Hodes, H. Reiser, J. G. Gribben, J. W. Ng, J. Kim, J. M. Goldberg, K. Hathcock, G. Laszlo, L. A. Lombard, S. Wang, G. S. Gray, L. M. Nadler, and A. H. Sharpe. 1993. Murine B7-2, an Alternative Ctla4 Counter-Receptor that Costimulates T-Cell Proliferation and Interleukin-2 Production. *J. Exp. Med.* 178: 2185-2192.

Goto, E., S. Ishido, Y. Sato, S. Ohgimoto, K. Ohgimoto, M. Nagano-Fujii, and H. Hotta. 2003. C-MIR, a human E3 ubiquitin ligase, is a functional homolog of herpesvirus proteins MIR1 and MIR2 and has similar activity. J. Biol. Chem. 278: 14657-14668.

Haase, C., T. N. Jorgensen, and B. K. Michelsen. 2002. Both exogenous and endogenous interleukin-10 affects the maturation of bone-marrow-derived dendritic cells in vitro and strongly influences T-cell priming in vivo. *Immunology* 107: 489-499.

Iida, T., H. Ohno, C. Nakaseko, M. Sakuma, M. Takeda-Ezaki, H. Arase, E. Kominami, T. Fujisawa, and T. Saito. 2000. Regulation of cell surface expression of CTLA-4 by secretion of CTLA-4-containing lysosomes upon activation of CD4(+) T cells. *Journal of Immunology* 165: 5062-5068.

Ikemizu, S., R. J. C. Gilbert, J. A. Fennelly, A. V. Collins, K. Harlos, E. Y. Jones, D. I. Stuart, and S. J. Davis. 2000. Structure and dimerization of a soluble form of B7-1. *Immunity* 12: 51-60.

Lapaque, N., J. L. Hutchinson, D. C. Jones, S. Meresse, D. W. Holden, J. Trowsdale, and A. P. Kelly. 2009. Salmonella regulates polyubiquitination and surface expression of MHC class II antigens.Proc. Natl. Acad. Sci. U. S. A. 106: 14052-14057.

Linsley, P. S., W. Brady, L. Grosmaire, A. Aruffo, N. K. Damle, and J. A. Ledbetter. 1991. Binding of the B-Cell Activation Antigen B7 to Cd28 Costimulates T-Cell Proliferation and Interleukin-2 Messenger-Rna Accumulation. *J. Exp. Med.* 173: 721-730.

Manzotti, C. N., M. X. P. Liu, F. Burke, L. Dussably, Y. Zheng, and D. M. Sansom. 2006. Integration of CD28 and CTLA-4 function results in differential responses of T cells to CD80 and CD86. *Eur. J. Immunol.* 36: 1413-1422.

Masteller, E. L., E. Chuang, A. C. Mullen, S. L. Reiner, and C. B. Thompson. 2000. Structural analysis of CTLA-4 function in vivo. *Journal of Immunology* 164: 5319-5327.

Matsuki, Y., M. Ohmura-Hoshino, E. Goto, M. Aoki, M. Mito-Yoshida, M. Uematsu, T. Hasegawa, H. Koseki, O. Ohara, M. Nakayama, K. Toyooka, K. Matsuoka, H. Hotta, A. Yamamoto, and S. Ishido. 2007. Novel regulation of MHC class II function in B cells. *EMBO J.* 26: 846-854.

Mead, K. I., Y. Zheng, C. N. Manzotti, L. C. A. Perry, M. K. P Liu, F. Burke, D. I. Powner, M. J. O. Wakelam and D. M. Sansom. 2005. Exocytosis of CTLA-4 is dependent on phospholipase D and ADP ribosylation factor-1 and stimulated during activation of regulatory T cells. *J. Immunol.* 174(8)4803-4811.

Pickart, C. M. 2001. Mechanisms underlying ubiquitination. *Annu. Rev. Biochem.* 70: 503-533.

Qureshi, O. S., Y. Zheng, K. Nakamura, K. Attridge, C. Manzotti, E. M. Schmidt, J. Baker, L. E. Jeffery, S. Kaur, Z. Briggs, T. Z. Hou, C. E. Futter, G. Anderson, L. S. K. Walker, and D. M. Sansom. 2011. Trans-Endocytosis of CD80 and CD86: A Molecular Basis for the Cell-Extrinsic Function of CTLA-4. *Science* 332: 600-603.

Sansom, D. M. 2000. CD28, CTLA-4 and their ligands: who does what and to whom? *Immunology* 101: 169-177.

Sansom, D. M., C. N. Manzotti, and Y. Zheng. 2003. What's the difference between CD80 and CD86? *Trends Immunol.* 24: 314-319.

Thery, C. and S. Amigorena. 2001. The cell biology of antigen presentation in dendritic cells. *Curr. Opin. Immunol.* 13: 45-51.

Thibodeau, J., M. Bourgeois-Daigneault, G. Huppe, J. Tremblay, A. Aumont, M. Houde, E. Bartee, A. Brunet, M. Gauvreau, A. de Gassart, E. Gatti, M. Baril, M. Cloutier, S. Bontron, K. Frueh, D. Lamarre, and V. Steimle. 2008. Interleukin-10-induced MARCH1 mediates intracellular sequestration of MHC class II in monocytes. *Eur. J. Immunol.* 38: 1225-1230.

Walseng, E., K. Furuta, B. Bosch, K. A. Weih, Y. Matsuki, O. Bakke, S. Ishido, and P. A. Roche. 2010. Ubiquitination regulates MHC class II-peptide complex retention and degradation in dendritic cells. *Proc. Natl. Acad. Sci. U. S. A.* 107: 20465-20470.

Zhang, X., J. Schwartz, S. Almo, and S. Nathenson. 2003. Crystal structure of the receptor-binding domain of human B7-2: Insights into organization and signaling. *Proc. Natl. Acad. Sci. U. S. A.* 100: 2586-2591.

Zhong, G. M., P. Romagnoli, and R. N. Germain. 1997. Related leucine-based cytoplasmic targeting signals in invariant chain and major histocompatibility complex class II molecules control endocytic presentation of distinct determinants in a single protein.*J. Exp. Med.* 185: 429-438.

Emily Halford

Project 2:

What is the Role of Lyp Phosphatase (PTPN22) in Phagocyte Signaling?

This project is submitted in partial fulfilment of the requirements for the award of the MRes

ABSTRACT

Background: A variant of lymphoid phosphatase (Lyp) (R620W) is associated with a broad range of autoimmune diseases and research has focused on its effect in T cells. However, phagocytes such as macrophages express higher levels of Lyp than T cells but little is known about the function of Lyp in these cells.

Methods: We used shRNA to knock down Lyp expression and an inhibitor to manipulate its activity in monocytic cell lines. We investigated the effect of this inhibitor on signaling through Toll-like Receptors and Fc Receptors as well as downstream effects including calcium flux and superoxide production.

Results: Attempts at knockdown were not successful, perhaps due to the toxicity of the selection antibiotic and the known difficulty of transfecting monocytic cells. Assessing calcium signals after CD32 (FcRγII) crosslinking was inconsistent, perhaps due to changes in expression/responses in the cell lines used. However, inhibition of Lyp increased the basal level of superoxide production within these cells. Further work is needed to expand this data.

Conclusion: The results suggest that Lyp may regulate production of cytotoxic mediators, such as superoxide in phagocytes. Dysregulation of this process, through expression of the Lyp variant in autoimmune disease may exacerbate inflammation and tissue damage.

ACKNOWLEDGEMENTS

Thank you to Dr Steve Young for providing such excellent and hands-on supervision. Thank you to Team Young for all their help, especially Rachel Bayley for teaching me the phosphatase assay and Western Blotting. Thank you to Dr Omar Qureshi for allowing me to use his electroporation equipment and to Dr Gillian McNab for showing me how to perform a plasmid extraction despite there being no obligation to do so. Thank you to the Rheumatology Research Group for being so welcoming (and for providing so much cake); it was a pleasure to be part of the group.

CONTENTS

LIST OF FIGURES

INTRODUCTION

The role of Lyp

Lymphoid phosphatase (Lyp) is a 105kDa protein encoded by the gene PTPN22 which is located at 1p13.1 (Cohen et al, 1999). It is a member of the protein tyrosine phosphatase (PTP) family of proteins which dephosphorylate tyrosine residues on their substrates (Fischer *et al.*, 1991). Phosphorylation is a post-translational modification which involves the addition of a phosphate to a protein substrate and is carried out by Protein Tyrosine Kinases (PTKs). As such phosphorylation is a key mechanism of signal transduction (Cohen *et al.*, 1999).

Lyp consists of an N-terminal catalytic domain, an interdomain and a C terminal portion containing four proline rich motifs termed P1-P4 (Vang *et al.*, 2007). Lyp is an intracellular phosphatase (Cohen *et al.*, 1999) and is found only in cells of haematopoietic origin. Upon initial characterization Lyp was found to be predominantly expressed in lymphoid tissues and cells (Cohen *et al.*, 1999) but it has subsequently been shown to be expressed at higher levels in neutrophils and monocytes than it is in T cells, as shown in **Figure 1** (Chien *et al.*, 2003).

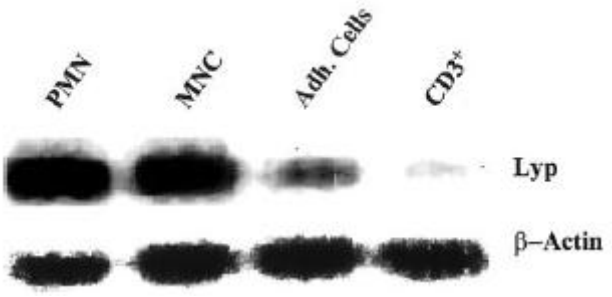

Figure 1: Lyp expression within polymorphonuclear neutrophils (PMN), mononuclear cells (MNC), adherent cells (Adh. Cells), and T cells ($CD3^+$) (Chien et al., 2003).

Much of what we understand about Lyp has emerged from studies of the mouse homolog, PEP (proline-, glutamic acid-, serine-, and threonine-rich [PEST]-domain Phosphatase), which is encoded by PTPN8. Lyp and PEP share 89% homology between their catalytic domains and 61% homology within their non-catalytic domains (Cohen *et al.*, 1999).

PTPs play a largely negative regulatory role in T cell activation (Iivanainen *et al.*, 1990) and indeed Lyp has been found to act as a negative regulator of signaling through the T cell Receptor (TCR) complex (Cloutier and Veillette, 1999). When a TCR recognises a Major Histocompatibility Complex (MHC) class II-peptide complex on the surface of an antigen presenting cell, CD45 dephosphorylates the inhibitory tyrosine residue of p56lck (Lck) and p59fyn (Fyn) which are Src family kinases (Mustelin *et al.*, 2005). Lck and Fyn initiate TCR signaling by phosphorylating the immunoreceptor tyrosine-based activation motifs (ITAMs) of CD3γ, CD3δ, CD3ε and TCRζ, which are chains of the TCR complex (Wange and Samelson, 1996). This creates binding sites for Src homology (SH) 2-domain containing proteins such as ZAP-70, which is also activated by Lck/Fyn. ZAP-70 binds the phosphorylated ITAM via its SH2 domain and then goes on to phosphorylate further signaling molecules, hence amplifying the signal and ultimately resulting in IL-2 gene expression.

Lyp negatively regulates Lck by dephosphorylating its activating tyrosine residue; Tyr-394 (Wu *et al.*, 2006). Lyp also interacts with the SH3 domain of a tyrosine kinase called Csk (P50csk) (C-terminal Src tyrosine kinase) via its P1 domain. This interaction is thought to target Lyp to the membrane so that it is in close proximity to Lck as Csk can bind PAG (phosphoprotein associated with glycosphingolipid-enriched membrane microdomains) (Brdicka *et al.*, 2000). In addition Csk is able to phosphorylate Lck on its inhibitory tyrosine residue; Tyr-505 (Gregersen and Batliwalla, 2005) and studies with PEP have shown that Csk and Lyp/PEP may act synergistically in this way to inhibit T cell signaling (Cloutier and Veillette, 1999; Gjorloff-Wingren *et al.*, 2000) and therefore increase the threshold for T cell activation. **Figure 2** depicts the process by which Lyp and Csk inactivate Lck. As a

mechanism of negative feedback Lck has been shown to phosphorylate Lyp (Fiorillo *et al.*, 2010) and phosphorylation of Lyp by Protein kinase C (PKC) leads to its inactivation (Yu *et al.*, 2007).

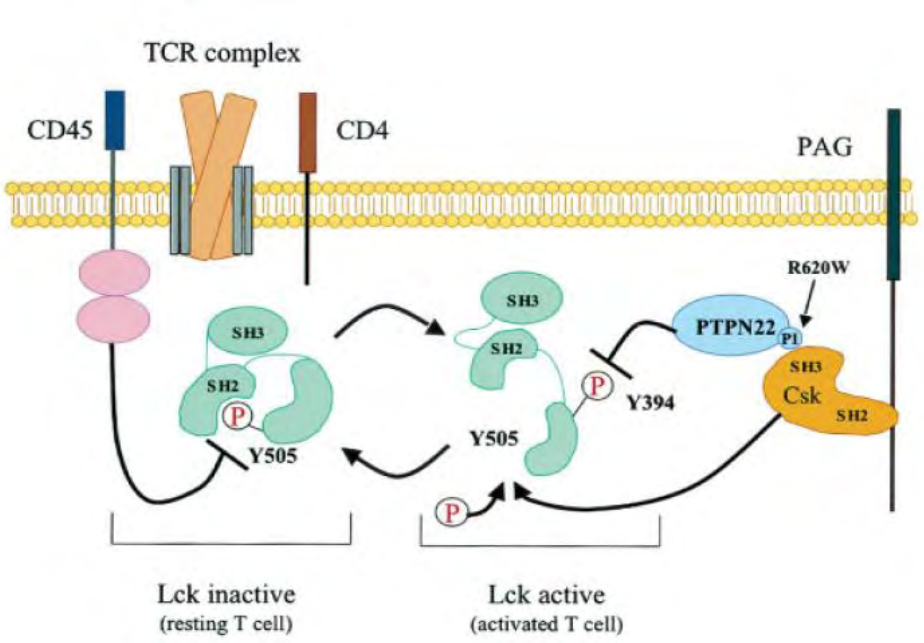

Figure 2: The role of Lyp within TCR signaling (Gregersen and Batliwalla, 2005)

Association of the R260W variant with Autoimmune Disease

In 2004 a single nucleotide polymorphism (SNP), 1858T, within PTPN22 which is linked with type 1 diabetes was discovered via a candidate gene approach (Bottini et. al). Autoimmune diseases such as type 1 diabetes are chronic inflammatory conditions which affect 3-5% of the population and occur as a result of recognition of self-antigen by autoreactive lymphocytes (Marrack *et al.*, 2001). This SNP leads to a missense mutation, in the form of an amino acid change from arginine (R) to tryptophan (W) at codon 620 (R620W). This variant was subsequently found to be associated with another autoimmune disease; rheumatoid arthritis (RA), with around 28% of white individuals with RA and 17% of white individuals without RA possessing the variant (Begovich *et al.*, 2004). The variant has also been found to be associated with further autoimmune diseases such as systemic lupus erythamatosus

(Kyogoku *et al.*, 2004) and Graves' disease (Velaga *et al.*, 2004) and therefore it has been termed a "shared autoimmunity" gene (Bottini *et al.*, 2006). Interestingly this fits in with the concept that common mechanisms lead to autoimmune disease (Gregersen and Batliwalla, 2005). However, the variant is not associated with multiple sclerosis (Begovich *et al.*, 2005) or Crohn's disease (Van Oene *et al.*, 2005). It may be that the variant only predisposes to autoimmune diseases in which autoantibodies have a prominent role rather than those which are largely T cell mediated such as multiple sclerosis and Graves disease.

In many PTPN22 R620-associated autoimmune diseases PTPN22 is the strongest genetic component outside the Major Histocompatibility Complex (MHC) complex, which is also a shared autoimmunity gene (Vang *et al.*, 2008) and therefore it would potentially be of use as a prognostic factor. The association has been found to be dose-dependent with homozygotes being at greater risk than heterozygotes of developing autoimmune disease such as rheumatoid factor positive RA (Lee *et al.*, 2005). Recently a loss of function mutation in PTPN22, R263Q, has been shown to be protective against systemic lupus erythematous (Orru *et al.*, 2009).

Potential mechanism by which the R260W variant is associated with Autoimmune Disease

A considerable amount of research has been carried out into the role of Lyp in T cells, but little is understood about its role in phagocytes, such as monocytes, macrophages and neutrophils, despite the high level of expression within these cells.

Phagocytes recognise pathogen-associated molecular patterns, such as LPS, a component of the cell wall of gram negative bacteria, using pathogen recognition receptors such as Toll-like receptors. In response to this these cells phagocytose and destroy pathogens using cytotoxic mediators, and release pro-inflammatory mediators such as cytokines and chemokines (Mosser and Edwards, 2008). Through the release of such mediators

phagocytes are believed to contribute to the pathogenesis of autoimmune diseases such as rheumatoid arthritis and therefore it is crucial that we understand the role of Lyp in these cells and can therefore explore the consequences of the variant.

The existing knowledge of the role of Lyp within T cells and the consequences of the variant within these cells and potentially B cells may give an indication as to its role in phagocytes such as macrophages. There are two main hypotheses about the effect of the variant which are the loss of function (LOF) and the gain of function (GOF). Both hypotheses will be explored within this report.

Hypothesis 1: Loss of function

The substitution of the arginine encoded by codon 260 to a tryptophan (R260W) in the variant is thought to disrupt the interaction between the P1 motif of Lyp and the SH3 domain of Csk (Bottini *et al.*, 2004; Begovich *et al.*, 2004). This would then hinder the inhibition of Lck by Lyp as it could no longer be targeted to the plasma membrane by Csk. Therefore R260W has been described as a loss of function (LOF) mutation. Indeed overexpression of wildtype Lyp in the context of Csk has been shown to lead to co-operative inhibition of TCR signaling and this is less so when R620W Lyp is overexpressed in this context (Zikherman *et al.*, 2009).

Loss of regulation of Lck activity would lead to increased phosphorylation of downstream targets such as PLC-γ1, resulting in lowering of the threshold for activation and therefore to T cell hyper-responsiveness. This could result in an increased likelihood of mounting an auto-immune response following immune stress such as viral infection. Indeed PEP deficient mice have been shown to exhibit enhanced phosphorylation of Lck and on a global scale an enhanced effector/memory T cell pool as well as an enlarged spleen and lymph nodes, although they do not develop autoimmune disease (Hasegawa *et al.*, 2004). Interestingly it

has been shown that if these mice also have the CD45 E613R allele then autoimmunity develops (Zikherman *et al.*, 2009).

There is a PEP variant (612W) which is very similar to the R620W variant of Lyp and studies with this variant have shown that it is degraded much more rapidly than wildtype PEP (Zhang *et al.*, 2011). As a consequence there would be lower levels of PEP protein which would lead to reduced inhibition of Lck and hence TCR signaling. This group then went on to show that levels of the variant form of Lyp were lower in human T and B cells than the wildtype form. However, this does not appear to be the case in human primary T cells, where levels of wildtype and variant PTPN22 mRNA are similar (Nielson *et al.*, 2007).

Hypothesis 2: Gain of function

In 2005 it was shown that the variant Lyp exhibits increased phosphatase activity therefore R620W may in fact be a gain of function (GOF) mutation (Vang *et al.*). This would suggest that there is increased inhibition of Lck and therefore decreased signaling through the T cell receptor. However, as previously discussed the variant is associated with aberrant T cell responses and this study showed that there was increased production of cytokines after T cell signaling in cells expressing the variant. When put into the context of T cell development this apparent paradox becomes clearer as decreased signaling through the TCR would lead to a greater number of auto-reactive cells escaping negative selection. Negative selection ensures that thymocytes which react strongly to self-antigens are deleted during development in the thymus. This is known as central tolerance and is a safeguard against autoimmunity. **Figure 3** shows that the presence of the R620W variant would lead to more T cells entering the periphery with moderate affinity for self and therefore would increase the risk of autoimmune disease developing. This hypothesis infers that it is the global effects of the SNP on the T cell pool rather on individual T cells which leads to the predisposition to autoimmune disease. Interestingly this may suggest that the reason that the PTPN22 variant

has been retained through evolution is that it enhances the T cell pool and hence the potential to respond to a greater variation of antigens. This could translate to enhanced defence against infection.

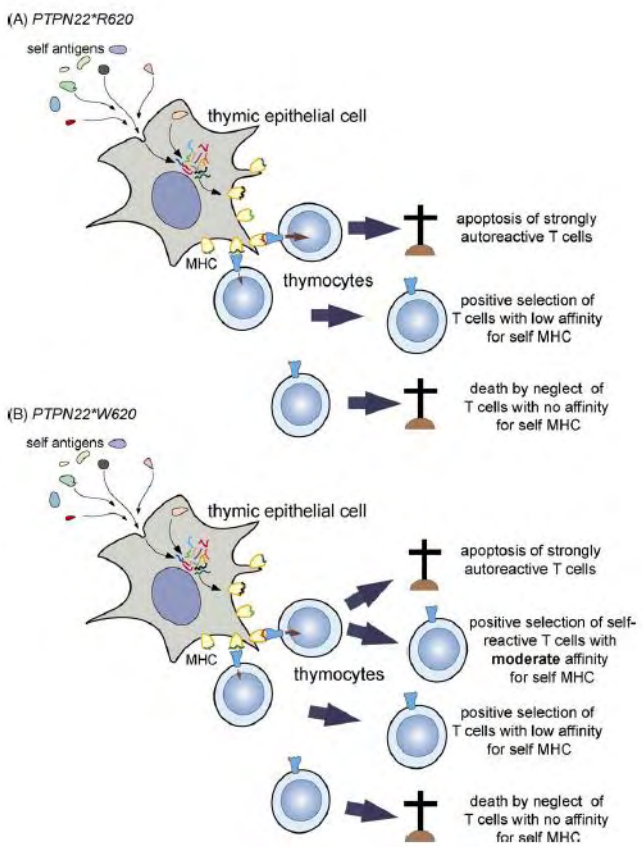

Figure 3: The effect of the variant on negative selection within the thymus (Bottini et al., 2006)

Another effect of the GOF mutant may be that this shift in the threshold for TCR activation reduces the functionality of regulatory T cells (Tregs). This would hinder suppression of auto-reactive T cells; a mechanism of peripheral tolerance. However PTPN22 deficient Tregs were not found to exhibit enhanced suppressive ability. Instead levels of Tregs were increased in the thymus as well as the periphery of PTPN22 deficient mice (Maine *et al.*, 2012). Tregs cells require a greater signal during development in the thymus (Wong *et al.*,

2001) and therefore a consequence of the GOF mutant may be that the number of Tregs in the periphery is reduced and hence peripheral tolerance is impaired.

The GOF hypothesis was given another dimension in 2010 when it was suggested that Lyp and Lck form a constitutive complex, facilitated by Csk, as is shown in **Figure 4**. This group therefore suggested that the reason for the gain of function was that the reduced interaction between the Lyp variant and Csk led to decreased phosphorylation of Lyp on its inhibitory tyrosine residue (Tyr-536) by Lck (Fiorillo *et al.*, 2010). This decreased inhibition of Lyp by Lck would then lead to increased phosphatase activity. However, preventing interactions between Lyp and Lck would also prevent dephosphorylation of Lck by Lyp and therefore this hypothesis requires further investigation.

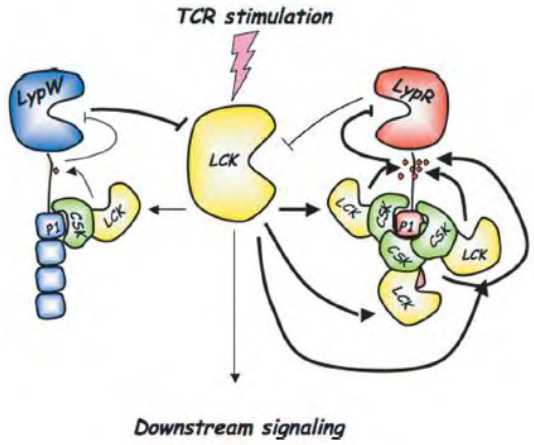

Figure 4: Effect of the variant on the negative feedback mechanism utilised by Lck. The presence of the variant Lyp disrupts the constitutive complex formed by wildtype Lyp, Csk and Lck and hence prevents inhibition of Lyp by Lck (Fiorillo et al 2010).

A recent paper has also proposed that Lyp and Csk form a constitutive complex and that in fact dissociation of Lyp from Csk is necessary for it to move to the membrane where it dephosphorylates Lck (Vang *et al.*, 2012). This contradicts the early LOF model and would

then mean that the variant Lyp exhibits increased phosphatase activity because the reduced association with Csk means that the variant Lyp can readily gain access to Lck.

The effect of the variant in B cells

The effects of the Lyp variant on B cells are not as well elucidated. PEP deficient mice have been shown to exhibit increased antibody production (Hasegawa *et al.*, 2004) and a recent meta-analysis has shown that the variant is significantly more prevalent in rheumatoid factor-positive than –negative RA (Lee *et al.*, 2012). There is however the possibility that any alterations in B cell activity are as a result of altered T cell help (Vang *et al.*, 2008).

Interestingly a recent study showed that possessing the variant increases an individual's likelihood of developing invasive pneumococcal infections or Gram positive empyema (Chapman *et al.*, 2006). As suggested by Vang *et al.* (2008) this could be due to effects of the variant in B cells, which result in reduced autoantibody production or in Neutrophils which are an important first line of defence to bacteria.

Potential targets of Lyp within phagocytes

To build on this knowledge about the role of Lyp it is useful to think about the targets of Lyp/PTP other than Lck, Fyn and ZAP-70 and whether they could have a role in phagocytes. These include CD3ε and TCRζ which are components of the TCR complex, a guanine nucleotide exchange factor called Vav1, and valosin-containing protein (VCP) which is an ATPase (Cloutier and Veillette, 1999; Wu *et al.*, 2006). The TCR complex is restricted to T cells and ZAP-70 is exclusively expressed in T cells and NK cells (Chan *et al.*, 1992). Similarly Lck and Fyn are predominantly expressed in T cells (Marth and Veillette, 1989).

VCP, on the other hand, is ubiquitously expressed (Wang *et al.*, 2003) and is involved in many cellular processes such as cell cycle control (Cao *et al.*, 2003). Indeed depletion of

VCP mRNA in HeLa cells has been shown to lead to reduced proliferation and increased apoptosis (Wojcik *et al.*, 2003). Therefore it has been suggested that VCP is important for cell proliferation and survival, particularly in T cells as VCP is phosphorylated during TCR signaling (Wu *et al.*, 2006). It may be that VCP is also involved in the proliferation and survival of phagocytes and that Lyp is involved in regulating this process.

Vav1 is also ubiquitously expressed in hematopoietic cells (Raab *et al.*, 1997), where it acts as a guanine nucleotide exchange factor for Rac and Rho (cdc42) which are small GTPases (Wu *et al.*, 2006). During TCR signaling in T cells, Vav1 becomes phosphorylated and is then able to activate Rac and Rho, which are involved in the actin cytoskeleton remodelling necessary for formation of the immunological synapse (Sechi and Wehland, 2004). The immunological synapse (IS) is formed when an MHC class II-peptide complex on an APC interacts with the TCR of a T cell and facilitates the sustained interaction that is necessary for T cell activation. Formation of the IS involves actin cytoskeleton remodelling such that clustering of MHC-peptide, TCR, co-receptors and co-stimulatory molecules occurs (Bromley *et al.*, 2004).

Vav1 has also been shown to play a role in phagocytosis (Patel *et al.*, 2002; Hall *et al.*, 2006), another process that requires actin cytoskeletal remodelling. Phagocytosis is the process of engulfing particles such as bacteria which are opsonised by antibodies or complement by phagocytes such as macrophages. It requires binding of either Fc Receptors (FcR) or complement receptors (CR3) to the opsonised particles and subsequent actin rearrangement such that phagocytic cup formation occurs. It results in destruction of the phagocytosed material by reactive oxygen and nitrogen species (ROS), reactive nitrogen species (RNS) and proteolytic enzymes and is therefore a mechanism of defence against infection. In addition the phagocytosis and destruction of cellular debris by M2 macrophages is an essential mechanism of repair and resolution (Mosser and Edwards, 2008).

Interestingly Vav1 has been shown to be necessary for FcγRII (CD32)-mediated phagocytosis in a macrophage cell line (Patel *et al.*, 2002) as well as primary murine macrophages (Hall *et al.*, 2006). This is again thought to be via activation of Rac, which then participates in the actin cytoskeleton remodelling necessary for phagocytosis. This is shown in **Figure 5** and may mean that Lyp is a regulator of phagocytosis within macrophages.

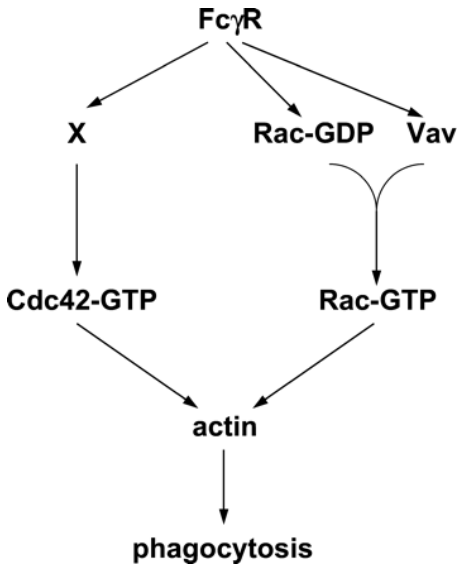

Figure 5: The process by which FcR (CD32) signaling results in phagocytosis (Patel et al., 2002).

Taking the findings of the recent literature into account we hypothesise that Lyp has a role in regulating the functional consequences of FcR and perhaps TLR signaling in macrophages, such as phagocytosis.

The aims of this study are:

- To study the effects of Lyp depletion/inhibition on signaling through FcRs and TLRs in monocytic cell lines
- To study the effects of Lyp depletion/inhibition on the functional consequences of FcR and TLR signaling in monocytic cell lines

MATERIALS AND METHODS

Unless otherwise stated reagents were purchased from Sigma.

DNA Constructs and Transfectants

KH10382N SureSilencing shRNA Plasmids for Human PTPN22 knock-down were purchased from SA Biosciences (Qiagen). Each vector expresses a short hairpin RNA, or shRNA, under control of the U1 promoter as well as the geneticin resistance gene. Three SureSilencing shRNA vectors and one Negative Control shRNA vector (a scrambled artificial sequence which does not match any human, mouse, or rat gene) were used. A Qiagen Plasmid Maxi Kit was used to purify the plasmids from transformed bacteria and a Nanodrop spectrophotometer was used to determine the yield.

Cell purification and Culture

All cell cultures were maintained at 37°C in a humidified incubator containing 5% CO_2. Promyelocytic HL60 cell line as well as U937 and THP-1 monocytic cell lines were obtained from Dr Steve Young. Cells were grown in complete RPMI 1640 medium supplemented with 2mM L-glutamine, 10% heat inactivated foetal calf serum (HIFCS; Biosera) and 1% penicillin and streptomycin. Cultures were maintained at a density of $1.0x10^6$ - $2.0x10^6$ cells/ml.

ShRNA plasmids were transfected into cells by electroporation using a Neon® Transfection System (Life Technologies). To determine the settings which would yield the highest efficiency of transfection, cells were transfected with a GFP-tagged construct using the 24 different settings and the level of GFP within cells was analysed by flow cytometry using a FACS Calibur flow cytometer as per the manufacturer's instructions. The optimal settings were found to be: 1 1600v pulse; width: 20 for THP-1 and U937 cells and 1 1700v pulse; width: 20 for HL60 cells.

Alternatively Attractene Tranfectant Reagent (Qiagen) was used. 1.5µl of Attractene was added to 0.4µg ShRNA plasmid diluted in 60µl of media without serum, proteins or antibiotics. These samples were kept for 10 min at RT before being added to 500µl media containing cells at a density of $1x10^5$cells/ml.

Successfully transfected cells were selected using geneticin (400µg/ml HL60; 600µg/ml THP-1; 700µg/ml U937) which was added 24 hours after transfection. This concentration was maintained for 8 days, with fresh media added every two days. After the 8 day period, the concentration of geneticin added was reduced by 50%. (Western blotting was to be performed on day 9).

Western blotting

Cells were washed twice in Ca^{2+} containing Hanks balanced saline solution (Ca^{2+} HBSS) (1x HBSS (Invitrogen), 25mM HEPES, 7.5% $NaHCO_3$) twice and once in ice-cold PBS/0.05% Tween 20 (PBST) before being lysed by incubation with TNE lysis buffer (20mM Tris, 150mM NaCl, 1mM EDTA in dH_2O) and 7x Protease Inhibitor Cocktail (7:1, Roche) for 30 minutes at 4°C. Samples were centrifuged at 13,000rpm for 10 min and 40µl of the supernatant was mixed with 10µl of 5x SDS loading buffer. The samples were then boiled for 5min at 100°C and stored at -20°C until required.

The samples were boiled for 5min at 100°C and electrophoresed along with SeeBlue Plus 2 Pre-stained Standard (Invitrogen) on a 10% SDS-polyacrylamide gel layered with a 5% stacking gel. The gel was run for 30min at 100V and then for an hour at 150V. The samples were then transferred to a polyvinylidene fluoride (PVDF) membrane for 2 hours at 450mA using a wet-blotting system. The transfer membrane was blocked with 5% Marvel in *PBST* for an hour at on a shaker at room temperature to prevent non-specific binding and then incubated with an anti-Lyp primary antibody (R&D Systems; clone 340113) (1:1000 in 5%

Marvel in PBST) overnight at 4°C on a shaker. The next day the membrane was washed 3x for 10min each in PBST and then incubated with an HRP-linked anti-mouse secondary antibody from sheep (GE Healthcare UK Ltd) (1:10000 in PBST) for 1 hour on a shaker at room temperature. The membrane was then washed 3x for 10min in TBST as before. After the last wash the PBST was discarded and Amersham ECL western blotting reagents (GE Healthcare Life Sciences) were added for 30 seconds. The blot was then placed in an X-ray cassette and the film was developed in a dark room.

The membrane was then re-probed for β-actin. Firstly the membrane was washed 2x for 10min in mild stripping buffer (15% glycine, 1% SDS; pH 2.2), 2x for 10min in PBS and 2x for 5min in PBST. All washes were at RT on a shaker. The transfer membrane was then blocked with 5% Marvel in PBST for an hour at on a shaker at room temperature before being incubated with an anti-β-actin primary antibody (Clone AC-15) (1:1000 in 5% Marvel in PBST) overnight at 4°C on a shaker. The next day the membrane was washed 3x for 10min each in PBST and then incubated with an HRP-linked anti-mouse secondary antibody from sheep (GE Healthcare UK Ltd) (1:10000 in PBST) for 1 hour on a shaker at room temperature. The membrane was then washed 3x for 10min in PBST as before. After the last wash the liquid was discarded and ECL reagents (GE Healthcare Life Sciences) were added for 30 seconds. The blot was then placed in an X-ray cassette and bands were detected by exposure of an X-ray autoradiography film in a dark room.

Phosphatase assay

The phosphatase assay used was adapted from the assay described in Rider *et al.* (2003). The wells of a 96 well maxisorp immunoplate (NUNC) were coated with 50µl of a 10µg/ml protein A/carbonate buffer (50mM pH 9.6) solution, sealed and incubated overnight at 4°C. The plate was then washed 3x with PBST using a Denley Wellwash4 plate washer and 50µl of an anti-Lyp monoclonal antibody (5µg/ml) in 1% BSA/0.05% Tween 20 solution was added

to the appropriate wells. This was then incubated for 2 hours at 37°C before being washed 3x with PBST. Subsequently to prevent non-specific binding of the lysate 100µl of blocking buffer (2% BSA/PBS) was added to each well and the plate was incubated at 37°c for 1 hour.

Cells were prepared such that there were enough for $1x10^6$ per well. The appropriate number of cells were washed twice in Ca^{2+} HBSS (1200rpm, 8 min) and then in ice-cold PBST. Cells were then lysed by incubation with TNE lysis buffer and 7x Protease Inhibitor Cocktail (7:1, Roche) for 30 minutes at 4°C with regular agitation. Cells were then centrifuged at 13000rpm for 10 min, the blocking buffer was tipped off the ELISA plate and 50µl of the cell lysate (supernatant) was added to each well. The plate was then incubated for 3 hours at 37°c and washed 3x with PBST and 3µl of 1M DL-dithiothreitol (DTT) was added. Next 50µl of 0.5mM 6,8-difluoro-4-methylumbelliferyl phosphate (DiFMUP) in phosphate reaction mixture (0.1M sodium acetate, 1mM EDTA, 0.2% Triton X-100, pH 6.0) was added to all wells and the activity of Lyp was measured using a Fluoroskan Ascent plate reader at 0, 1 hour and 2 hours using the 355nm/460nm filter pair.

Ca2+ Signaling

Cells were incubated overnight with 100nM phorbol 12-myristate 13-acetate (PMA) at 37°C with regular agitation as done by Azenabor *et al.* (2009) to induce differentiation into macrophage-like cells. 1.5million per cells per agonist were collected the next day. These were then centrifuged, the media was discarded and fresh media was added such that the concentration of cells was no greater than $2x10^6$/ml. 1µM Indo-1 AM (Invitrogen) reconstituted in dimethyl sulfoxide (DMSO) was added and then cells were incubated at 37°C for 40min. Following incubation cells were washed 3x in Ca^{2+} HBSS and after the final wash cells were resuspended in Ca^{2+} HBSS at $1x10^6$ cells/ml. 1.5ml of cell suspension was then placed in a disposable cuvette, kept at 37°C for 5min and then loaded into a Perkin Elmer LS50B Spectrofluorimeter with a magnetic stirrer to maintain constant agitation so that cells

were kept in suspension. 10µg/ml LPS or 5µg/ml mouse anti-human CD32 antibody (ImmunoTools) was added after 120 seconds of recording, followed by 10µg/ml of an Fc specific goat anti-mouse IgG antibody as per Metes *et al.* (1999). The recording was continued until 300 seconds had passed. An Indo-1 AM dual emission protocol generated in FL Winlab Version 2.1 software was used to collect this data.

Superoxide Production Assays

Cells were incubated overnight with 100nM phorbol 12-myristate 13-acetate (PMA) at 37°C with regular agitation.

Cells were then prepared so that they were at a density of $3.3x10^6$ cells/ml of Ca^{2+} HBSS. These cells were incubated at 37°C for 15min. After this time 100µl of 500µM Cytochrome C/Ca^{2+} HBSS was added to each well of the pre-warmed 96 well plate, followed by 60µl of cells, Ca^{2+} HBSS or 100mM sodium dithionite/ Ca^{2+} HBSS solution and the optical density was measured using an Anthos HTIII plate reader (550nm). Agonists were then added and readings taken every 10min. Agonists used were 10µg/ml LPS, 200nM PMA or 5µg/ml mouse anti-human CD32 antibody (ImmunoTools) followed by 10µg/ml anti-mouse antibody. Stingray version 1.5 software was used to collect the data.

Alternatively, after PMA incubation cells were prepared so that they were at a density of $4x10^6$ cells/ml of medium. 200µl of the cell suspension was placed in each FACS tube and the tubes were incubated with or without the LYP inhibitor (1.5µM, Calbiochem) at 37°C for 30min (as per Karver *et al.*, 2009). Dihydrorhodamine (DHR) solution (10µM) was then added to each tube and they were incubated at 37°C for 5min. After this time the agonists were added if appropriate and the level of fluorescence measured using FL1 of a Dako CyAn ADP flow cytometer. Agonists were again 10µg/ml LPS, 200nM PMA or 5µg/ml mouse anti-human CD32 antibody (ImmunoTools) followed by 10µg/ml anti-mouse antibody.

RESULTS

Expression of Lyp within monocytic cell lines

To investigate whether the three monocytic cell lines express Lyp, a western blot of the cell lysate was performed using an anti-Lyp antibody. As can be seen in **Figure 6** (top section) there were bands in the lanes containing the HL60 lysate and the U937 lysate but not the one containing THP-1 lysate. These bands were present at 150kDa which is 45kDa over the mass of Lyp (105kDa). It may be that Lyp is associated with its binding partner Csk, which is 45kDa. The membrane was subsequently stripped and re-probed using an anti-β-actin antibody. The β-actin bands shown in the bottom section of **Figure 6** are of similar density for all three cell lines. Overall this figure indicates that Lyp is expressed in HL60 and U937 cells, but not THP-1 -cells.

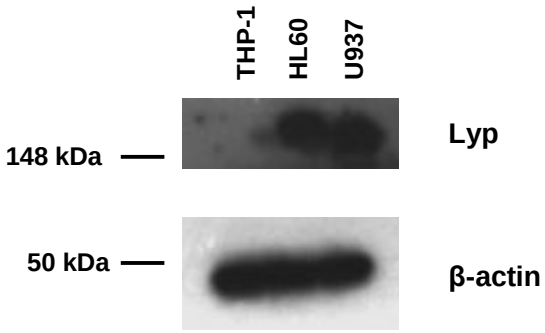

Figure 6: Expression of Lyp in monocytic cell lines. Lysate from HL60, THP-1 and U937 cells was electrophoresed along with SeeBlue Plus 2 Pre-stained Standard on a 10% SDS-polyacrylamide gel. The proteins were then transferred to a membrane and a western blot for Lyp was performed. The membrane was then stripped and re-probed for β-actin**.** The upper panel shows the blot for Lyp and the lower panel the blot for β-actin.

Lyp knockdown/Inhibition

Initially we worked on obtaining stable knockdown of Lyp in the three cell lines using transfection with plasmids containing short hairpin RNA (shRNA) inserts and a geneticin resistance gene. shRNA constructs are short sections of mRNA in a hairpin conformation which can be used to specifically knock down expression of a protein using existing cellular machinery. Geneticin was added 24 hours after transfection to select for the successfully transfected cells. The concentrations of geneticin had been determined by a previous student who had performed antibiotic titrations to identify the concentration which would cause massive cell death by day 7 and would kill all cells by day 14.

Electroporation was used as the method of transfection because preliminary work using the chemical transfection agent Attractene had not led to efficient knockdown within these cells (data not shown). We optimised the electroporation settings using the Neon optimisation protocol and flow cytometric analysis of cells which had been transfected with an unrelated GFP-tagged construct. **Supplementary Figure 1** shows the optimisation for THP-1 for which setting 4 was able to achieve the highest efficiency of transfection (25%). However we found that the majority of cells had died within 2 days of geneticin addition and therefore we were not able to perform a western blot to determine whether knock down had occurred. We therefore used Attractene as an alternative transfection strategy but again cells did not survive. As we had found a commercially available inhibitor, we decided to concentrate on experiments using this due to the short timescale of the project.

Phosphatase activity of Lyp within monocytic cell lines

In order to investigate the phosphatase activity of Lyp within our cell lines and determine whether the inhibitor is able to ameliorate this activity, an assay was carried out to probe the activity of captured Lyp using DiFMUP (6,8-difluoro-4-methylumbelliferyl phosphate), which can be dephosphorylated to yield a fluorescent product: DiFMU (6,8-difluoro-7-hydroxy-4-methylcoumarin). DL-dithiothreitol (DTT) was added to the captured Lyp prior to DiFMUP to reduce the Lyp. This is necessary as if the key cysteine residue in the active site of Lyp is oxidised it is unable to dephosphorylate its substrates. The fluorescence intensity was measured after DiFMUP addition (0hrs) and again after incubation for 2 hours at 37°C. **Figure 7** shows the results of this experiment when carried out with Lyp captured from HL60 cell lysate. We were able to observe a 40% increase in fluorescence intensity in the sample containing Lyp between 0 and 2 hours. In comparison there was only an 8% increase for the negative control, for which no anti-Lyp antibody was added to the plate to capture Lyp. Therefore the results of this experiment indicate that Lyp from HL60 cells is able to dephosphorylate DiFMUP and hence exhibits phosphatase activity.

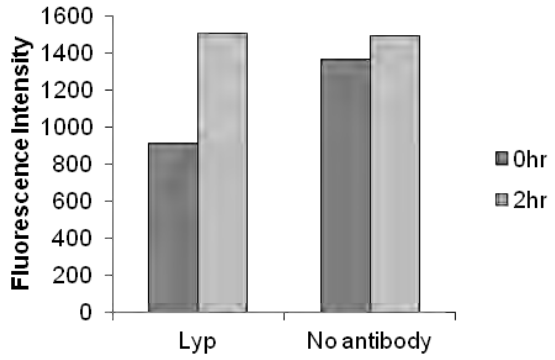

Figure 7: Phosphatase activity of Lyp in HL60 cell line. HL60 cells were lysed and incubated for 3hrs in wells of an 96 well plate which had been coated with an anti-Lyp antibody or wells which did not contain antibody, as a negative control. The captured Lyp was reduced using DTT and its phosphatase activity was investigated using DiFMUP which changes colour when dephosphorylated. A Fluoroskan Ascent plate reader was used to detect any colour changes after 0 and 2 hours (Ex/Em = 355nm/460nm). All conditions were done in triplicates. The histogram shows the fluorescence intensity at 0 and 2 hours.

This experiment was then extended to the other two cell lines and another control was added in which DTT was not added prior to DiFMUP. Three individual experiments were carried out using this setup and the results are shown in **Figure 8** as the percentage increase in fluorescence intensity between 0 and 2hrs. In all three cell types the percentage increase for the no antibody control was similar or higher than the percentage increase for the sample containing Lyp. In addition the percentage increase for the DTT control was very large when, much like for the no antibody control, we should have seen little to no increase. Therefore this experiment produced inconclusive results and we were not able to determine the phosphatase activity of Lyp within THP-1 or U937 cells. As a consequence we were not able to then investigate the effect of the Lyp inhibitor on the phosphatase activity of Lyp.

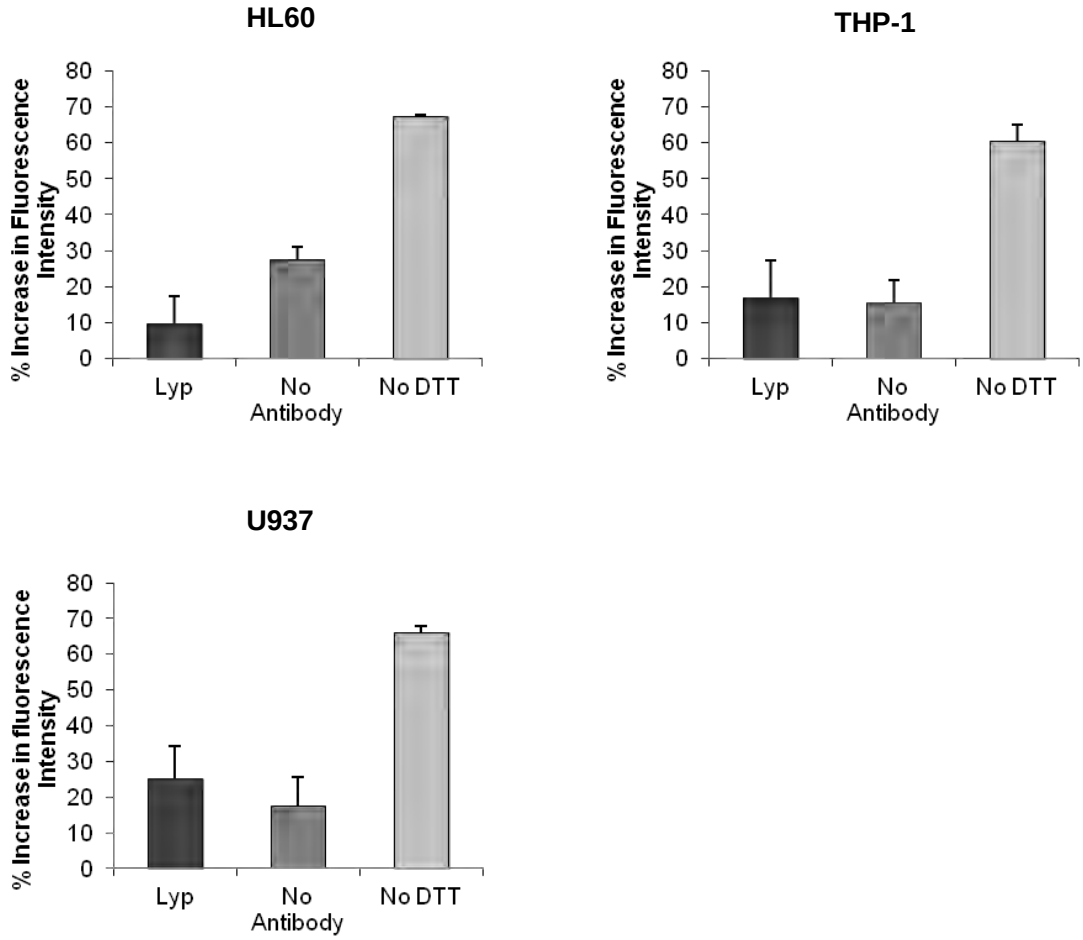

Figure 8: Phosphatase activity of Lyp in HL60, THP-1 and U937 cells. Cells were lysed and incubated for 3hrs in wells of an 96 well plate which had been coated with an anti-Lyp antibody or wells which did not contain antibody, as a negative control. The captured Lyp was reduced using DTT in all wells except the no DTT negative control wells and the phosphatase activity of the Lyp was investigated using DiFMUP which changes colour when dephosphorylated. All conditions were done in triplicates and a Fluoroskan Ascent plate reader was used to detect any colour changes after 0 and 2 hours (Ex/Em = 355nm/460nm). Histograms showing the results of three independent experiments as a % increase in fluorescence intensity between the readings at 0 and 2 hours. Error bars show the standard error of the mean.

Measuring Toll like receptor (TLR) and Fc receptor (FcR) signaling within monocytic cell lines

To investigate the effect of Lyp inhibition on TLR and FcR signaling in our cell lines, an experiment which measures Ca^{2+} flux was performed. Cells were first treated overnight with PMA (phorbol 12-myristate 13-acetate) at 37°C to differentiate them into macrophage-like cells. A ratio metric calcium sensitive dye, Indo-1 AM was then used to measure Ca^{2+} flux in response to LPS, a Toll-like receptor (TLR) agonist. Indo-1 AM is able to enter cells and it emits fluorescence at a higher wavelength when bound to Ca^{2+}. The fluorimeter can detect both the lower and higher wavelength and calculate an emission ratio. This can then be converted to an absolute Ca^{2+} concentration using the values obtained from adding ionomycin to stimulate the cells (Rmax) and then EDTA to chelate the Ca^{2+} (Rmin). This was done with HL60 cells and is shown in **Figure 9a**. However when LPS was added to the HL60, THP-1 or U937 cells there was no change in the emission ratio (**Figure 9b)** and therefore we were not able to investigate the effect of the inhibitor on TLR signalling.

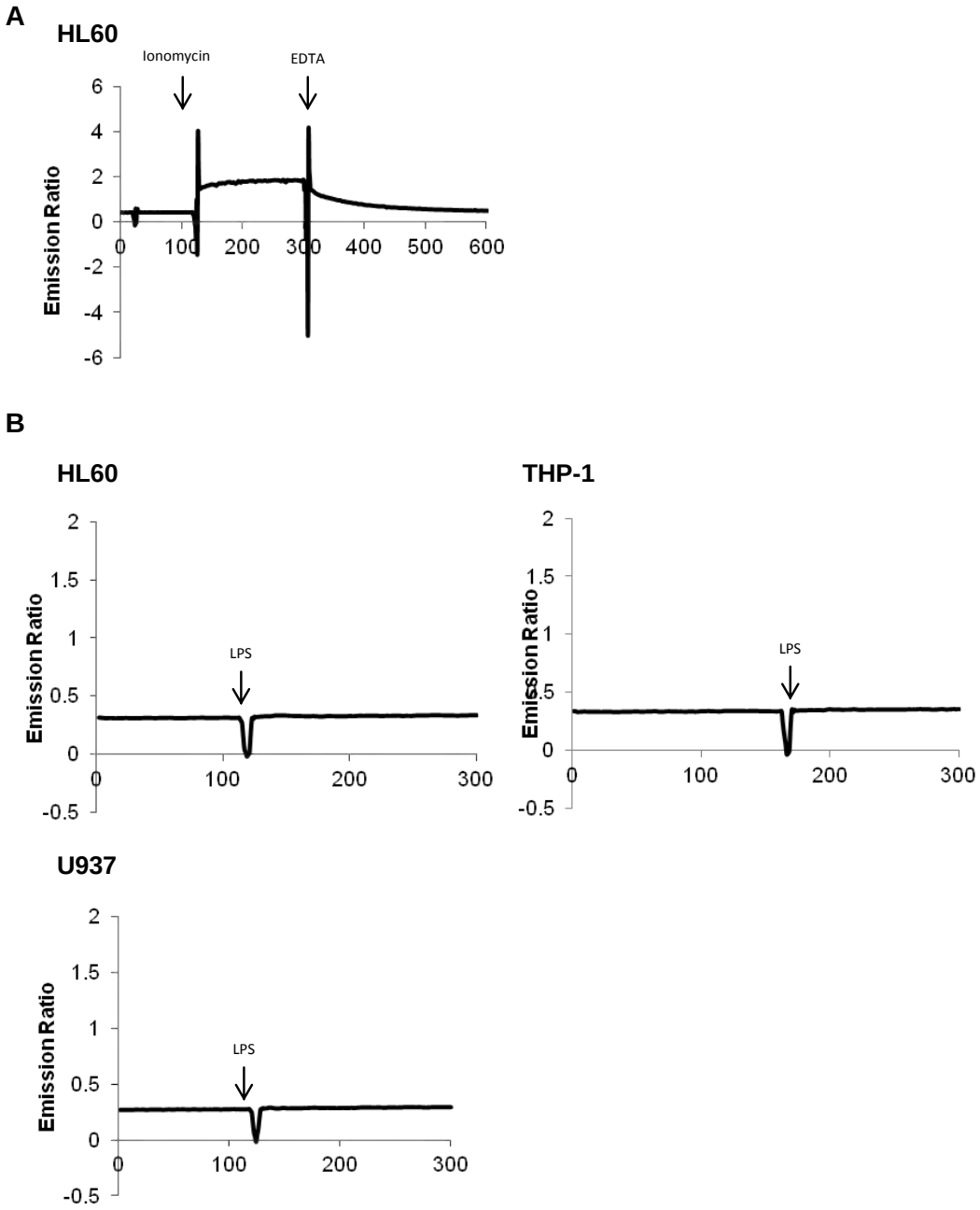

Figure 9: Detection of Ca^{2+} release by monocytic cell lines in response to TLR signalling Cells were centrifuged and resuspended in Ca^{2+} HBSS, incubated with Indo-1 AM calcium sensitive dye for 45 min at 37°C and then washed 3x in Ca^{2+} HBSS. A Perkin Elmer Spectrofluorimeter was used to measure the emission ratio before and after an agonist was added. (A) Graph showing the change in emission ratio when Ionomycin and EDTA were added to HL60 cells. These readings would allow conversion of the Ca^{2+} ratio to absolute Ca^{2+} concentration. (B) Graphs showing any changes in emission ratio upon addition of the TLR4 agonist LPS (10µg/ml) to HL60, THP-1 and U937 cells which had been pre-treated with 100nM PMA overnight to allow differentiation into macrophage-like cells.

We then sought to measure Ca^{2+} flux in response to in response to FcR signalling. To induce signaling through an FcR we crosslinked FcγRII (CD32) using a mouse anti-human CD32 antibody followed by an anti-mouse antibody. Initially this was done using HL60 cells and a small increase in the Ca^{2+} ratio was observed (**Figure 10a**). After 60-120 seconds additional anti-mouse antibody was added and again we were able to observe an increase in the Ca^{2+} ratio. However when this was repeated on the HL60 cells (**Figure 10b**) and also carried out using THP-1 and U937 cells (**Figure 10c**); no increase in Ca^{2+} ratio was observed. Therefore this experiment was not able to detect any changes in Ca^{2+} flux in response to TLR or FcR agonists and was not extended to include use of the inhibitor.

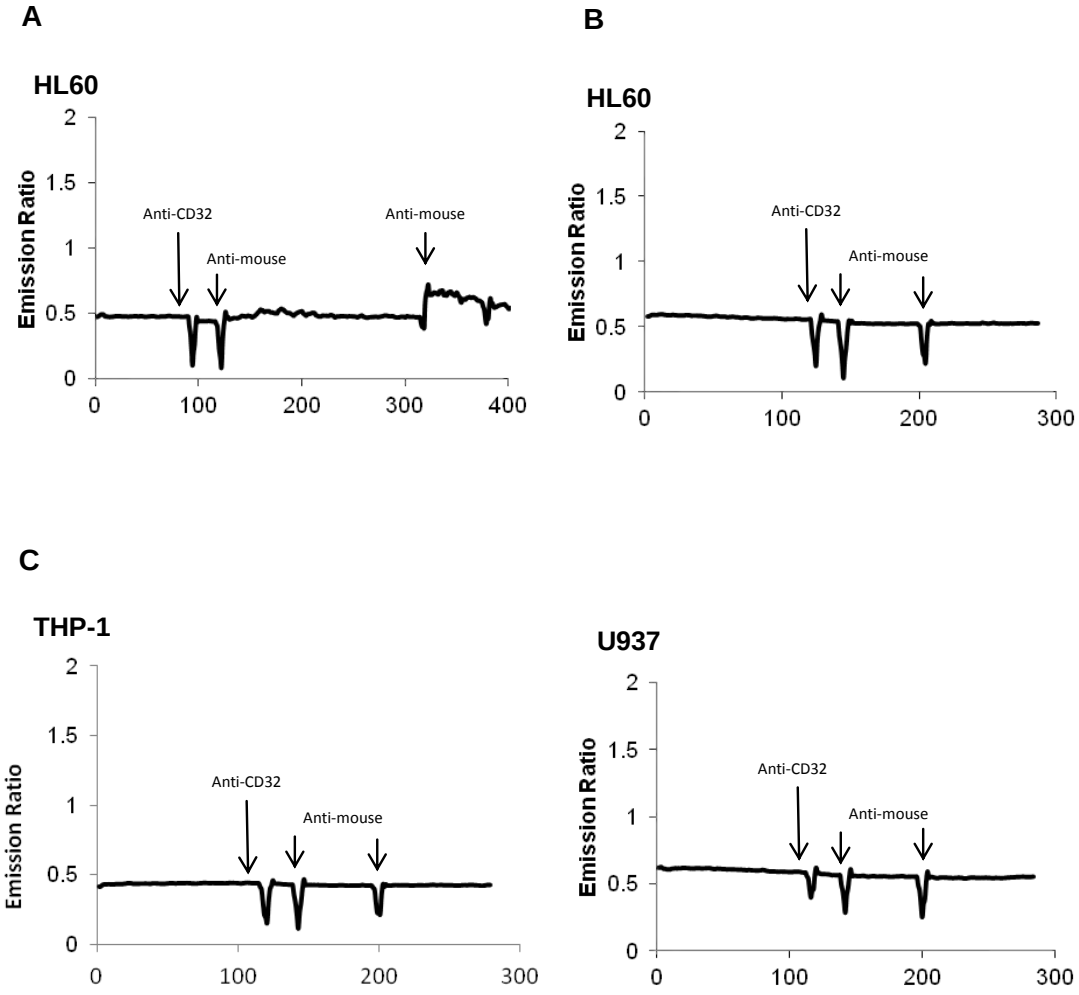

Figure 10: Detection of Ca^{2+} release by monocytic cell lines in response to FcR signalling. Cells were pre-treated with 100nM PMA overnight, centrifuged and resuspended in Ca^{2+} HBSS before being incubated for 45 min at 37°C with Indo-1 AM, a ratiometric calcium sensitive dye. Cells were then washed 3x in Ca^{2+} HBSS and a spectrofluorimeter was used to measure the emission ratio before and after CD32 crosslinking. To crosslink CD32 a mouse anti-human CD32 antibody (5µg/ml) followed by an anti-mouse antibody (10µg/ml) was added to cells (A) Graph showing any changes in the emission ratio upon CD32 crosslinking on HL60 cells (B) Graph showing a repeat of the HL60 CD32 crosslinking experiment (C) Graphs showing any changes in the emission ratio following CD32 crosslinking on THP-1 (on the left) and U937 cells (on the right).

Measuring functional consequences of phagocyte signaling

To investigate the effect of Lyp inhibition on the functional consequences of phagocyte signaling, an assay was performed which uses detection of superoxide as a measurable indicator. We differentiated HL60 cells by overnight incubation with PMA and then used a fluorimeter to detect the colour change associated with reduction of Fe(III) in Cytochrome C to Fe(II) by superoxide produced in response to LPS, PMA and CD32 crosslinking. Ca^{2+} HBSS was used as a negative control and sodium dithionite (DT) was used as a positive control as it is a strong reducing agent. As is shown in **Figure 11**, the optical density (OD) of the positive control was around 40% higher than the negative control. The OD of the unstimulated HL60 cells was similar to that of the negative control but upon addition of agonist we were not able to observe any increase in OD over 20 minutes. Therefore we were not able to measure superoxide production by HL60 cells using this assay and an alternative method was sought.

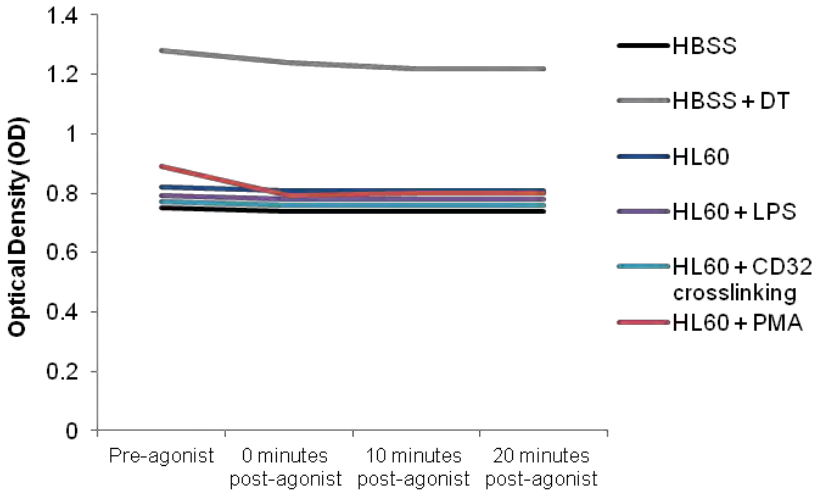

Figure 11: Detection of superoxide production by HL60 cells by reduction of Cytochrome C. HL60 cells were pre-treated with 100nM PMA overnight, washed and resuspended in Ca^{2+} HBSS. This cell suspension, Ca^{2+} HBSS as a negative control, or Ca^{2+} HBSS containing sodium dithionite (DT) as a positive control were added to wells containing 500µM Cytochrome C solution. The optical density at 550nm was recorded using a plate reader. Agonists (10µg/ml LPS, 200µM PMA or 5µg/ml mouse anti-CD32 antibody followed by 10µg/ml anti-mouse antibody) were then added and readings were taken every 10min. The graph shows the optical density of the samples over the time points.

The second method of superoxide production used dihydrorhodamine (DHR), which is a cell permeable dye that can be oxidised by superoxide to produce a fluorescent product: rhodamine. PMA differentiated HL60, THP-1 or U937 cells were pre-warmed at 37°C for 30min, 10μM DHR was added and cells were incubated for a further 5min at 37°C. The agonists (LPS, PMA or CD32 crosslinking) were then added and any resulting changes in fluorescence were detected using FL1 of a flow cytometer. DHR was not added to one of the samples so that this could be used as a negative control

Figure 12 contains the results for the HL60 cells. The gating used to exclude dead cells (left dot plot) and include only single cells (right dot plot) is included in **Figure 12a**. As we can see in **Figure 12b**, the fluorescence intensity was low in the sample lacking DHR, with an overall MFI of 6. The fluorescence intensity in cells of the unstimulated sample however was high; with an MFI of 1648 for Region 1 (R1). Cells which had been treated with agonists did not appear to contain higher levels of fluorescence than the unstimulated sample and instead the R1 MFIs were all lower than that of the unstimulated sample. Similar results were observed for THP-1 (**Figure 13)** and U937 cells (**Figure 14**), although the MFIs of were much lower than those of the HL60 cells at 132 and 325 respectively.

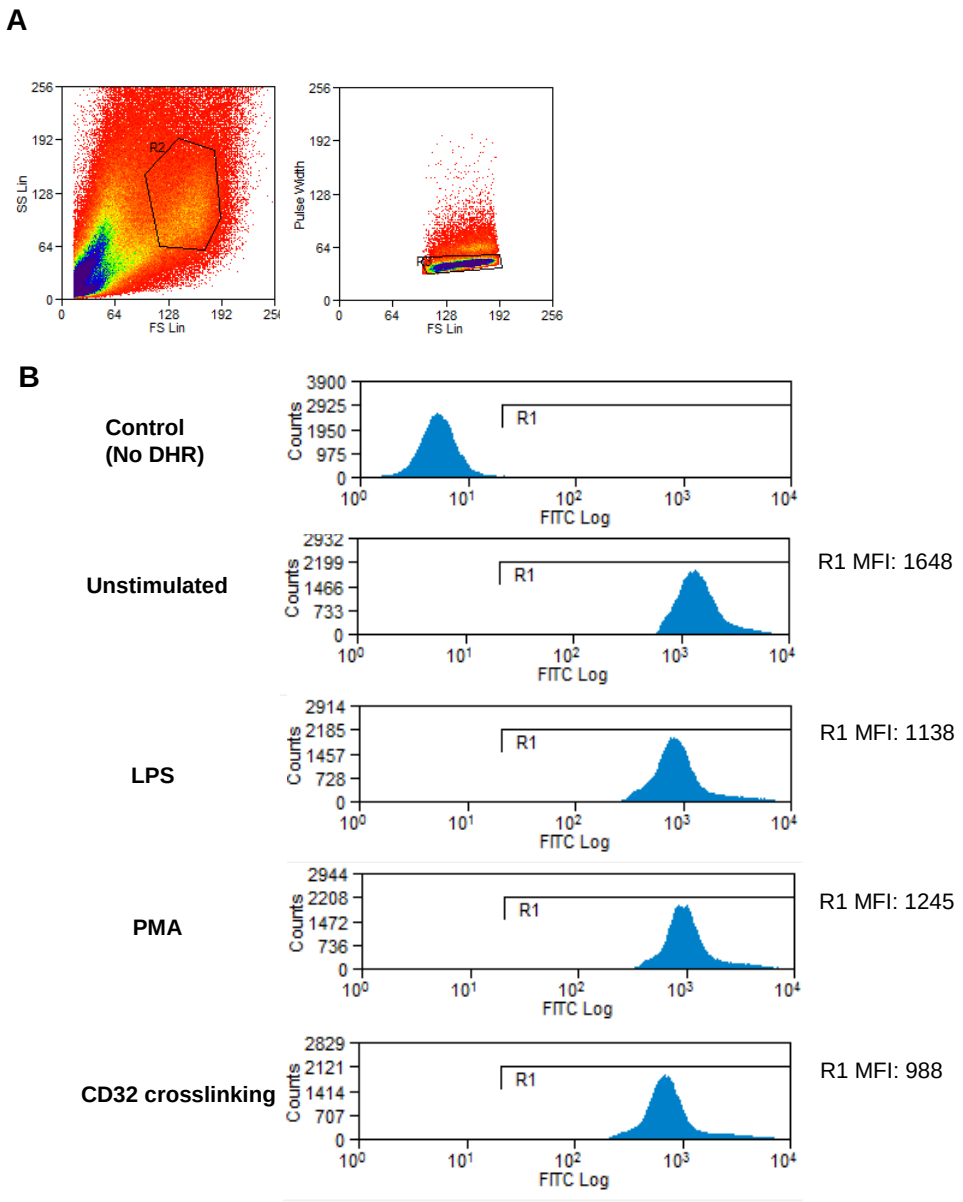

Figure 12: Detection of superoxide production by HL60 cells using Dihydrorhodamine (DHR). HL60 cells were pre-treated with 100nM PMA overnight, washed and resuspended in media. 1x10^6 cells were placed in each FACS tube and incubated for 15min at 37°C. 10µM DHR was added to all tubes except one as a negative control and the cells were incubated at 37°C for a further 5min. Agonists (10µg/ml LPS, 200µM PMA or 5µg/ml mouse anti-CD32 antibody followed by 10µg/ml anti-mouse antibody) were added and the level of fluorescence analysed by flow cytometry. (A) Dotplots showing the gating used to exclude dead cells (left) and include only single cells (right).(B) Histograms of the level of fluorescence in the control sample, unstimulated sample and agonist stimulated samples. Mean fluorescence intensity (MFI) values are shown at the right of each histogram.

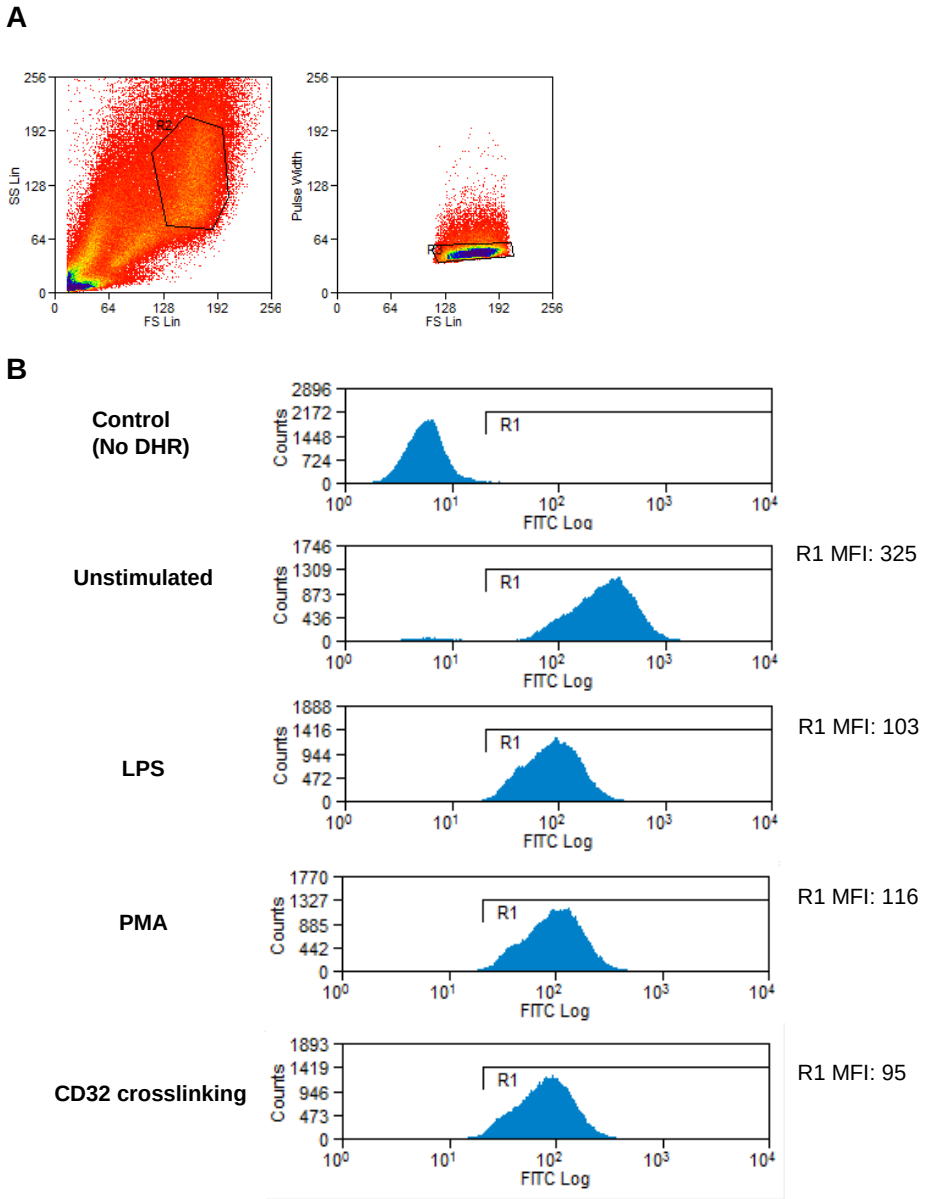

Figure 13: Detection of superoxide production by THP-1 cells using Dihydrorhodamine (DHR). THP-1 cells were pre-treated with 100nM PMA overnight, washed and resuspended in media. 1x10^6 cells were placed in each FACS tube and incubated for 15min at 37°C. 10µM DHR was added to all tubes except one as a negative control and the cells were incubated at 37°C for a further 5min. Agonists (10µg/ml LPS, 200µM PMA or 5µg/ml mouse anti-CD32 antibody followed by 10µg/ml anti-mouse antibody) were added and the level of fluorescence analysed by flow cytometry. (A) Dotplots showing the gating used to exclude dead cells (left) and include only single cells (right).(B) Histograms of the level of fluorescence in the control sample, unstimulated sample and agonist stimulated samples. Mean fluorescence intensity (MFI) values are shown at the right of each histogram.

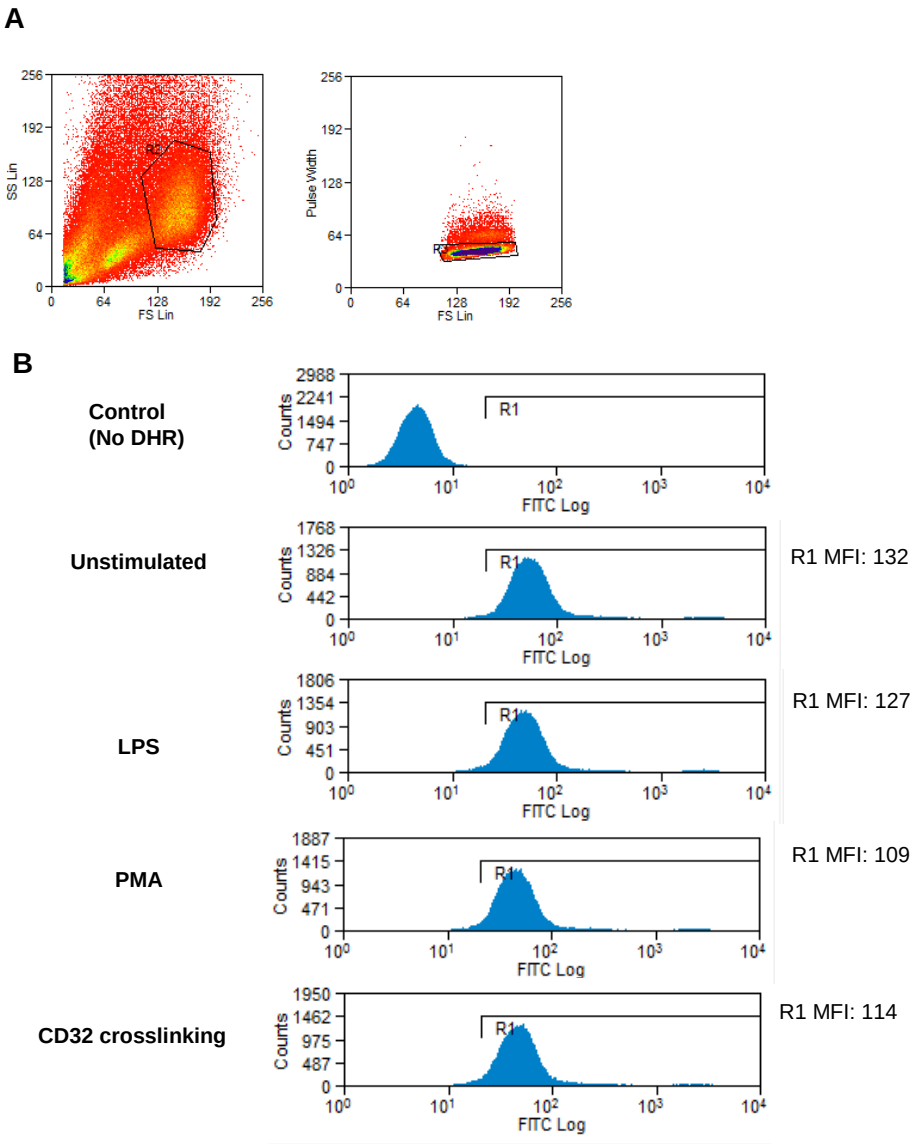

Figure 14: Detection of superoxide production by U937 cells using Dihydrorhodamine (DHR). U937 cells were pre-treated with 100nM PMA overnight, washed and resuspended in media. 1x10^6 cells were placed in each FACS tube and incubated for 15min at 37°C. 10µM DHR was added to all tubes except one as a negative control and the cells were incubated at 37°C for a further 5min. Agonists (10µg/ml LPS, 200µM PMA or 5µg/ml mouse anti-CD32 antibody followed by 10µg/ml anti-mouse antibody) were added and the level of fluorescence analysed by flow cytometry. (A) Dotplots showing the gating used to exclude dead cells (left) and include only single cells (right).(B) Histograms of the level of fluorescence in the control sample, unstimulated sample and agonist stimulated samples. Mean fluorescence intensity (MFI) values are shown at the right of each histogram.

To investigate whether the Lyp inhibitor would have any effect on the level of fluorescence in the unstimulated cells, this experiment was repeated for the negative control, unstimulated cells and additionally for unstimulated cells which had been pre-treated with the Lyp inhibitor for 30min. As shown by the histograms and graphs in **Figure 15** we observed a high level of fluorescence in the unstimulated sample for all cell types. In contrast to the previous experiment the level was similar in all three cell types (MFI ~150). Addition of the Lyp inhibitor led to an increase of approximately 60% in the level of fluorescence within the HL60 cells, a 40% increase in the THP-1 cells, and a 4% increase in the U937 cells.

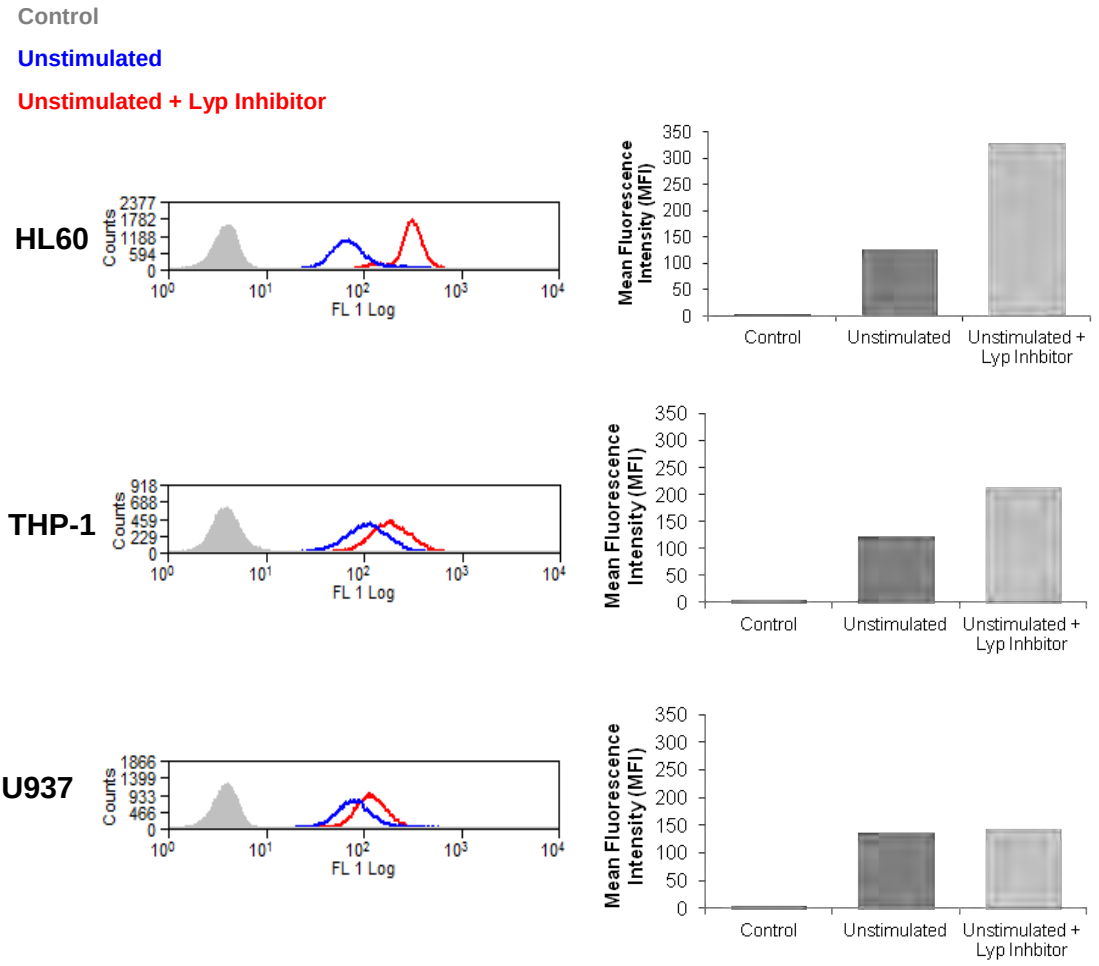

Figure 15: The effect of Lyp inhbitor on superoxide production by unstimulated HL60, THP-1 and U937 cells using Dihydrorhodamine (DHR). Cells were pre-treated with 100nM PMA overnight, washed and resuspended in media. 1x106 cells were placed in each FACS tube and incubated for 30min with or without Lyp Inhbitor (1.5µM) at 37°C. 10µM DHR was added to all tubes except one as a negative control and the cells were incubated at 37°C for a further 5min. The level of fluorescence was analysed by flow cytometry. Histograms show the level of fluorescence in the HL60 cells (top), THP-1 cells (middle) and U937 cells (bottom) of the control (grey), unstimulated (red) and unstimulated Inhibitor treated (red) samples. This data is also shown graphically on the right of each histogram in the form of Mean Fluorescence Intensity (MFI).

DISCUSSION

Lyp is expressed at high levels in macrophages and considering the strong association of the R620W variant with many autoimmune diseases it is of vital importance that we understand what the role of Lyp is in these cells and then what effect the variant has on their function. This may lead to a greater understanding about how the variant contributes to the development and the pathogenesis of autoimmune disease.

Three monocytic cell lines were used in these experiments: HL60 which is derived from an individual with acute promyelocytic leukaemia, THP-1 which is derived from an individual with acute monocytic leukaemia, and U937 which is derived from an individual with diffuse histiocytic leukaemia (Harris and Ralph, 1985; Fleit and Kobasiuk 1991). All three cell lines resemble the progenitors of monocytes/macrophages (Harris and Ralph, 1985), with the promyelocytic HL60 cells resembling the earliest progenitor, and can be induced to differentiate into different cell types (Collins, 1987).

The results within this report indicate that Lyp is expressed within HL60 and U937 cells, but not THP-1 cells. As can be seen in **Figure 16**, Chien *et al.* (2003) have shown that THP-1 cells express lower levels of Lyp than HL60 and U937 cells. It may be that Lyp is present within the THP-1 cells in our experiment but as it is at a lower level our experiment is not sensitive enough to detect it. As the β-actin levels were similar in all three cell lines we can rule out a loading discrepancy. Alternatively our THP-1 cells may have lost Lyp expression.

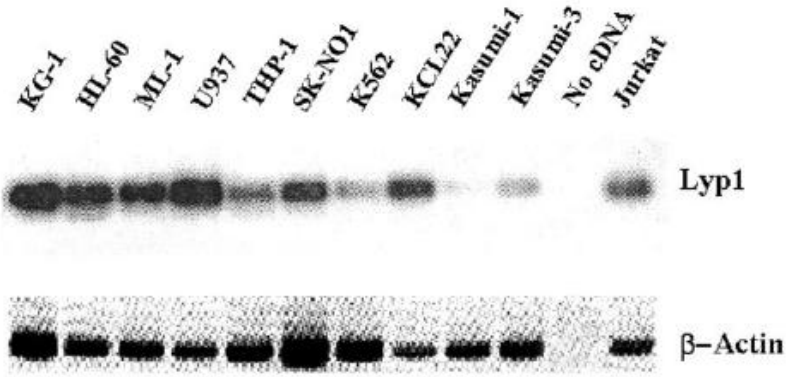

Figure 16: Lyp expression in cell lines (Chien et al., 2003)

The results also suggested that Lyp may be associated with Csk within our samples. Indeed findings from recent publications, which provide evidence for the gain of function hypothesis, have suggested that Lyp and Csk are constitutively associated with each other within T cells (Fiorello *et al.*, 2010; Vang *et al.*, 2012) and this may also be the case in monocytes/macrophages. However the loss of function hypothesis, for which there is also evidence, centres round the concept that Csk associates with Lyp only when TCR signaling occurs, and that this association targets Lyp to the membrane (Bottini *et al.*, 2004; Begovich *et al.*, 2004; Zikherman *et al.*, 2009).

We originally attempted to deplete Lyp in the cell lines and study the effects upon signaling and the resulting functional consequences. After unsuccessful attempts to stably knock down Lyp whilst maintaining viable cells and the discovery of a commercially available inhibitor for Lyp we altered our strategy to one of inhibition. The reason that the cells did not survive transfection and selection may have been because the antibiotic concentration was too high and therefore even cells which had taken up the plasmid with the geneticin resistance gene were unable to survive. Alternatively cells may have responded to the plasmid DNA, via signaling through Toll-like receptor 3 (TLR3), for example. After becoming activated by the

DNA the cells may subsequently have gone into apoptosis, which is a mechanism of tailing down the immune response.

An assay which measures the phosphatase activity of Lyp was used to determine whether the Lyp inhibitor can indeed reduce its enzymatic activity. Although this assay worked in the initial experiment using HL60 cells and we were able to gain an insight into its phosphatase activity, we were unable to reproduce this as the two negative controls did not work thereafter for the HL60, or the THP-1 and U937 cells. Potential reasons for the high level of activity in the controls could be that the blocking was not effective, although the use of fresh blocking buffer did not alter this. Alternatively it could be that the washing step after incubation with the cell lysate was not effective enough. In future an extra control could be added which would be that the plate would be coated not with an anti-Lyp antibody but an isotype matched antibody to a different target which has no phosphatase activity.

Assays were then used to measure phagocyte signaling and the resulting functional consequences with the intention of using the inhibitor to determine whether Lyp may have a functional role within signaling and hence an effect on its downstream effects. We used Ca^{2+} flux assays to study phagocyte signaling as during signaling Ca^{2+} can be released into the cytosol from the endoplasmic reticulum (Ca^{2+} flux) where it then acts as a second messenger, leading to further signal transduction. Ca^{2+} flux is a downstream event which is common to many signaling pathways and is therefore a good method of detecting signaling through the TLRs and FcRs of our cells. However as we saw no increase in Ca^{2+} flux in response to TLR or FcR agonists in these assays we were not able to explore the effect of the lyp inhibitor on phagocyte signaling. One potential explanation for this could be that the absence of serum and therefore, for example, LPS binding protein, prevents TLR4 stimulation, however at this high LPS concentration that is perhaps unlikely. It is also possible that the crosslinking was not effective or that these early progenitors of monocytes/macrophages do not express CD32. All three cell lines have previously been

shown to express CD32 (Chi *et al.*, 2002; Fleit and Kobasiuk, 1991; Kwiatkowska *et al.*, 2002) but in future we could determine whether our cells express Lyp by staining CD32 with a fluorochrome conjugated anti-CD32 antibody and analysing the level of fluorescence using flow cytometry.

Similarly in both superoxide production assays, which were used to study production of superoxide as a functional consequence of TLR and FcR signaling, we were not able to observe any increase in response to the agonists. This was unexpected as reactive oxygen species (ROS), such as superoxide, are produced by NADPH oxidase when a phagocyte recognises pathogen associated molecular patterns via pattern recognition receptors such as TLRs or has bound opsonised bacteria via the FcRs. Upon phagocytosis, these reactive species, such as superoxide, are used to destroy the pathogen. It is possible that the previously discussed limitations of using the agonists in this way may again apply. When the cytochrome C method of detecting superoxide production was used we saw no increase in superoxide production for any of the samples, except the positive control (a strong reducing agent). This assay detects superoxide which has been released from cells and therefore the reason that we saw no increase in optical density for any of the cellular samples may be because the assay is not sensitive enough. The DHR method detects intracellular superoxide and therefore is more sensitive. Indeed when using this second method we were able to detect superoxide.

Superoxide is known to exist at a low concentration in unstimulated cells (Sies, 1993), which may account for the fact that the level of fluorescence in the unstimulated cells was quite high across the two individual DHR experiments when compared to the negative control. The level detected in the unstimulated HL60s in the initial experiment was very high which suggests that these cells had previously been stimulated and therefore responded by producing high levels of superoxide. This may be as a result of the overnight pre-treatment with PMA which was necessary to differentiate in particular the promyelocytic HL60 cells into

macrophage-like cells. However in the second experiment the level detected in the HL60 cells was much lower and was more in the order of the level in the other two cell types.

When cells were treated with the Lyp inhibitor the fluorescence increased by 60% for the HL60 cells and by 40% for the THP-1 cells but there was little change in the fluorescence for the U937 cells. This suggests that inhibition of Lyp is able to increase the production of superoxide within HL60 and THP-1 cells and therefore Lyp may be involved in regulating this process. We would need to repeat this experiment to validate this observation but we were able to rule out the possibility that the inhibitor itself is providing this increase in fluorescence as it does not emit within the range detected by FL1 of the flow cytometer (520-540nm) and instead its emission peak is at approximately 640nm (**Supplementary Figure 2**). Further identification of targets of Lyp may provide more clues about where in this process Lyp may act.

To further investigate the effects of the inhibitor on the functional consequences of phagocyte signaling we could carry out a phagocytosis assay where the uptake of fluorescently labelled bacteria by inhibitor-treated or control cells is investigated. Considering that Lyp may have effects on phagocytosis via Vav1, this would be a very interesting experiment. In addition we could perform a whole cell phosphotyrosine immunoblot from inhibitor-treated and control cells and blot for Vav1. This would give us an indication as to whether Lyp dephosphorylates Vav1. We could also determine the effect of Lyp inhibition on cell adhesion by performing an adhesion assay. For example cells in suspension could be added to a plate which is coated with an extra-cellular matrix protein, washes performed, the adherent cells lysed and then detected using a cell quantification dye.

Continuing to work on achieving stable knock down would allow us to eventually perform these assays in cells which lack Lyp expression. Knock down would allow us to overcome

some of the limitations of inhibition, for example, the possibility that other phosphatases, such as CD45, are also inhibited.

Once assays have been optimised and the effects of Lyp inhibition investigated we could then extend these to primary monocytes and macrophages to obtain results from a more physiological source. Once an understanding about the role of Lyp within monocytes and macrophages has been obtained, we could design experiments to be performed on monocytes and macrophages from individuals who are heterozygous or homozygous for the variant of Lyp. Then by comparing the results to those obtained from control individuals we may gain an insight into the effect of the variant within phagocytes and whether this may contribute to the pathogenesis of autoimmune diseases such as rheumatoid arthritis.

APPENDIX

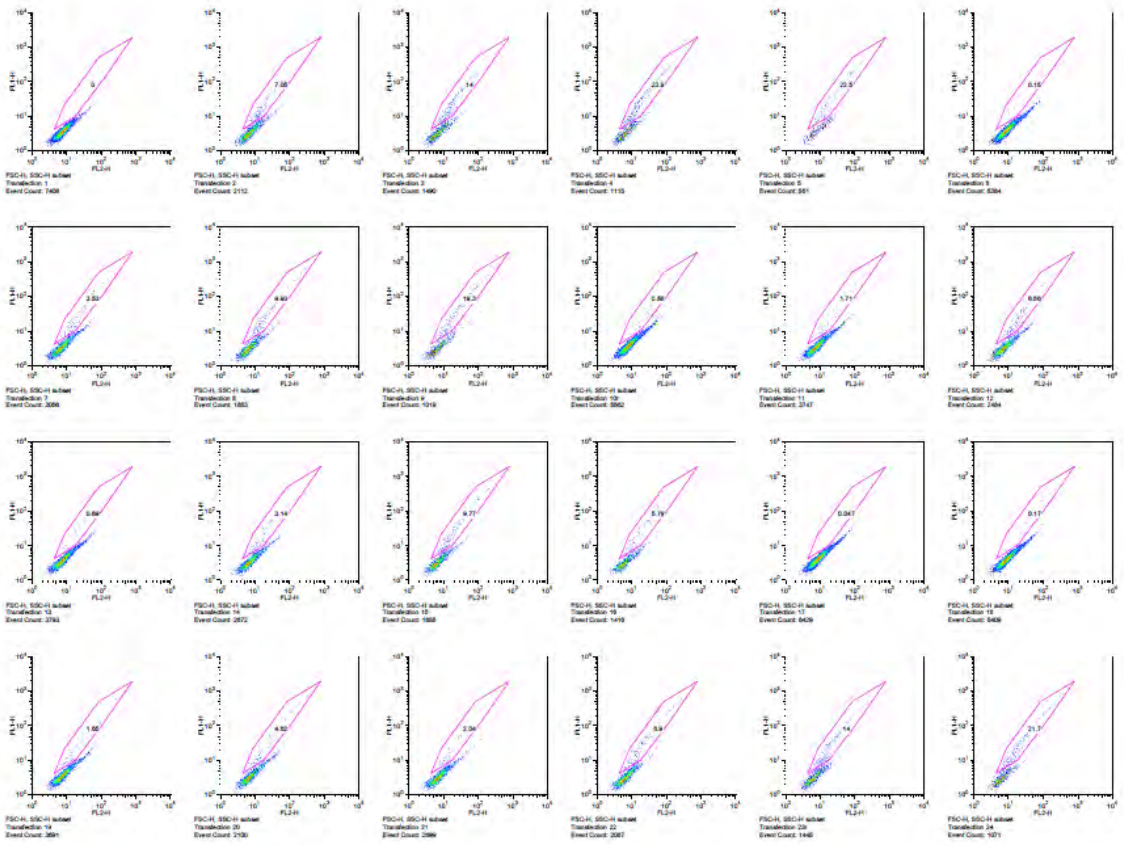

Supplementary figure 1: Transfection optimisation of THP-1 cells. A Neon transfection system was used to transfect THP-1 cells with a GFP-tagged construct using the Neon optimisation protocol. A FACS Calibur Flow Cytometer was then used to analyse GFP expression within the cells and hence determine the efficiency of transfection at each of the 24 different settings.

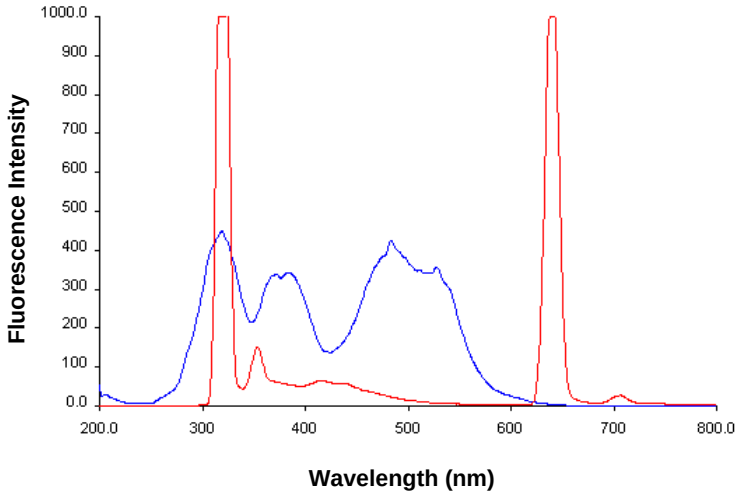

Supplementary Figure 2: Excitation and emission peaks for the Lyp Inhibitor. A wavelength scan was performed for 750μM Lyp Inhibitor (in DMSO).

REFERENCES

Azenabor, A.A., P. Kennedy, and J. York. 2009. Free intracellular Ca2+ regulates bacterial lipopolysaccharide induction of iNOS in human macrophages. *Immunobiology* 214:143-152.

Begovich, A.B., S.J. Caillier, H.C. Alexander, J.M. Penko, S.L. Hauser, L.F. Barcellos, and J.R. Oksenberg. 2005. The R620W polymorphism of the protein tyrosine phosphatase PTPN22 is not associated with multiple sclerosis. *Am. J. Hum. Genet.* 76:184-187.

Begovich, A.B., V.E.H. Carlton, L.A. Honigberg, S.J. Schrodi, A.P. Chokkalingam, H.C. Alexander, K.G. Ardlie, Q.Q. Huang, A.M. Smith, J.M. Spoerke, M.T. Conn, M. Chang, S.Y.P. Chang, R.K. Saiki, J.J. Catanese, D.U. Leong, V.E. Garcia, L.B. McAllister, D.A. Jeffery, A.T. Lee, F. Batliwalla, E. Remmers, L.A. Criswell, M.F. Seldin, D.L. Kastner, C.I. Amos, J.J. Sninsky, and P.K. Gregersen. 2004. A missense single-nucleotide polymorphism in a gene encoding a protein tyrosine phosphatase (PTPN22) is associated with rheumatoid arthritis. *Am. J. Hum. Genet.* 75:330-337.

Bottini, N., L. Musumeci, A. Alonso, S. Rahmouni, K. Nika, M. Rostamkhani, J. MacMurray, G.F. Meloni, P. Lucarelli, M. Pellecchia, G.S. Eisenbarth, D. Comings, and T. Mustelin. 2004. A functional variant of lymphoid tyrosine phosphatase is associated with type I diabetes. *Nature Genetics* 36:337-338.

Bottini, N., T. Vang, F. Cucca, and T. Mustelin. 2006. Role of PTPN22 in type 1 diabetes and other autoimmune diseases. *Semin. Immunol.* 18:207-213.

Brdicka, T., D. Pavlistova, E. Bruyns, V. Korinek, J. Scherer, P. Angelisova, A. Shevchenko, I. Hilgert, V. Horejsi, and B. Schraven. 2000. PAG (phosphoprotein associated with glycosphingolipid-enriched microdomains), a novel ubiquitously expressed transmembrane adaptor protein, binds the protein tyrosine kinase Csk and is involved in regulation of T cell

activation. *Immunobiology* 203:105.

Bromley, S.K., W.R. Burack, K.G. Johnson, K. Somersalo, T.N. Sims, C. Sumen, M.M. Davis, A.S. Shaw, P.M. Allen, and M.L. Dustin. 2001. The immunological synapse. *Annual Review of Immunology* 19:375-396.

Burn, G.L., L. Svensson, C. Sanchez-Blanco, M. Saini, and A.P. Cope. 2011. Why is PTPN22 a good candidate susceptibility gene for autoimmune disease? *Febs Letters* 585:3689-3698.

Cao, K., R. Nakajima, H.H. Meyer, and Y.X. Zheng. 2003. The AAA-ATPase Cdc48/p97 regulates spindle disassembly at the end of mitosis. *Cell* 115:355-367.

Chan, A.C., M. Iwashima, C.W. Turck, and A. Weiss. 1992. ZAP-70 - A 70 kD protein-tyrosine kinase that associates with the TCR zeta-chain. *Cell* 71:649-662.

Chapman, S.J., C.C. Khor, F. O Vannberg, N.A. Maskell, C.W. Davies, E.L. Hedley, S. Segal, C.E. Moore, K. Knox, N.P. Day, S.H. Gillespie, D.W. Crook, R.J. Davies, and A.V. Hill. 2006. PTPN22 and invasive bacterial disease. *Nature Genetics* 38:499-500.

Chi, M., S. Tridandapani, W.J. Zhong, K.M. Coggeshall, and R.F. Mortensen. 2002. C-reactive protein induces signaling through Fc gamma RIIa on HL-60 granulocytes. *J. Immunol.* 168:1413-1418.

Chien, W.W., N. Tidow, E.A. Williamson, L.Y. Shih, U. Krug, A. Kettenbach, A.C. Fermin, C.M. Roifman, and H.P. Koeffler. 2003. Characterization of a myeloid tyrosine phosphatase, Lyp, and its role in the Bcr-Abl signal transduction pathway. *Journal of Biological Chemistry* 278:27413-27420.

Cloutier, J.F., and A. Veillette. 1999. Cooperative inhibition of T-cell antigen receptor signaling by a complex between a kinase and a phosphatase. *J. Exp. Med.* 189:111-121.

Cohen, S., H. Dadi, E. Shaoul, N. Sharfe, and C.M. Roifman. 1999. Cloning and characterization of a lymphoid-specific, inducible human protein tyrosine phosphatase, Lyp. *Blood* 93:2013-2024.

Collins, S.J. 1987. The HL-60 promyelocytic leukemia-cell line - proliferation, differentiation, and cellular oncogene expression. *Blood* 70:1233-1244.

Fiorillo, E., V. Orru, S.M. Stanford, Y. Liu, M. Salek, N. Rapini, A.D. Schenone, P. Saccucci, L.G. Delogu, F. Angelini, M.L.M. Bitti, C. chmedt, A.C. Chan, O. Acuto, and N. Bottini. 2010. Autoimmune-associated PTPN22 R620W Variation Reduces Phosphorylation of Lymphoid Phosphatase on an Inhibitory Tyrosine Residue. *Journal of Biological Chemistry* 285:26506-26518.

Fischer, E.H., H. Charbonneau, and N.K. Tonks. 1991. Protein tyrosine phosphatases - A diverse family of intracellular and transmembrane enzymes. *Science* 253:401-406.

Fleit, H.B., and C.D. Kobasiuk. 1991. The human monocyte-like cell-line thp-1 expresses Fc-gamma-RI and Fc-gamma-RII. *Journal of Leukocyte Biology* 49:556-565.

Gjorloff-Wingren, A., M. Saxena, S. Williams, D. Hammi, and T. Mustelin. 1999. Characterization of TCR-induced receptor-proximal signaling events negatively regulated by the protein tyrosine phosphatase PEP. *Eur. J. Immunol.* 29:3845-3854.

Gregersen, P.K., and F. Batliwalla. 2005. PTPN22 and rheumatoid arthritis: Gratifying replication. *Arthritis Rheum.* 52:1952-1955.

Hall, A.B., M.A.M. Gakidis, M. Glogauer, J.L. Wilsbacher, S. Gao, W. Swat, and J.S. Brugge. 2006. Requirements for Vav guanine nucleotide exchange factors and Rho GTPases in Fc gamma R- and complement-mediated phagocytosis. *Immunity* 24:305-316.

Harris, P., and P. Ralph. 1985. Human-leukemic models of myelomonocytic development - a

review of the HL-60 and U937 cell-lines. *Journal of Leukocyte Biology* 37:407-422.

Hasegawa, K., F. Martin, G.M. Huang, D. Tumas, L. Diehl, and A.C. Chan. 2004. PEST domain-enriched tyrosine phosphatase (PEP) regulation of effector/memory T cells. *Science* 303:685-689.

Huang, J.Y., D. Tilly, A. Altman, K. Sugie, and H.M. Grey. 2000. T-cell receptor antagonists induce Vav phosphorylation by selective activation of Fyn kinase. *Proc. Natl. Acad. Sci. U. S. A.* 97:10923-10929.

Iivanainen, A.V., C. Lindqvist, T. Mustelin, and L.C. Andersson. 1990. Phosphotyrosine phosphatases are involved in reversion of t-lymphoblastic proliferation. *Eur. J. Immunol.* 20:2509-2512.

Karver, M.R., D. Krishnamurthy, R.A. Kulkarni, N. Bottini, and A.M. Barrios. 2009. Identifying Potent, Selective Protein Tyrosine Phosphatase Inhibitors from a Library of Au(I) Complexes. *Journal of Medicinal Chemistry* 52:6912-6918.

Kwiatkowska, K., J. Frey, and A. Sobota. 2003. Phosphorylation of Fc gamma RIIA is required for the receptor-induced actin rearrangement and capping: the role of membrane rafts. *Journal of Cell Science* 116:537-550.

Kyogoku, C., C.D. Langefeld, W.A. Ortmann, A. Lee, S. Selby, V.E.H. Carlton, M. Chang, P. Ramos, E.C. Baechler, F.M. Batliwalla, J. Novitzke, A.H. Williams, C. Gillett, P. Rodine, R.R. Graham, K.G. Ardlie, P.M. Gaffney, K.L. Moser, M. Petri, A.B. Begovich, P.K. Gregersen, and T.W. Behrens. 2004. Genetic association of the R620W polymorphism of protein tyrosine phosphatase PTPN22 with human SLE. *Am. J. Hum. Genet.* 75:504-507.

Lee, A.T., W. Li, A. Liew, C. Bombardier, M. Weisman, E.M. Massarotti, J. Kent, F. Wolfe, A.B. Begovich, and P.K. Gregersen. 2005. The PTPN22 R620W polymorphism associates

with RF positive rheumatoid arthritis in a dose-dependent manner but not with HLA-SE status. *Genes Immun.* 6:129-133.

Lee, Y.H., S.-C. Bae, and G.G. Song. 2012. The association between the functional PTPN22 1858 C/T and MIF-173 C/G polymorphisms and juvenile idiopathic arthritis: a meta-analysis. *Inflammation Research* 61:411-415.

Marrack, P., J. Kappler, and B.L. Kotzin. 2001. Autoimmune disease: why and where it occurs. *Nature Medicine* 7:899-905.

Metes, D., M. Manciulea, D. Pretrusca, H. Rabinowich, L.K. Ernst, L. Popescu, A. Calugaru, A. Sulica, W.H. Chambers, R.B. Herberman, and P.A. Morel. 1999. Ligand binding specificities and signal transduction pathways of Fc gamma receptor IIc isoforms: the CD32 isoforms expressed by human NK cells. *Eur. J. Immunol.* 29:2842-2852.

Mosser, D.M., and J.P. Edwards. 2008. Exploring the full spectrum of macrophage activation. *Nature Reviews Immunology* 8:958-969.

Mustelin, T., T. Vang, and N. Bottini. 2005. Protein tyrosine phosphatases and the immune response. *Nature Reviews Immunology* 5:43-57.

Orru, V., S.J. Tsai, B. Rueda, E. Fiorillo, S.M. Stanford, J. Dasgupta, J. Hartiala, L. Zhao, N. Ortego-Centeno, S. D'Alfonso, F.C. Arnett, H. Wu, M.A. Gonzalez-Gay, B.P. Tsao, B. Pons-Estel, M.E. Alarcon-Riquelme, Y. He, Z.-Y. Zhang, H. Allayee, X.S. Chen, J. Martin, N. Bottini, and G. Italian Collaborative. 2009. A loss-of-function variant of PTPN22 is associated with reduced risk of systemic lupus erythematosus. *Human Molecular Genetics* 18:569-579.

Patel, J.C., A. Hall, and E. Caron. 2002. Vav regulates activation of Rac but not Cdc42 during Fc gamma R-mediated phagocytosis. *Molecular Biology of the Cell* 13:1215-1226.

Raab, M., A.J. daSilva, P.R. Findell, and C.E. Rudd. 1997. Regulation of Vav-SLP-76 binding

by ZAP-70 and its relevance to TCR zeta/CD3 induction of interleukin-2. *Immunity* 6:155-164.

Rider, D.A., and S.P. Young. 2003. Measuring the specific activity of the CD45 protein tyrosine phosphatase. *J. Immunol. Methods* 277:127-134.

Sechi, A.S., and J. Wehland. 2004. Interplay between TCR signaling and actin cytoskeleton dynamics. *Trends Immunol.* 25:257-265.

Sies, H. 1993. Strategies of antioxidant defence. *European Journal of Biochemistry* 215:213-219.

van Oene, M., R.F. Wintle, X.D. Liu, M. Yazdanpanah, X.J. Gu, B. Newman, A. Kwan, B. Johnson, J. Owen, W. Greer, D. Mosher, W. Maksymwych, E. Keystone, L.A. Rubin, C.I. Amos, and K.A. Siminovitch. 2005. Association of the lymphoid tyrosine phosphatase R620W variant with rheumatoid arthritis, but not Crohn's disease, in Canadian populations. *Arthritis Rheum.* 52:1993-1998.

Vang, T., M. Congia, M.D. Macis, L. Musumeci, V. Orru, P. Zavattari, K. Nika, L. Tautz, K. Tasken, F. Cucca, T. Mustelin, and N. Bottini. 2005. Autoimmune-associated lymphoid tyrosine phosphatase is a gain-of-function variant. *Nature Genetics* 37:1317-1319.

Vang, T., W.H. Liu, L. Delacroix, S. Wu, S. Vasile, R. Dahl, L. Yang, L. Musumeci, D. Francis, J. Landskron, K. Tasken, M.L. Tremblay, B.A. Lie, R. Page, T. Mustelin, S. Rahmouni, R.C. Rickert, and L. Tautz. 2012. LYP inhibits T-cell activation when dissociated from CSK. *Nature Chemical Biology* 8:437-446.

Wang, Q., C.C. Song, and C.C.H. Li. 2003. Hexamerization of p97-VCP is promoted by ATP binding to the D1 domain and required for ATPase and biological activities. *Biochem. Biophys. Res. Commun.* 300:253-260.

Wange, R.L., and L.E. Samelson. 1996. Complex complexes: Signaling at the TCR. *Immunity* 5:197-205.

Wojcik, C., M. Yano, and G.N. DeMartino. 2004. RNA interference of valosin-containing protein (VCP/p97) reveals multiple cellular roles linked to ubiquitin/proteasome-dependent proteolysis. *Journal of Cell Science* 117:281-292.

Wong, P., G.M. Barton, K.A. Forbush, and A.Y. Rudensky. 2001. Dynamic tuning of T cell reactivity by self-peptide-major histocompatibility complex ligands. *J. Exp. Med.* 193:1179-1187.

Wu, J.S., A. Katrekar, L.A. Honigberg, A.M. Smith, M.T. Conn, J. Tang, D. Jeffery, K. Mortara, J. Sampang, S.R. Williams, J. Buggy, and J.M. Clark. 2006. Identification of substrates of human protein-tyrosine phosphatase PTPN22. *Journal of Biological Chemistry* 281:11002-11010.

Yu, X., J.P. Sun, Y.T. He, X.L. Guo, S.J. Liu, B. Zhou, A. Hudmon, and Z.Y. Zhang. 2007. Structure, inhibitor, and regulatory mechanism of Lyp, a lymphoid-specific tyrosine phosphatase implicated in autoimmune diseases. *Proc. Natl. Acad. Sci. U. S. A.* 104:19767-19772.

Zhang, J., N. Zahir, Q. Jiang, H. Miliotis, S. Heyraud, X. Meng, B. Dong, G. Xie, F. Qiu, Z. Hao, C.A. McCulloch, E.C. Keystone, A.C. Peterson, and K.A. Siminovitch. 2011. The autoimmune disease-associated PTPN22 variant promotes calpain-mediated Lyp/Pep degradation associated with lymphocyte and dendritic cell hyperresponsiveness. *Nature Genetics* 43:902-U122.

Zikherman, J., M. Hermiston, D. Steiner, K. Hasegawa, A. Chan, and A. Weiss. 2009. PTPN22 Deficiency Cooperates with the CD45 E613R Allele to Break Tolerance on a Non-Autoimmune Background. *J. Immunol.* 182:4093-4106.